UNIVERSIDADE FEDERAL DE VIÇOSA

Isolation and characterization of foodborne pathogen-infecting phages and genetic determinants of phage susceptibility in *Staphylococcus aureus*

Paloma Cavalcante Cunha
Doctor Scientiae

VIÇOSA - MINAS GERAIS
2025

PALOMA CAVALCANTE CUNHA

Isolation and characterization of foodborne pathogen-infecting phages and genetic determinants of phage susceptibility in *Staphylococcus aureus*

Thesis submitted to the Agricultural Microbiology Graduate Program of the Universidade Federal de Viçosa in partial fulfillment of the requirements for the degree of *Doctor Scientiae*.

Adviser: Sergio Oliveira de Paula

Co-adviser: Roberto Sousa Dias

VIÇOSA - MINAS GERAIS
2025

Ficha catalográfica elaborada pela Biblioteca Central da Universidade Federal de Viçosa - Campus Viçosa

T
C972i
2025

Cunha, Paloma Cavalcante, 1996-
Isolation and characterization of foodborne pathogen-infecting phages and genetic determinants of phage susceptibility in *Staphylococcus aureus* / Paloma Cavalcante Cunha. – Viçosa, MG, 2025.
1 tese eletrônica (131 f.): il. (algumas color.).

Texto em inglês.
Orientador: Sérgio Oliveira de Paula.
Tese (doutorado) - Universidade Federal de Viçosa, Departamento de Microbiologia, 2025.
Inclui bibliografia.
DOI: https://doi.org/10.47328/ufvbbt.2025.375
Modo de acesso: World Wide Web.

1. *Salmonella enterica*. 2. *Staphylococcus aureus*. 3. Sistemas de controle biológico. 4. Bacteriófagos. I. Paula, Sérgio Oliveira de, 1976-. II. Universidade Federal de Viçosa. Departamento de Microbiologia. Programa de Pós-Graduação em Microbiologia Agrícola. III. Título.

CDD 22. ed. 579.344

Bibliotecário(a) responsável: Bruna Silva CRB-6/2552

PALOMA CAVALCANTE CUNHA

Isolation and characterization of foodborne pathogen-infecting phages and genetic determinants of phage susceptibility in *Staphylococcus aureus*

Thesis submitted to the Agricultural Microbiology Graduate Program of the Universidade Federal de Viçosa in partial fulfillment of the requirements for the degree of *Doctor Scientiae*.

APPROVED: May 21, 2025.

Assent:

Paloma Cavalcante Cunha
Author

Sergio Oliveira de Paula
Adviser

ACKNOWLEDGMENTS

This journey would not have been possible without the presence, support, and love of very special people, to whom I express my deepest gratitude.

To my mother, for giving me life and for being, every day, a reference of strength, determination, and resilience. To my sister, my lifelong companion, for walking beside me with love and unwavering support. To my grandmother, for making me believe in education as a tool to change the world and for always encouraging me to pursue my dreams with courage.

To my beloved partner, Feliphe, for his unconditional support and patience, and for being my safe haven, my comfort, and my peace.

To my family, both by blood and by heart – especially Ana Paula and Dora – for their constant affection and support.

To my friends, who make life lighter and more beautiful, I offer my heartfelt thanks. A special thank you to my dear housemates, Marília and Juliana, who became my family and shared such meaningful moments with me. I also warmly thank Pernille, Marie-Aida, and Glória, who became such special friends during my time in Norway and whose companionship made the Norwegian winter feel so much warmer.

To all the interns who worked with me during this project, thank you for your commitment and collaboration. In particular, I thank Ana Julia and Isabella, whose dedication was essential to the development of this research.

To all my professors who have guided and inspired me throughout the years, and to my advisors, Sérgio and Roberto, thank you for your guidance, encouragement, and for accompanying me throughout this scientific journey.

To all my colleagues and friends from the Laboratório de Imunovirologia Molecular (LIVM), thank you for the companionship, support, and for all the enriching scientific and personal exchanges we shared throughout these years.

To Vinícius and Professor Davide, thank you for welcoming me so warmly into the lab during my exchange period in Norway and for contributing so positively and kindly to the realization of my sandwich PhD dream.

To the Universidade Federal de Viçosa (UFV), the Departamento de Microbiologia, the Departamento de Biologia Geral, and the Programa de Pós-Graduação em Microbiologia Agrícola, thank you for the academic

training, infrastructure, and support throughout this journey. To the Núcleo de Microscopia e Microanálise (NMM), thank you for the technical assistance with microscopy. I also extend my gratitude to the Brazilian public education system for making free and high-quality education possible.
Finally, I thank God for the gift of life and for writing such a beautiful story for me.
This work has been sponsored by the following Brazilian research agencies: Coordination for the Improvement of Higher Education Personnel (CAPES; Financing code 001), Minas Gerais State Foundation for Research Aid (FAPEMIG) and National Council of Scientific and Technological Development (CNPq).

ABSTRACT

CUNHA, Paloma Cavalcante, D.Sc., Universidade Federal de Viçosa, May, 2025. **Isolation and characterization of foodborne pathogen-infecting phages and genetic determinants of phage susceptibility in *Staphylococcus aureus***. Adviser: Sergio Oliveira de Paula. Co-adviser: Roberto Sousa Dias.

The growing prevalence of antibiotic-resistant bacterial pathogens in clinical, veterinary, and food production settings demands alternative control strategies. Bacteriophages (phages), due to their host specificity and safety, have emerged as promising antimicrobial agents for both therapeutic and biocontrol applications. This thesis explores the isolation, genomic and functional characterization, and application of lytic phages targeting *Salmonella enterica* and *Staphylococcus aureus*, two major foodborne and zoonotic pathogens. The study also investigates bacterial genetic determinants that modulate susceptibility to phage infection. In Chapter 1, the polyvalent *Tequintavirus* phage UFVCit2 was isolated and shown to infect *Citrobacter freundii, Shigella flexneri,* and different *S. enterica* serovars. Genomic analysis confirmed its strictly lytic nature and genetic safety. UFVCit2 significantly reduced S. enterica counts on chicken meat and lettuce in food model experiments, highlighting its potential for biocontrol applications in complex matrices. Chapter 2 presents the characterization of phage CapO46, a newly identified *Rosenblumvirus* with broad activity against *S. aureus* strains from clinical and environmental origins. CapO46 exhibited rapid adsorption kinetics, a short latent period, and stable lytic activity in ultra-high-temperature (UHT) milk, achieving up to 7.2 log10 CFU/mL reduction after 12 hours. Genomic analyses confirmed the absence of lysogeny, virulence, or resistance genes, further supporting its suitability as a safe and effective biocontrol agent for dairy applications. In Chapter 3, a genome-wide CRISPR interference (CRISPRi-seq) screen was conducted to identify host factors in *S. aureus* that influence susceptibility to CapO46. The screen revealed that repression of mgrA, sarZ, and SAOUHSC_00695 conferred resistance to infection, while silencing rpiRc increased susceptibility. Functional validation via bacterial growth, phage replication, adhesion, and biofilm formation assays confirmed the involvement of these genes in regulating both phage sensitivity and surface-associated virulence traits. Altogether, this work demonstrates the potential of phages as targeted, safe, and sustainable alternatives to antibiotics, and underscores the importance of genetic context in modulating bacterial susceptibility. The integration of phage genomics, food model applications, and functional bacterial genetics provides a comprehensive framework for the rational development of

phage-based biocontrol and therapeutic strategies.

Keywords: *Salmonella enterica*; *Staphylococcus aureus*; Biocontrol; CRISPR interference; Host factors; Phage resistance.

RESUMO

CUNHA, Paloma Cavalcante, D.Sc., Universidade Federal de Viçosa, maio de 2025. **Isolamento e caracterização de fagos que infectam patógenos alimentares e determinantes genéticos da susceptibilidade fágica em *Staphylococcus aureus***. Orientador: Sergio Oliveira de Paula. Coorientador: Roberto Sousa Dias.

A crescente prevalência de patógenos bacterianos resistentes a antibióticos em contextos clínico, veterinário e de produção de alimentos exige estratégias de controle alternativas. Os bacteriófagos (fagos), devido à sua especificidade de hospedeiro e segurança, surgem como agentes antimicrobianos promissores tanto para aplicações terapêuticas quanto de biocontrole. Esta tese aborda o isolamento, caracterização genômica e funcional, e aplicação de fagos líticos direcionados a *Salmonella enterica* e *Staphylococcus aureus*, dois importantes patógenos de origem alimentar e zoonótica. O estudo também investiga determinantes genéticos bacterianos que modulam a susceptibilidade à infecção fágica. No Capítulo 1, foi isolado o fago polivalente UFVCit2, pertencente ao gênero *Tequintavirus*, com atividade lítica contra *Citrobacter freundii*, *Shigella flexneri* e diferentes sorovares de *S. enterica*. A análise genômica confirmou sua natureza estritamente lítica e perfil genético seguro. Em experimentos com modelos alimentares, UFVCit2 reduziu significativamente as contagens de *S. enterica* em carne de frango e alface, destacando seu potencial como agente de biocontrole em matrizes complexas. O Capítulo 2 apresenta a caracterização do fago CapO46, um *Rosenblumvirus* recém-identificado com ampla atividade contra cepas de *S. aureus* de origens clínicas e ambientais. CapO46 demonstrou cinética de adsorção rápida, curto período de latência e atividade lítica em leite UHT, alcançando até 7,2 log10 CFU/mL de redução após 12 horas. As análises genômicas confirmaram a ausência de genes relacionados à lisogenia, virulência ou resistência, reforçando sua adequação como agente seguro e eficaz para aplicações em produtos lácteos. No Capítulo 3, foi realizada uma triagem genômica por CRISPR de interference (CRISPRi-seq) para identificar fatores do hospedeiro em *S. aureus* que influenciam a susceptibilidade ao fago CapO46. A triagem revelou que a repressão dos genes *mgrA*, *sarZ* e SAOUHSC_00695 conferiu resistência à infecção, enquanto o silenciamento de *rpiRc* aumentou a susceptibilidade. A validação funcional por meio de ensaios de crescimento bacteriano, replicação fágica, adesão e formação de biofilme confirmou o envolvimento desses genes na regulação da sensibilidade ao fago e em características associadas à virulência superficial. Em conjunto, este trabalho demonstra o potencial dos fagos como alternativas

direcionadas, seguras e sustentáveis aos antibióticos, e destaca a importância do contexto genético na modulação da susceptibilidade bacteriana. A integração entre genômica de fagos, testes em modelos alimentares e genética funcional bacteriana fornece uma base abrangente para o desenvolvimento racional de estratégias terapêuticas e de biocontrole baseadas em fagos.

Palavras-chave: *Salmonella entérica*; *Staphylococcus aureus*; Biocontrole; Interferência por CRISPR; Fatores do hospedeiro; Resistência a fagos

SUMMARY

GENERAL INTRODUCTION

Antibiotic resistance represents one of the greatest threats to public health, food safety, and the sustainability of animal production in the 21st century [1]. The indiscriminate use of antibiotics in both human medicine and agriculture has accelerated the selection of multidrug-resistant strains, which challenge conventional treatments and contribute to the persistence of infectious outbreaks worldwide [1,2]. It is estimated that by 2050, infections caused by resistant bacteria could result in up to 10 million deaths annually if effective measures are not adopted [3]. In this context, alternative therapies that combine antimicrobial efficacy with safety and specificity—such as bacteriophage therapy—are gaining increased attention.

Bacteriophages (phages) are viruses that specifically infect bacteria. They are recognized as the most abundant and genetically diverse biological entities on the planet, yet it is estimated that only a tiny fraction—less than 0.0002%—of their diversity has been explored to date [4,5]. These viruses are widespread and can be isolated from a range of ecosystems, including terrestrial soil, marine and freshwater bodies, and even extreme environments [6]. Phages coevolve with their bacterial hosts and play critical roles in shaping microbial ecology and evolution—either through bacterial cell lysis or by mediating horizontal gene transfer, including the dissemination of virulence and resistance determinants [7,8].

Structurally, phages consist of a protein capsid enclosing genetic material, which can be single- or double-stranded DNA or RNA. They may possess long contractile or non-contractile tails, short non-contractile tails, or lack a tail entirely, which defines their morphology [5]. According to the current International Committee on Taxonomy of Viruses (ICTV) taxonomy, most tailed phages belong to the order *Caudoviricetes* and are classified into families and genera based on phylogenomic criteria, genome organization, and virion structure. Although taxonomy is no longer based solely on tail morphology, such descriptors remain widely used for comparative and descriptive purposes [9].

Phage infection is a stepwise and coordinated process that begins with adsorption, in which the phage recognizes and attaches to specific receptors on the bacterial surface. This is typically mediated by tail structures—such as fibers, spikes, or baseplates—or other capsid components. Adsorption occurs in two stages: a reversible primary interaction driven by electrostatic forces, and a subsequent

irreversible binding that involves tighter association with a secondary receptor, often requiring the action of hydrolase enzymes [10,11]. Receptor-binding proteins (RBPs), usually located at the distal ends of the tail, mediate host specificity and are responsible for both initial contact and stable attachment [12,13]. Phage receptors include a range of bacterial surface components such as lipopolysaccharides (LPS), wall teichoic acids (WTAs), outer membrane proteins, as well as structures like pili and flagella [14–16]. The recognition of secondary receptors typically triggers conformational changes in the virion structure that lead to genome ejection through a channel formed across the bacterial cell wall, often involving pores created by phage-encoded enzymes such as lysins [10,11,17]. Once the phage genome enters the host cytoplasm, the subsequent events depend on the biological cycle of the phage. In the case of lytic phages, the genome undergoes replication, transcription, and translation [5]. These steps culminate in the assembly of progeny virions, which are released when phage-encoded lytic enzymes—such as holins and endolysins—degrade the bacterial cell wall, thereby completing the infection cycle [18].

The lytic cycle, during which phages replicate immediately after infection and lyse the bacterial cell, represents a critical step in the application of phages for therapeutic and industrial purposes. Its fast-acting nature and efficiency in eliminating target bacteria make lytic phages highly suitable for biocontrol applications, especially when compared to temperate phages, which follow a distinct biological strategy. While lytic phages act swiftly to eliminate their hosts, temperate phages that follow the lysogenic cycle integrate their genome into the bacterial chromosome and may remain latent for extended periods [19]. These phages may also facilitate the transfer of harmful genes, such as toxins and virulence genes, and antibiotic resistance factors [8]. For these reasons, lysogenic phages are generally not suitable for therapeutic or industrial applications. Instead, strictly lytic phages are preferred for biocontrol strategies [20].

Furthermore, one of the most relevant features of phages is their higher host specificity when compared to conventional antimicrobials. This characteristic stands in contrast to the broad-spectrum activity of antibiotics, which often target a wide range of bacterial species indiscriminately. Such general activity can disrupt the host microbiota and promote collateral damage [21], whereas phages act with much greater precision, typically infecting only specific bacterial strains or species. While this specificity is advantageous for minimizing off-target effects and preserving beneficial microorganisms [22,23], it may pose limitations in polymicrobial infections or cases

where the exact pathogen is not known. In such contexts, the narrow spectrum of individual phages can limit treatment efficacy [24].

To overcome this, phage cocktails composed of multiple complementary phages are often formulated to broaden the spectrum of bacterial targets [25,26]. An alternative or complementary approach involves the use of polyvalent phages—those capable of infecting multiple bacterial strains or even different species or genera [27,28]. These phages can be particularly useful in scenarios where precise pathogen identification is challenging, or where infections involve mixed bacterial populations [29]. Both strategies aim to enhance therapeutic coverage while maintaining the advantages of phage specificity, but they require robust characterization of phage host range and careful selection to avoid redundancy or interference among phages in the cocktail [20,30]. The success of this strategy also relies on accurate pathogen identification and continuous monitoring of host range coverage. This specificity contributes to minimizing disruption of beneficial microbiota, while also enhancing phage persistence and efficacy at the site of infection [29,31].

In addition, phages can degrade bacterial biofilms—complex matrices that impair antimicrobial penetration and contribute to persistent infections [32–34]. These biofilm-disrupting properties, combined with the targeted and residue-free nature of phage action, align well with sustainable practices in food and agricultural industries [20,35]. As a result, bacteriophages are increasingly being considered as practical interventions in production chains, not only for environmental reasons but also for their potential to address persistent microbial threats where conventional sanitization methods fail [35].

This relevance becomes even more apparent when considering the growing problem of antimicrobial resistance in industrial and agricultural settings. Pathogens such as *Salmonella enterica* and *Staphylococcus aureus* are among the most critical agents responsible for economic losses in these sectors [36–38]. *S. aureus*, for instance, is a frequent cause of bovine mastitis and also foodborne intoxications, forming biofilms that further complicate sanitation efforts [38–40]. Meanwhile, *Salmonella* remains a leading cause of foodborne outbreaks, with serovars like Enteritidis and Typhimurium being widespread in poultry production systems [41–43]. Together, these pathogens contribute to substantial economic burdens—including discarded products, veterinary treatment costs, reduced productivity, and health-related expenses [36,37,44]. Against this backdrop, phage-based biocontrol strategies

emerge as promising, safe, and cost-effective alternatives to conventional antimicrobial methods [45–47].

Several studies have demonstrated the effectiveness of phages in controlling pathogens in food and animal systems. Commercial products such as Salmonelex™ and SalmoFresh™ are already used to control *Salmonella* in meat, vegetables, eggs, and even on glass and stainless steel surfaces [48–51]. Other commercially available phage-based formulations include Listex™ P100, approved for use against *Listeria monocytogenes* in meat and ready-to-eat foods [52,53], and EcoShield™, which targets *Escherichia coli* O157:H7 on different types of meat and leafy greens [54,55]. These products exemplify the expanding role of phage biocontrol in food safety across a variety of bacterial pathogens and food matrices. In the case of *S. aureus*, phages have been investigated for treating bovine mastitis in murine models and decontaminating dairy products [45,56–58]. These findings support the utility of phages as tools for biosafety in productive systems.

The success of phage therapy, however, depends on a deep understanding of phage-host interactions, especially in the context of bacterial resistance. Similar to antibiotics, bacteria can develop resistance to phages via several mechanisms: receptor loss or modification, restriction-modification systems, CRISPR-Cas immunity, and superinfection exclusion, among others [59,60]. In *Salmonella*, for example, variation in outer membrane proteins such as FhuA and OmpC can prevent phage adsorption [61]. In *S. aureus*, alterations in genes related to wall teichoic acid biosynthesis, DNA repair systems, or phage adsorption structures, have been shown to influence phage susceptibility in *S. aureus* and other species [62–64]. The emergence of phage resistance is therefore a critical limitation, necessitating combinatory strategies such as phage cocktails, engineered RBPs, and functional genetic screens to identify relevant host factors [59,60,65].

In this context, the chapters presented in this thesis address key aspects of bacteriophage-based therapy and bacterial biocontrol—from the characterization of phages active against *S. aureus* and *Salmonella*, to the identification of genetic factors modulating bacterial susceptibility. Chapter 1 focuses on a *Tequintavirus* phage with activity against multiple Enterobacteriaceae, including *Salmonella*, and its application was validated in food models using chicken meat and lettuce; Chapter 2 explores a *Rosenblumvirus* phage effective against multiple *S. aureus* strains, including efficacy tests conducted in UHT milk; and Chapter 3 details a genome-wide CRISPRi screen

that uncovered genes involved in phage resistance in *S. aureus*. Together, these studies contribute to a better understanding of phages as sustainable and effective tools for controlling pathogenic bacteria in animal health and food safety.

REFERENCES

1. WORLD HEALTH ORGANIZATION (WHO) **Antibiotic Resistance**, Available online: https://www.who.int/news-room/fact-sheets/detail/antibiotic-resistance (accessed on 28 February 2023).

2. FOUNOU, L.L.; FOUNOU, R.C.; ESSACK, S.Y. **Antibiotic Resistance in the Food Chain: A Developing Country-Perspective**. *Front Microbiol* **2016**, *7*, doi:10.3389/fmicb.2016.01881.

3. O'NEILL, J. ***Tackling Drug-Resistant Infections Globally: Final Report and Recommendations***; London, UK, 2016;

4. IGNACIO-ESPINOZA, J.C.; AHLGREN, N.A.; FUHRMAN, J.A. **Long-Term Stability and Red Queen-like Strain Dynamics in Marine Viruses**. *Nat Microbiol* **2019**, *5*, 265–271, doi:10.1038/s41564-019-0628-x.

5. SULAKVELIDZE, A. *BACTERIOPHAGES*; KUTTER, E., SULAKVELIDZE, A., Eds.; CRC Press, 2004; ISBN 9780203491751.

6. CLOKIE, M.R.J.; MILLARD, A.D.; LETAROV, A. V.; HEAPHY, S. **Phages in Nature.** ***Bacteriophage*** **2011**, *1*, 31–45, doi:10.4161/bact.1.1.14942.

7. KOSKELLA, B.; BROCKHURST, M.A. **Bacteria–Phage Coevolution as a Driver of Ecological and Evolutionary Processes in Microbial Communities.** *FEMS Microbiol Rev* **2014**, *38*, 916–931, doi:10.1111/1574-6976.12072.

8. BRÜSSOW, H.; CANCHAYA, C.; HARDT, W.-D. **Phages and the Evolution of Bacterial Pathogens: From Genomic Rearrangements to Lysogenic Conversion**. *Microbiology and Molecular Biology Reviews* **2004**, *68*, 560–602, doi:10.1128/MMBR.68.3.560-602.2004.

9. INTERNATIONAL COMMITTEE ON TAXONOMY OF VIRUSES VIRUS TAXONOMY: 2023 Release Available online: https://ictv.global/taxonomy (accessed on 30 April 2025).

10. NOBREGA, F.L.; VLOT, M.; DE JONGE, P.A.; DREESENS, L.L.; BEAUMONT, H.J.E.; LAVIGNE, R.; DUTILH, B.E.; BROUNS, S.J.J. **Targeting Mechanisms of Tailed Bacteriophages**. *Nat Rev Microbiol* **2018**, *16*, 760–773, doi:10.1038/s41579-018-0070-8.

11. LETAROV, A. V.; KULIKOV, E.E. **Adsorption of Bacteriophages on Bacterial Cells.** ***Biochemistry (Moscow)*** **2017**, *82*, 1632–1658, doi:10.1134/S0006297917130053.

12. MILLER, E.S.; KUTTER, E.; MOSIG, G.; ARISAKA, F.; KUNISAWA, T.; RÜGER, W. **Bacteriophage T4 Genome.** ***Microbiology and Molecular Biology Reviews*** **2003**, *67*, 86–156, doi:10.1128/MMBR.67.1.86-156.2003.

13. BARTUAL, S.G.; OTERO, J.M.; GARCIA-DOVAL, C.; LLAMAS-SAIZ, A.L.; KAHN, R.; FOX, G.C.; VAN RAAIJ, M.J. Structure of the Bacteriophage T4 Long Tail Fiber Receptor-Binding Tip. *Proceedings of the National Academy of Sciences* **2010**, *107*, 20287–20292, doi:10.1073/pnas.1011218107.

14. BROWN, S.; XIA, G.; LUHACHACK, L.G.; CAMPBELL, J.; MEREDITH, T.C.; CHEN, C.; WINSTEL, V.; GEKELER, C.; IRAZOQUI, J.E.; PESCHEL, A.; ET AL. **Methicillin Resistance in *Staphylococcus Aureus* Requires Glycosylated Wall Teichoic Acids.** *Proceedings of the National Academy of Sciences* **2012**, *109*, 18909–18914, doi:10.1073/pnas.1209126109.

15. RABSCH, W.; MA, L.; WILEY, G.; NAJAR, F.Z.; KASERER, W.; SCHUERCH, D.W.; KLEBBA, J.E.; ROE, B.A.; GOMEZ, J.A.L.; SCHALLMEY, M.; et al. **FepA- and TonB-Dependent Bacteriophage H8: Receptor Binding and Genomic Sequence.** *J Bacteriol* **2007**, *189*, 5658–5674, doi:10.1128/JB.00437-07.

16. BRAUN, V.; SCHALLER, K.; WOLFF, H. A **Common Receptor Protein for Phage T5 and Colicin M in the Outer Membrane of Escherichia Coli B.** *Biochimica et Biophysica Acta (BBA) - Biomembranes* **1973**, *323*, 87–97, doi:10.1016/0005-2736(73)90433-1.

17. GUTIÉRREZ, D.; BRIERS, Y. **Lysins Breaking down the Walls of Gram-Negative Bacteria, No Longer a No-Go.** *Curr Opin Biotechnol* **2021**, *68*, 15–22, doi:10.1016/j.copbio.2020.08.014.

18. CHATURONGAKUL, S.; OUNJAI, P. Phage–Host Interplay: **Examples from Tailed Phages and Gram-Negative Bacterial Pathogens**. *Front Microbiol* **2014**, *5*, doi:10.3389/fmicb.2014.00442.

19. HOBBS, Z.; ABEDON, S.T. **Diversity of Phage Infection Types and Associated Terminology: The Problem with 'Lytic or Lysogenic.**' *FEMS Microbiol Lett* **2016**, *363*, fnw047, doi:10.1093/femsle/fnw047.

20. ABEDON, S.T.; GARCÍA, P.; MULLANY, P.; AMINOV, R. Editorial: **Phage Therapy: Past, Present and Future.** *Front Microbiol* **2017**, *8*, doi:10.3389/fmicb.2017.00981.

21. MIKKELSEN, K.H.; ALLIN, K.H.; KNOP, F.K. **Effect of Antibiotics on Gut Microbiota, Glucose Metabolism and Body Weight Regulation: A Review of the Literature.** *Diabetes Obes Metab* **2016**, *18*, 444–453, doi:10.1111/dom.12637.

22. GALTIER, M.; DE SORDI, L.; MAURA, D.; ARACHCHI, H.; VOLANT, S.; DILLIES, M.; DEBARBIEUX, L. **Bacteriophages to Reduce Gut Carriage of Antibiotic Resistant Uropathogens with Low Impact on Microbiota Composition.** *Environ Microbiol* **2016**, *18*, 2237–2245, doi:10.1111/1462-2920.13284.

23. MAI, V.; UKHANOVA, M.; REINHARD, M.K.; LI, M.; SULAKVELIDZE, A. **Bacteriophage Administration Significantly Reduces *Shigella* Colonization and Shedding by *Shigella* -Challenged Mice without Deleterious Side Effects and Distortions in the Gut Microbiota.** *Bacteriophage* **2015**, *5*, e1088124, doi:10.1080/21597081.2015.1088124.

24. SERVICK, K. Beleaguered **Phage Therapy Trial Presses On.** *Science (1979)* **2016**, *352*, 1506–1506, doi:10.1126/science.352.6293.1506.

25. PHOTHAWORN, P.; SUPOKAIVANICH, R.; LIM, J.; KLUMPP, J.; IMAM, M.; KUTTER, E.; GALYOV, E.E.; DUNNE, M.; KORBSRISATE, S. **Development of a Broad-Spectrum Salmonella Phage Cocktail Containing Viunalike and Jerseylike Viruses Isolated from Thailand.** *Food Microbiol* **2020**, *92*, 103586, doi:10.1016/j.fm.2020.103586.

26. GUTIÉRREZ, D.; VANDENHEUVEL, D.; MARTÍNEZ, B.; RODRÍGUEZ, A.; LAVIGNE, R.; GARCÍA, P. **Two Phages, PhilPLA-RODI and PhilPLA-C1C, Lyse Mono- and Dual-Species Staphylococcal Biofilms.** *Appl Environ Microbiol* **2015**, *81*, 3336–3348, doi:10.1128/AEM.03560-14.

27. DUC, H.M.; SON, H.M.; YI, H.P.S.; SATO, J.; NGAN, P.H.; MASUDA, Y.; HONJOH, K.; MIYAMOTO, T. **Isolation, Characterization and Application of a Polyvalent Phage Capable of Controlling Salmonella and Escherichia Coli O157:H7 in Different Food Matrices.** *Food Research International* **2020**, *131*, 108977, doi:10.1016/j.foodres.2020.108977.

28. YU, P.; MATHIEU, J.; LU, G.W.; GABIATTI, N.; ALVAREZ, P.J. **Control of Antibiotic-Resistant Bacteria in Activated Sludge Using Polyvalent Phages in Conjunction with a Production Host.** *Environ Sci Technol Lett* **2017**, *4*, 137–142, doi:10.1021/acs.estlett.7b00045.

29. LIN, D.M.; KOSKELLA, B.; LIN, H.C. **Phage Therapy: An Alternative to Antibiotics in the Age of Multi-Drug Resistance.** ***World*** *J Gastrointest Pharmacol Ther* **2017**, *8*, 162, doi:10.4292/wjgpt.v8.i3.162.

30. SCHMERER, M.; MOLINEUX, I.J.; BULL, J.J. **Synergy as a Rationale for Phage Therapy Using Phage Cocktails.** *PeerJ* **2014**, *2*, e590, doi:10.7717/peerj.590.

31. FERNÁNDEZ, L.; DUARTE, A.C.; RODRÍGUEZ, A.; GARCÍA, P. **The Relationship between the Phageome and Human Health: Are Bacteriophages Beneficial or Harmful Microbes?** *Benef Microbes* **2021**, *12*, 107–120, doi:10.3920/BM2020.0132.

32. BANSAL, S.; HARJAI, K.; CHHIBBER, S. **Depolymerase Improves Gentamicin Efficacy during Klebsiella Pneumoniae Induced Murine Infection.** *BMC Infect Dis* **2014**, *14*, 456, doi:10.1186/1471-2334-14-456.

33. DEL POZO, J.L. **Biofilm-Related Disease.** *Expert Rev Anti Infect Ther* **2018**, *16*, 51–65, doi:10.1080/14787210.2018.1417036.

34. URUÉN, C.; CHOPO-ESCUIN, G.; TOMMASSEN, J.; MAINAR-JAIME, R.C.; ARENAS, J. **Biofilms as Promoters of Bacterial Antibiotic Resistance and Tolerance.** *Antibiotics* **2020**, *10*, 3, doi:10.3390/antibiotics10010003.

35. GOODRIDGE, L.D.; BISHA, B. **Phage-Based Biocontrol Strategies to Reduce Foodborne Pathogens in Foods.** *Bacteriophage* **2011**, *1*, 130–137, doi:10.4161/bact.1.3.17629.

36. WORLD HEALTH ORGANIZATION WHO **Estimates of the Global Burden of Foodborne Diseases: Foodborne Disease Burden Epidemiology Reference Group** 2007–2015, Available online: https://www.who.int/publications/i/item/9789241565165 (accessed on 1 May 2025).

37. FERRARI, R.G.; ROSARIO, D.K.A.; CUNHA-NETO, A.; MANO, S.B.; FIGUEIREDO, E.E.S.; CONTE-JUNIOR, C.A. Worldwide **Epidemiology of *Salmonella* Serovars in ANIMAL-BASED FOODS: A META-ANALYSIS.** *Appl Environ Microbiol* **2019**, *85*, doi:10.1128/AEM.00591-19.

38. LÉGUILLIER, V.; PINAMONTI, D.; CHANG, C.-M.; GUNJAN; MUKHERJEE, R.; HIMANSHU; COSSETINI, A.; MANZANO, M.; ANBA-MONDOLONI, J.; MALET-

VILLEMAGNE, J.; et al. **A Review and Meta-Analysis of Staphylococcus Aureus Prevalence in Foods.** *The Microbe* **2024**, *4*, 100131, doi:10.1016/j.microb.2024.100131.

39. VASUDEVAN, P.; NAIR, M.K.M.; ANNAMALAI, T.; VENKITANARAYANAN, K.S. **Phenotypic and Genotypic Characterization of Bovine Mastitis Isolates of Staphylococcus Aureus for Biofilm Formation.** *Vet Microbiol* **2003**, *92*, 179–185, doi:10.1016/S0378-1135(02)00360-7.

40. BABRA, C.; TIWARI, J.G.; PIER, G.; THEIN, T.H.; SUNAGAR, R.; SUNDARESHAN, S.; ISLOOR, S.; HEGDE, N.R.; DE WET, S.; DEIGHTON, M.; et al. **The Persistence of Biofilm-Associated Antibiotic Resistance of Staphylococcus Aureus Isolated from Clinical Bovine Mastitis Cases in Australia**. *Folia Microbiol (Praha)* **2013**, *58*, 469–474, doi:10.1007/s12223-013-0232-z.

41. NAIR, D.V.T.; KOLLANOOR JOHNY, A. **Salmonella in Poultry Meat Production. In *Food Safety in Poultry Meat Production*;** Springer International Publishing: Cham, 2019; pp. 1–24.

42. WESSELS, K.; RIP, D.; GOUWS, P. **Salmonella in Chicken Meat: Consumption, Outbreaks, Characteristics, Current Control Methods and the Potential of Bacteriophage Use.** *Foods* **2021**, *10*, 1742, doi:10.3390/foods10081742.

43. MECHESSO, A.F.; MOON, D.C.; KIM, S.-J.; SONG, H.-J.; KANG, H.Y.; NA, S.H.; CHOI, J.-H.; KIM, H.-Y.; YOON, S.-S.; LIM, S.-K. **Nationwide Surveillance on Serotype Distribution and Antimicrobial Resistance Profiles of Non-Typhoidal Salmonella Serovars Isolated from Food-Producing Animals in South Korea.** *Int J Food Microbiol* **2020**, *335*, 108893, doi:10.1016/j.ijfoodmicro.2020.108893.

44. RAINARD, P.; FOUCRAS, G.; FITZGERALD, J.R.; WATTS, J.L.; KOOP, G.; MIDDLETON, J.R. **Knowledge Gaps and Research Priorities in *Staphylococcus Aureus* Mastitis Control.** *Transbound Emerg Dis* **2018**, *65*, 149–165, doi:10.1111/tbed.12698.

45. CUNHA, P.C.; DE SOUZA, P.S.; ROSSETO, A.J.D.; RODRIGUES, I.R.; DIAS, R.S.; DA SILVA DUARTE, V.; PORCELLATO, D.; DA SILVA, C.C.; DE PAULA, S.O. **Characterization of Newly Isolated Rosenblumvirus Phage Infecting Staphylococcus Aureus from Different Sources.** *Microorganisms* **2025**, *13*, 664, doi:10.3390/microorganisms13030664.

46. CLAVIJO, V.; BAQUERO, D.; HERNANDEZ, S.; FARFAN, J.C.; ARIAS, J.; ARÉVALO, A.; DONADO-GODOY, P.; VIVES-FLORES, M. **Phage Cocktail SalmoFREE® Reduces Salmonella on a Commercial Broiler Farm.** *Poult Sci* **2019**, *98*, 5054–5063, doi:10.3382/ps/pez251.

47. CLAVIJO, V.; MORALES, T.; VIVES-FLORES, M.J.; REYES MUÑOZ, A. **The Gut Microbiota of Chickens in a Commercial Farm Treated with a Salmonella Phage Cocktail.** *Sci Rep* **2022**, *12*, 991, doi:10.1038/s41598-021-04679-6.

48. SUKUMARAN, A.T.; NANNAPANENI, R.; KIESS, A.; SHARMA, C.S. **Reduction of Salmonella on Chicken Meat and Chicken Skin by Combined or Sequential Application of Lytic Bacteriophage with Chemical Antimicrobials.** *Int J Food Microbiol* **2015**, *207*, 8–15, doi:10.1016/j.ijfoodmicro.2015.04.025.

49. ZHANG, X.; NIU, Y.D.; NAN, Y.; STANFORD, K.; HOLLEY, R.; MCALLISTER, T.; NARVÁEZ-BRAVO, C. **SalmoFresh™ Effectiveness in Controlling Salmonella on Romaine Lettuce, Mung Bean Sprouts and Seeds.** *Int J Food Microbiol* **2019**, *305*, 108250, doi:10.1016/j.ijfoodmicro.2019.108250.

50. WOOLSTON, J.; PARKS, A.R.; ABULADZE, T.; ANDERSON, B.; LI, M.; CARTER, C.; HANNA, L.F.; HEYSE, S.; CHARBONNEAU, D.; SULAKVELIDZE, A. **Bacteriophages Lytic for Salmonella Rapidly Reduce Salmonella Contamination on Glass and Stainless Steel Surfaces.** *Bacteriophage* **2013**, *3*, e25697, doi:10.4161/bact.25697.

51. GRANT, A.; PARVEEN, S.; SCHWARZ, J.; HASHEM, F.; VIMINI, B. **Reduction of Salmonella in Ground Chicken Using a Bacteriophage.** *Poult Sci* **2017**, *96*, 2845–2852, doi:10.3382/ps/pex062.

52. CHIBEU, A.; AGIUS, L.; GAO, A.; SABOUR, P.M.; KROPINSKI, A.M.; BALAMURUGAN, S. **Efficacy of Bacteriophage LISTEX™P100 Combined with Chemical Antimicrobials in Reducing Listeria Monocytogenes in Cooked Turkey and Roast Beef.** *Int J Food Microbiol* **2013**, *167*, 208–214, doi:10.1016/j.ijfoodmicro.2013.08.018.

53. ALLENDE, A. *et al.* **Evaluation of the Safety and Efficacy of Listex™ P100 for Reduction of Pathogens on Different Ready-to-eat (RTE) Food Products.** *EFSA Journal* **2016**, *14*, doi:10.2903/j.efsa.2016.4565.

54. CARTER, C.D.; PARKS, A.; ABULADZE, T.; LI, M.; WOOLSTON, J.; MAGNONE, J.; SENECAL, A.; KROPINSKI, A.M.; SULAKVELIDZE, A. **Bacteriophage Cocktail Significantly Reduces Escherichia Coli O157**. *Bacteriophage* **2012**, *2*, 178–185, doi:10.4161/bact.22825.

55. VIKRAM, A.; TOKMAN, J.I.; WOOLSTON, J.; SULAKVELIDZE, A. **Phage Biocontrol Improves Food Safety by Significantly Reducing the Level and Prevalence of Escherichia Coli O157:H7 in Various Foods.** *J Food Prot* **2020**, *83*, 668–676, doi:10.4315/0362-028X.JFP-19-433.

56. NGASSAM-TCHAMBA, C.; DUPREZ, J.N.; FERGESTAD, M.; DE VISSCHER, A.; L'ABEE-LUND, T.; DE VLIEGHER, S.; WASTESON, Y.; TOUZAIN, F.; BLANCHARD, Y.; LAVIGNE, R.; et al. **In Vitro and in Vivo Assessment of Phage Therapy against Staphylococcus Aureus Causing Bovine Mastitis.** *J Glob Antimicrob Resist* **2020**, *22*, 762–770, doi:10.1016/j.jgar.2020.06.020.

57. GENG, H.; ZOU, W.; ZHANG, M.; XU, L.; LIU, F.; LI, X.; WANG, L.; XU, Y. **Evaluation of Phage Therapy in the Treatment of Staphylococcus Aureus-Induced Mastitis in Mice.** *Folia Microbiol (Praha)* **2020**, *65*, 339–351, doi:10.1007/s12223-019-00729-9.

58. KWAK, H.; KIM, J.; RYU, S.; BAI, J. **Characterization of KMSP1, a Newly Isolated Virulent Bacteriophage Infecting Staphylococcus Aureus, and Its Application to Dairy Products.** *Int J Food Microbiol* **2023**, *390*, 110119, doi:10.1016/j.ijfoodmicro.2023.110119.

59. LABRIE, S.J.; SAMSON, J.E.; MOINEAU, S. **Bacteriophage Resistance Mechanisms.** *Nat Rev Microbiol* 2010, *8*, 317–327.

60. HYMAN, P.; ABEDON, S.T. **Bacteriophage Host Range and Bacterial Resistance.** In; 2010; pp. 217–248.

61. KIM, M.; RYU, S. **Spontaneous and Transient Defence against Bacteriophage by Phase-variable Glucosylation of <scp>O</Scp> -antigen in *<scp>S</Scp> Almonella Enterica* Serovar <scp>T</Scp> Yphimurium**. *Mol Microbiol* **2012**, *86*, 411–425, doi:10.1111/j.1365-2958.2012.08202.x.

62. MOLLER, A.G.; LINDSAY, J.A.; READ, T.D. **Determinants of Phage Host Range in *Staphylococcus* Species.** *Appl Environ Microbiol* **2019**, *85*, doi:10.1128/AEM.00209-19.

63. JURADO, A.; FERNÁNDEZ, L.; RODRÍGUEZ, A.; GARCÍA, P. **Understanding the Mechanisms That Drive Phage Resistance in Staphylococci to Prevent Phage Therapy Failure.** *Viruses* **2022**, *14*, 1061, doi:10.3390/v14051061.

64. AZAM, A.H.; HOSHIGA, F.; TAKEUCHI, I.; MIYANAGA, K.; TANJI, Y. **Analysis of Phage Resistance in Staphylococcus Aureus SA003 Reveals Different Binding Mechanisms for the Closely Related Twort-like Phages ϕSA012 and ϕSA039.** *Appl Microbiol Biotechnol* **2018**, *102*, 8963–8977, doi:10.1007/s00253-018-9269-x.

65. ROUSSET, F.; CUI, L.; SIOUVE, E.; BECAVIN, C.; DEPARDIEU, F.; BIKARD, D. **Genome-Wide CRISPR-DCas9 Screens in E. Coli Identify Essential Genes and Phage Host Factors.** *PLoS Genet* **2018**, *14*, e1007749, doi:10.1371/journal.pgen.1007749.

CHAPTER 1

Isolation and characterization of the polyvalent enterobacteria-infecting phage UFVCit2 with potential for biocontrol applications

ABSTRACT

Salmonella enterica is a major foodborne pathogen globally, often associated with poultry and fresh produce. The rising prevalence of multidrug-resistant strains and the limited efficacy of conventional decontamination methods highlight the need for alternative, targeted strategies. Bacteriophages have emerged as promising biocontrol agents due to their specificity, safety, and potential for direct application in food systems. In this study, we isolated and characterized the polyvalent lytic phage UFVCit2 and evaluated its effectiveness against *S. enterica* in two food matrices: chicken meat and lettuce. UFVCit2 belongs to the *Tequintavirus* genus and showed lytic activity against *Citrobacter freundii*, *Shigella flexneri*, and different *S. enterica* serovars. Genomic analysis confirmed the absence of virulence, antibiotic resistance, or lysogeny-related genes, supporting its classification as genetically safe. The phage remained stable across a broad range of pH values and temperatures. In biocontrol assays, UFVCit2 significantly reduced *S. enterica* serovar Enteritidis counts on lettuce at room temperature by 1.83, 1.84, and 1.55 $\log_{10}$ CFU/mL after 1, 2, and 24 hours, respectively. In refrigerated chicken meat (4 °C), reductions of 0.79, 0.84, 0.76, and 0.69 $\log_{10}$ CFU/mL were observed at 1, 6, 24, and 48 hours post-treatment, respectively. Phylogenetic and protein identity analyses suggest that UFVCit2 likely targets the outer membrane receptor FhuA, similarly to phage T5. Future studies should aim to optimize MOI and cocktail formulations to improve host range and efficacy, as well as assess phage stability across different food matrices. Taken together, these findings support UFVCit2 as a promising candidate for the development of phage-based interventions to enhance food safety.

Keywords: *Salmonella*; *Citrobacter*; *Shigella*; *Tequintavirus*; Biocontrol; Food safety

1. INTRODUÇÃO

Non-typhoidal *Salmonella* (NTS) is one of the leading causes of foodborne illnesses worldwide, responsible for millions of cases of gastrointestinal infection each year [1]. Globally, it is estimated that over 90 million cases of human salmonellosis occur annually, with approximately 155,000 deaths attributed to this [2]. In Brazil, *Salmonella* has consistently ranked among the most frequently identified etiological agents in foodborne outbreaks [3]. Although NTS infections usually cause mild, short-duration illness with low fatality, individuals with risk factors such as malnutrition, age extremes, HIV, malaria, or sickle-cell disease are more susceptible to invasive disease [4]. A growing concern is the emergence of multidrug-resistant (MDR) *Salmonella* strains, driven by the widespread and often indiscriminate use of antibiotics in both human and veterinary settings [1]. This selective pressure has led to resistant serotypes that circulate in the food chain, reducing the effectiveness of conventional therapies and complicating epidemiological control efforts [1,5].

The genus *Salmonella* belongs to the Enterobacteriaceae family and comprises two recognized species: *Salmonella enterica* and *Salmonella bongori*. The vast majority of human and animal infections are caused by *S. enterica*, which is further divided into six subspecies - *enterica, arizonae, diarizonae, salamae, houtenae,* and *indica* - and over 2,600 serovars [6]. Among them, serovars such *Salmonella enterica* subsp. *enterica* serovar Enteritidis (*S.* Enteritidis) and *Salmonella enterica* subsp. *enterica* serovar Typhimurium (*S.* Typhimurium) are most frequently associated with foodborne outbreaks worldwide [7]. These bacteria are facultative intracellular pathogens commonly found in the gastrointestinal tracts of animals, particularly poultry, swine, and cattle, which serve as reservoirs and vehicles of transmission. Environmental sources such as water, soil, and food processing surfaces can also harbor the pathogen, contributing to cross-contamination along the food production chain [7–9].

Contamination can occur at multiple stages throughout the food production chain, including animal farming, slaughter, processing, transportation, retail, and even during food handling and preparation by consumers. Poultry meat—particularly chicken—is one of the most common sources of *Salmonella* contamination [10,11]. To mitigate its spread, several control strategies are employed, including good agricultural and manufacturing practices, microbiological monitoring, cleaning and disinfection

protocols, and hazard analysis and critical control point (HACCP) systems [12,13]. In Brazil, microbiological criteria for food safety are established by the Brazilian Health Regulatory Agency (ANVISA) through Normative Instruction No. 161/2022, which mandates the absence of *Salmonella* in all food products [14,15]. Similar regulations exist in other countries, such as the United States and the European Union [16,17]. However, despite standard sanitation efforts, *Salmonella* remains difficult to eliminate and persist in poultry production systems [10].

Therefore, the control of *Salmonella* in food matrices is of fundamental importance and must be improved in order to reduce the risk of this pathogen reaching humans [8]. Although there are different products and conventional methods for controlling food pathogens, decontaminating *Salmonella* in food still presents challenges. Irradiation, for example, a very effective and widely used physical method, can lead to lipid oxidation, changes in texture, color and odor, and loss of nutrients from food [18,19]. Chlorine, one of the most common sanitizers, can have some negative effects on human health, such as the formation of carcinogenic by-products [20]. Furthermore, extensive use of chlorine can induce the development of bacterial resistance to this substance, which will reduce its effectiveness in subsequent applications [21,22]. Comparably, the extensive and inappropriate use of antibiotics in farm animals has resulted in the increasingly frequent isolation of multidrug-resistant *Salmonella* from animals, food, and clinical samples [23–25]. Therefore, new antimicrobial agents have become increasingly necessary and urgent to control this pathogen [26,27].

In light of the growing challenge posed by antimicrobial resistance and the limitations of conventional sanitation methods, bacteriophage-based biocontrol has emerged as a promising alternative for food safety applications. Bacteriophages (phages) are viruses that infect and lyse specific bacterial hosts without disrupting the beneficial microbiota or posing a threat to human or animal health [28,29]. In the food industry, phage applications have focused primarily on two strategies: oral administration to reduce *Salmonella* colonization in the gastrointestinal tract of poultry, and surface disinfection of food products and processing equipment during post-harvest stages [30,31]. These strategies can prevent cross-contamination of the final product and thus provide a significant reduction in the concentration of these bacteria in poultry products [32].

Phages offer several advantages over traditional antimicrobials, including high specificity, self-amplification at the site of infection, and compatibility with direct application on food surfaces or in complex food matrices [28,33,34]. Importantly, their use has been shown not to alter the visual, textural, or sensory properties of treated foods, making them suitable candidates for both biocontrol of foodborne pathogens and biopreservation strategies aimed at extending shelf life [35–37]. In addition, a broad host range makes phages particularly appealing for industrial use, as polyvalent phages can expand the spectrum of bacterial targets in phage formulations and allow propagation in non-pathogenic strains, thereby minimizing the risk of cross-contamination with the target pathogen during production [34,39]. Numerous studies have demonstrated the efficacy of phage-based interventions in reducing *Salmonella* contamination across a variety of food products. Commercial formulations such as SalmoFresh™ and Salmonelex™ have proven effective in meats, vegetables, and eggs, highlighting their potential as practical tools in food safety management [33,38].

In this context, this chapter aimed to isolate and characterize a lytic bacteriophage with activity against *Salmonella enterica*, evaluating its biological, genomic, and physicochemical properties to determine its potential for biocontrol applications in food systems. Specifically, we assessed the phage's host range within the *Enterobacteriaceae* family, performed genomic analyses to ensure the absence of undesired genes related to lysogeny, antibiotic resistance, or virulence, and evaluated its stability under different pH and temperature conditions. Furthermore, we tested its antimicrobial efficacy in two relevant food models—chicken meat and lettuce—artificially contaminated with *S. enterica*. The findings presented here contribute to the growing body of knowledge on phage-based biocontrol strategies for enhancing food safety.

2. MATERIALS AND METHODS

2.1 Bacterial strains and growth conditions

Citrobacter freundii ATCC 8090 was used as the isolation host for phage UFVCit2. All bacterial strains used in this study are listed in Table 1 and were employed to investigate the host range of the phage. *Escherichia coli* strains were kindly provided by Dr. Maria Aparecida Moreira, Laboratório de Doenças Bacterianas of the Universidade Federal de Viçosa (UFV), Viçosa, Brazil. *Serratia marcescens* was kindly

provided by Dr. Maria Cristina Vanetti, Laboratório de Microbiologia Industrial, UFV. Some of the of the *Salmonella enterica* subs. *enterica* strains were isolated from mesenteric lymph nodes of pigs and kindly provided by Dr. Ricardo Yamatogi, Departamento de Medicina Veterinária, UFV, while others were isolated from poultry farming and kindly provided by a partner company.

The strains were cultivated in Luria-Bertani (LB) broth (10 g/L of $NaCl_2$, 10 g/L of peptone and 5 g/L of yeast extract) at a temperature of 37 °C. XLD agar (Kasvi) was used to identify and differentiate *Salmonella* in food tests. The optical density (OD) of the cultures was measured on a spectrophotometer at a wavelength of 600 nm (OD600) to infer the phase of bacterial growth.

2.2 Phage isolation and propagation

The phage used in this study, named *Citrobacter* phage UFVCit2, was isolated from urban sewage samples collected in the city of Viçosa (Minas Gerais, Brazil). For the isolation, the Twest and Kropinski (2009) [40] enrichment protocol was carried out. Briefly, the samples were centrifuged at 10,000 ×g and 4 °C for 10 minutes and the supernatant was filtered through a 0.22 µm PES membrane (Millipore, Billerica, MA, USA). Then, 5 mL of sterile double-strength LB broth plus 2 mM $CaCl_2$ (0.22 g/L) was inoculated with 0.1 mL of a *C. freundii* culture (Table 1) in logarithmic growth phase (OD_{600} ~ 0.5) and mixed with 5 mL of the filtered sewage sample. The mixture was incubated at 37 ºC and 100 rpm for approximately 24 hours. After that, the mixture was centrifuged at 10,000 ×g and 4 °C for 10 minutes and the supernatant (lysate) was filtered (0.22 µm membrane). The lysate was then subjected to the double-layer agar (DLA) technique [41,42], and incubated overnight.

Among the resulting lysis plates, one plaque was selected, excised, and subjected to the double-layer agar method for further propagation. This procedure—plaque picking followed by re-plating—was repeated at least three times to ensure the isolation of a single, clonal phage population. The purified phage was then propagated in LB broth supplemented with 2 mM $CaCl_2$, following the protocol described by Sambrook *et al*. (2001) [43], titrated as previously reported [42], and stored at 4 °C. For experiments involving *S.* Enteritidis, the phage was also propagated using this bacterial host.

2.3 Host range

The ability of phage UFVCit2 to infect different bacterial strains was initially assessed by spotting 10 µL of phage suspension onto the surface of double-layer agar plates previously inoculated with the test bacteria (Table 1). Plates were incubated overnight at 37 °C. Bacterial strains that exhibited clear zones or lysis plaques at the spot site were considered susceptible to the phage and were selected for subsequent efficiency of plating (EOP) assays.

To determine the host range and more accurately evaluate productive infection, the EOP was calculated as described by Khan Mirzaei *et al*. (2015) [44]. Briefly, phage lysates were serially diluted and plated on susceptible strains using the DLA technique. Plates were incubated overnight at 37 °C, and plaque-forming units per milliliter (PFU/mL) were determined the following day. The EOP was calculated by dividing the average PFU/mL obtained on the test strain by the average PFU/mL obtained on the original host strain. EOP was classified as high (≥ 0.5), moderate (0.2–0.49), low (0.001–0.199), or inefficient (≤ 0.001), following Khan Mirzaei *et al*. (2015) [44].

2.4 Morphology analysis

Phage morphology was analyzed by transmission electron microscopy (TEM). The phage suspension was first concentrated and purified by ultracentrifugation over a 20% sucrose cushion at 15,000 rpm for 7 hours at 4 °C. After centrifugation, the supernatant was discarded and the pellet was resuspended in 100 µL of ultrapure water. A 10 µL aliquot of this suspension was applied to Formvar®-coated grids. After 5 minutes, excess liquid was removed with filter paper, and the sample was negatively stained with 2% (w/v) uranyl acetate for 15 seconds. Grids were left in a desiccator for 24 hours before imaging with a Zeiss EM 109 transmission electron microscope (Zeiss, Oberkochen, Germany) at the Center for Microscopy and Microanalysis (UFV).

Capsid and tail dimensions were measured using three independent micrographs of distinct phage particles, and average values were calculated using ImageJ v1.54g software (National Institutes of Health, Bethesda, MD, USA).

2.5 One-step growth curves

One-step growth curves were performed to determine the burst size and latent period of phage UFVCit2 in *C. freundii* ATCC 8090 and *S.* Enteritidis ATCC 13076,

following the protocol described by Niu *et al*. (2012) [45]. Briefly, 10 mL of host bacterial culture at approximately 10^8 CFU/mL was infected with phage suspension at a multiplicity of infection (MOI) of 0.0001. The mixture was incubated at 37 °C for 10 minutes to allow phage adsorption, then centrifuged at 10,000 × g for 10 minutes to remove unadsorbed phages. The pellet containing infected cells was resuspended in 10 mL of LB broth, and a 100 µL aliquot was immediately collected to determine the initial phage titer (time zero).

The culture was incubated at 37 °C with shaking (100 rpm) for a total of 90 minutes. Samples of 100 µL were collected every 5 minutes for the first 40 minutes, and then every 10 minutes thereafter, and titrated using the DLA method. The latent period was defined as the time between adsorption and the onset of the first burst. The burst size was calculated as the ratio between the final number of phage particles and the initial count.

2.6 Multiplicity of Infection influence

To evaluate the influence of multiplicity of infection (MOI) on host bacterial growth, optical density-based growth curves were performed using 96-well polystyrene microplates. Briefly, phage UFVCit2 was diluted in SM buffer (5.8 g/L NaCl, 2.0 g/L $MgSO_4 \cdot 7H_2O$, 50 mL of 1 M Tris-HCl, 5 mL of 2% gelatin; pH 7.5), and 20 µL of the phage suspension was added to 180 µL of bacterial culture in early exponential phase (OD_{600} = 0.1, approximately 1.5 × 10^7 CFU/mL) in LB medium, to achieve final MOIs of 0.1, 1, and 10. Control wells received 20 µL of SM buffer instead of phage. Microplates were incubated at 37 °C in a Multiskan™ GO spectrophotometer (Thermo Scientific, USA), and bacterial growth (OD_{600}) was recorded every 15 minutes over a 21-hour period.

2.7 Thermal and pH stability

Stability assays were conducted to assess the potential application of phage UFVCit2 under different food processing and storage scenarios. The phage was evaluated for pH and thermal stability following the protocol described by Sváb *et al*. (2018) [46], with minor modifications. In all cases, the final phage concentration was adjusted to 1 × 10^7 PFU/mL. Immediately after treatment, phage preparations were

diluted in SM buffer, plated using the DLA method, and titrated. All assays were performed in triplicate.

For pH stability testing, 10 µL of phage suspension was added to 990 µL of LB broth adjusted to various pH values (ranging from pH 2 to pH 12), and incubated at 25 °C for 2 hours. LB broth at pH 7 served as the control. For thermal stability, phage suspensions in LB broth (pH 7.0) were incubated for 48 h at -20 ºC, for 2 hours at 25, 40, 50, 60, and 70 °C, and for 5 minutes at 80 and 90 °C. A non-heated aliquot kept at 4 °C was used as the control.

2.8 *In Vitro* phage challenge at low temperature

A bacterial culture of *S.* Enteritidis at OD_{600} = 0.4 (approximately 5 × 10^8 CFU/mL) was diluted in LB broth to a final concentration of 1 × 10^5 CFU/mL. Subsequently, 100 µL of the UFVCit2 phage lysate was added to 9.9 mL of this bacterial suspension to achieve multiplicities of infection (MOIs) of 100 and 1000. Control tubes received 100 µL of SM buffer instead of phage. All tubes were incubated at 4 °C, and culture samples were collected at 0, 1, 3, 5, 24, and 48 hours post-inoculation. At each time point, aliquots were serially diluted in phosphate-buffered saline (PBS; 137 mM NaCl, 2.7 mM KCl, 10 mM Na_2HPO_4, 1.8 mM KH_2PO_4; pH 7.4), plated on LB agar using the spread plate method, and incubated overnight at 37 °C. Bacterial counts (CFU/mL) were determined the following day.

2.9 Biocontrol of *S.* Enteritidis in food

2.9.1. Biocontrol in fresh lettuce

This assay was based on the methodology described by Spricigo *et al*. (2013) [47], with modifications. *S.* Enteritidis was grown in LB broth until mid-log phase (OD_{600} = 0.4, approximately 5 × 10^8 CFU/mL). The culture was centrifuged at 9000 rpm for 15 minutes, the supernatant was discarded, and the bacterial pellet was resuspended in 10 mL of 0.9% NaCl sterile solution. The suspension was then diluted to a final concentration of 1 × 10^5 CFU/mL. Phage UFVCit2 was diluted in 0.9% NaCl to a final titer of 1 × 10^8 PFU/mL. Fresh lettuce was washed under running tap water and surface-disinfected by immersion in a sodium hypochlorite solution (200 ppm) for 15 minutes. The leaves were then rinsed with sterile distilled water to remove residual chlorine.

To contaminate the surface with *S.* Enteritidis, the lettuce leaves were immersed in the bacterial suspension prepared before for 5 minutes at room temperature, then transferred to sterile Petri dishes and allowed to dry under aseptic conditions for approximately 15 minutes. The dried leaves were cut into smaller sections, and 5 g was weighed into each Petri dish to serve as an individual replicate. Samples were then immersed in 10 mL of the phage solution, and incubated for 10 minutes. Control samples were treated similarly but received phage-free 0.9% NaCl instead. A negative control group, consisting of lettuce leaves that were not inoculated with either bacteria or phage, was included to confirm the effectiveness of the hypochlorite disinfection procedure.

After treatment, the leaves were transferred to new sterile Petri dishes and left to dry for an additional 15 minutes. Once dried, the samples were stored at room temperature (~25 ºC) in sterile tubes. Samples were collected at 0, 1, 2, and 24 hours post-treatment. To recover bacteria, 2 mL of 0.9% NaCl was added to each sample and gently agitated for 5 minutes to dislodge bacterial cells. The resulting suspension was plated on XLD agar using the spread plate method and incubated at 37 °C overnight. The number of viable *Salmonella* cells (CFU/mL) was determined the following day.

2.9.2. Biocontrol in chicken meat

This assay was adapted from the methods described by Sukumaran *et al*. (2015) [38] and Pelyuntha *et al*. (2022) [48], with modifications. The preparation of *S*. Enteritidis inoculum and phage UFVCit2 solution was performed as described in the previous section (Biocontrol in fresh lettuce).

Chicken breast fillets were purchased from a local supermarket and aseptically cut into ~2 × 2 cm^2 cubes. The meat pieces were then immersed in a 50 ppm chlorine solution, prepared with autoclaved distilled water, for 5 minutes to reduce background microorganisms. To remove residual chlorine, each meat piece was sequentially transferred through three separate beakers containing sterile distilled water, remaining immersed for 5 minutes in each. Excess water was removed, and the meat pieces were air-dried in the biological safety cabinet for 15 minutes at room temperature.

Each side of the disinfected meat cube received 50 µL of the bacterial suspension (100 µL total per piece) and was left undisturbed for 5 minutes to allow bacterial

attachment. Excess liquid was removed, and the contaminated pieces were transferred to new Petri dishes and left to dry for an additional 15 minutes. Then, 50 µL of the phage suspension was surface-applied to each side (100 µL total per piece). Control groups received the same volume of sterile saline instead of phage solution. After 10 minutes of phage exposure, each meat piece was placed into an individual sterile tube and stored at 4 °C.

Samples were collected at 0, 1, 6, 24, 48, and 72 hours post-treatment. To recover bacteria, 2 mL of PBS was added to each tube and samples were agitated for 5 minutes to release attached bacterial cells. The resulting liquid was serially diluted and plated on XLD agar using the spread plate method. Plates were incubated at 37 °C for 24 hours, and typical black-centered *Salmonella* colonies were enumerated. A negative control group, consisting of meat pieces not inoculated with either bacteria or phage, was included to confirm the absence of *Salmonella* after disinfection with the 50 ppm chlorine solution.

2.10. Genomic characterization and phylogenomic analysis

2.10.1. Phage DNA isolation and sequencing

Phage genomic DNA was extracted using the PCI/SDS protocol available at PhagesDB (PCI/SDS DNA Extraction 2.2013, http://phagesdb.org). Briefly, 1 mL of high-titer phage lysate (≥10^9 PFU/mL) was treated with $MgCl_2$ (1 M, 12.5 µL), DNase I (2000 U/mL, 0.4 µL), and RNase A (100 mg/mL, 1 µL), followed by incubation at room temperature for 30 minutes. Subsequently, EDTA (0.5 M, 40 µL), Proteinase K (10 mg/mL, 5 µL), and SDS (10%, 50 µL) were added, and the sample was incubated at 55 °C for 1 hour. DNA was then purified through two rounds of extraction with an equal volume of phenol:chloroform:isoamyl alcohol (25:24:1), followed by gentle mixing and centrifugation at 12,000 × g for 5 minutes. The upper aqueous phase was recovered and precipitated with 95% ethanol (1 mL) and sodium acetate (3 M, 50 µL), and incubated on ice for 5 minutes. After centrifugation at 12,000 × g for 10 minutes and a wash with 70% ethanol, the DNA pellet was air-dried and resuspended in nuclease-free water or TE buffer. DNA quality was assessed by spectrophotometry and agarose gel electrophoresis.

Sequencing was performed on the Illumina NovaSeq 6000 platform by Novogene Bioinformatics Technology Co., Ltd. (Davis, CA, USA). Raw read quality was assessed

with FastQC (version 0.11.9; https://github.com/s-andrews/FastQC). Adapter sequences were removed using TrimGalore (version 0.6.7; default settings), and further trimming was conducted with Trimmomatic (version 0.36), using the parameters HEADCROP:10, CROP:140, SLIDINGWINDOW:4:20, and MINLEN:130. High-quality reads were assembled *de novo* using SPAdes (version 3.15.4), with all odd K-mer sizes between 21 and 99. Assembly quality was assessed using Assembly-Stats (version 1.0.1), and contigs shorter than 1,000 bp were excluded. Candidate phage contigs were identified based on size and coverage, and confirmed by BLASTn alignment against the NCBI nucleotide database.

2.10.2. Genome annotation, analysis and taxonomic assessment

Prediction and initial annotation of open reading frames (ORFs) were performed using the RAST server (https://rast.nmpdr.org/rast.cgi) in May 2021. Each predicted ORF was subsequently manually curated using the BLASTp algorithm at NCBI (https://blast.ncbi.nlm.nih.gov/BlastAlign.cgi) and the InterProScan web service (https://www.ebi.ac.uk/interpro/) to generate the final consensus annotation table and to search for possible protein domains. Additional *in silico* analyses were performed to assess genomic features of interest. The presence of putative tRNA genes was evaluated using the tRNAscan-SE tool (Galaxy Version 0.4) via the Phage Galaxy server (https://phage.usegalaxy.eu/) (Lowe and Chan, 2016). Screening for antimicrobial resistance genes and virulence factors was carried out using ResFinder v4.7.2 [49–51] and VirulenceFinder v2.0.5 [52,53], both hosted at the CGE web platform (https://cge.food.dtu.dk/). The visual genomic map of UFVCit2 was generated using the Proksee platform (https://proksee.ca/) and integrated into the annotation process to support the manual curation of predicted ORFs and structural feature identification.

To identify the closest relatives and determine the taxonomic placement of phage UFVCit2, its complete genome sequence was compared against the NCBI nucleotide database using the BLASTn tool. A randomized subset of RefSeq genomes from the *Markadamsvirinae* subfamily (taxonomy ID 2732013) was retrieved from the NCBI Virus database (https://www.ncbi.nlm.nih.gov/labs/virus/vssi/#/). The genome of UFVCit2 was then added to this dataset and analyzed through the ViPTree server (https://www.genome.jp/viptree/) to construct a proteomic-based phylogenetic tree and

infer evolutionary relationships. Intergenomic similarity was assessed using the VIRIDIC web tool (http://rhea.icbm.uni-oldenburg.de/viridic/), applying ICTV thresholds of 95% and 70% to delineate species and genus boundaries, respectively.

The complete genome of UFVCit2 was deposited in the NCBI GenBank in October 2022 and is available under the accession number OP745948.1.

2.10.3. Phylogenetic analysis of RBP and Llp sequences

The amino acid sequence of the receptor-binding protein (RBP) and the superinfection exclusion protein (Llp) of phage UFVCit2, along with RBPs and Llps from *Markadamsvirinae* phages with known bacterial receptors, was aligned using MAFFT v7 at MPI Bioinformatics Toolkit (https://toolkit.tuebingen.mpg.de/tools/mafft) with the L-INS-i strategy. The phylogenetic tree was reconstructed using the Maximum Likelihood method implemented in MEGA 12. The LG model with Gamma-distributed rates among sites (LG+G) was applied, and gaps were treated with the "Use All Sites" option. Branch support was assessed by standard bootstrap analysis with 1000 replicates, and bootstrap values greater than 70% were considered indicative of strong phylogenetic support. Trees were analyzed to assess the clustering of UFVCit2 relative to phages with experimentally characterized receptors (FhuA, BtuB, or FepA), enabling inference of the most probable receptor used by UFVCit2 based on its phylogenetic proximity to functionally annotated phages.

2.11. Statistical analysis

All experiments were performed in triplicate. Statistical analyses were conducted using GraphPad Prism software, version 8.3.0 (538). Data normality was assessed using the Shapiro–Wilk test prior to statistical analysis, and appropriate tests were selected based on the results. For growth curve comparisons, multiple unpaired t tests (one per time point) were performed, with statistical significance determined using the Holm–Sidák method and an alpha level of 0.05. Each time point was analyzed independently, without assuming a consistent standard deviation (SD). For the stability assays, low-temperature infectivity tests, and food biocontrol experiments, unpaired t tests were used to compare the means between control and UFVCit2-treated groups for each condition.

3. RESULTS

3.1 Phage host range and morphology

The phage used in this study was isolated from *C. freundii* ATCC 8090 and named *Citrobacter* phage vB_CfrD-UFVCit2 (hereafter referred to as UFVCit2). The phage was able to reach high titers, exceeding 10^9 PFU/mL, within a few hours (~7 h) when propagated in this host, producing small (~1 mm), translucent plaques on LB agar. The host range of UFVCit2 is presented in Table 1. Efficiency of plating (EOP) assays were performed only for strains that yielded positive results, i.e., growth inhibition (+) in spot tests. The results showed that UFVCit2 was able to infect representatives of three genera within the *Enterobacteriaceae* family. In addition to its original isolation host (*C. freundii*), UFVCit2 successfully infected different serovars of *S. enterica* (*S.* Enteritidis, *S.* Typhimurium, *S.* 1,4,[5],12:-:1,2, and *S.* Panama), as well as a strain of *Shigella flexneri* (ATCC 12022). Highly productive infections (EOP ≥ 0.5) were observed in *S.* Enteritidis, *S.* Typhimurium, and *S. flexneri*. In contrast, infection in *S.* Panama was classified as moderately productive (EOP 0.2 to <0.5), and infection in *S.* 1,4,[5],12:-:1,2 as low productivity (EOP 0.001 to <0.2).

Although UFVCit2 caused visible growth inhibition in some *E. coli* and *Salmonella* strains in the spot test, no lysis plaques were detected by double-layer agar assay (DLA), suggesting that the observed effects may be attributed to mechanisms other than productive infection, such as lysis from without. Future assays quantifying the phage titer (PFU/mL) in these cultures should be performed to determine whether phage replication is occurring.

Microscopy analysis revealed that phage UFVCit2 has an isometric head measuring 55 nm in diameter and a long, thin, flexible tail approximately 200 nm in length (Figure 1A). One-step growth curves were performed using the original isolation host (*C. freundii*) and the host with the highest efficiency of plating (*S. Enteritidis*). The results showed that both the latency period and burst size of UFVCit2 varied between the two hosts: the latency period was 30 minutes in *C. freundii* (Figure 1B) and 25 minutes in *S. Enteritidis* (Figure 1C), while the burst size was 434 PFU/cell in *C. freundii* and 100 PFU/cell in *S. Enteritidis*.

Table 1. Host range of phage UFVCit2. Bacterial strains were tested by spot assay for susceptibility to infection. Efficiency of plating (EOP) was determined only for strains that produced visible growth inhibition in spot tests. EOP values were categorized as follows: high (≥0.5), moderate (0.2 to <0.5), low (0.001 to <0.2), and no plaque formation (0). "+" indicates visible growth inhibition in spot assay; "-" indicates no visible alterations.

Strain	Source	Spot-test	Average title (PFU/mL)	EOP
C. freundii ATCC 8090	TC	+	$5,9 \times 10^8$	Host
S. flexneri ATCC 12022	TC	+	1×10^9	1,7
S. Enteritidis ATCC 13076	TC	+	$1,5 \times 10^9$	2,5
S. Typhimurium	Swine	+	$3,0 \times 10^8$	0,5
S. 1,4,[5],1:-:1,2	Swine	+	$1,6 \times 10^6$	0,002
S. Panama	Swine	+	$2,8 \times 10^8$	0,47
S. Infantis	Swine	+	0	0
S. Derby	Swine	+	0	0
S. Cerro	Swine	-		
S. Heidelberg 63623	Poultry (BC)	+	0	0
S. Heidelberg 65499	Poultry (SH)	+	0	0
S. Minnesota 64303	Poultry (BC)	-		
S. Minnesota 65374	Poultry (BB)	-		
*S.*Mbandaka 64166	Poultry (FF)	-		
S. Mbandaka 64188	Poultry (FF)	-		
E. coli ATCC 29214	TC	+	0	0
E. coli K12	TC	+	0	0
E. coli 304	HH	+	0	0
E. coli 30	BM	+	0	0
E. coli 4	BM	-		
E. coli 20	BM	-		
E. coli CDC0111ab	TC	-		
E. cloacae ATCC 13047	TC	-		
S. marcescens MIND01	Environmental	-		

TC = Type collection; Poultry: BC = Broiler chicken, BB = broiler breeder, FM = feed mill, SH = slaughterhouse; BM = Bovine mastitis; HH = Human hospital.

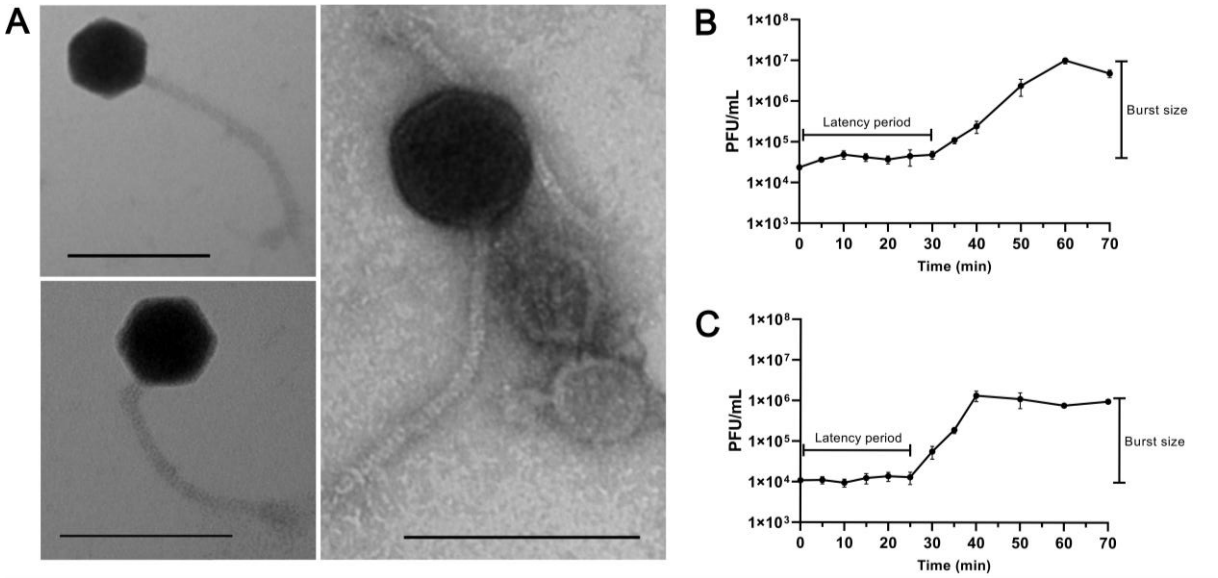

Figure 1. Transmission electron microscopy (TEM) image of phage UFVCit2, with the scale bar representing 100 µm (A). One-step growth curves of the phage in its original isolation host *Citrobacter freundii* (B) and in the host exhibiting the highest efficiency of plating (EOP), *Salmonella Enteritidis* (C).

3.2 Genome analysis and taxonomic assessment

3.2.1 Genome analysis

The UFVCit2 phage has a double-stranded DNA genome of 111,610 bp with a G+C content of 39.1%. A total of 146 putative ORFs were identified, of which 58 were predicted to encode functional proteins, while 88 were annotated as hypothetical proteins of unknown function. Additionally, 21 tRNA-encoding genes were found, with one remaining unclassified (Table 2). Although the genome topology (linear or circular) was not experimentally determined, the genome map was represented as circular (Figure 2) for visualization purposes. Functional ORFs were grouped into seven categories based on their predicted roles: DNA, RNA, and nucleotide metabolism; auxiliary metabolic genes and host takeover; head and packaging; connector; tail; lysis; and other functions. The genomic map also depicts tRNA genes, GC content, and GC skew profiles.

Table 2. Transfer RNA (tRNA) genes predicted in the genome of phage UFVCit2 using tRNAscan-SE. The table lists the corresponding amino acid, anticodon, genomic position, and prediction score.

tRNA	Anti Codon	Begin	End	Cove Score
Undet	-	41738	41667	21.25
Arg	TCT	41164	41093	45.87
Ser	GCT	37453	37368	60.60
Met	CAT	37358	37284	40.78
Leu	TAA	36774	36701	60.37
Tyr	GTA	35760	35683	46.56
Glu	TTC	35130	35059	55.65
Cys	GCA	34531	34459	46.27
Asn	GTT	34303	34224	56.07
Lys	CTT	33663	33591	70.94
Pro	TGG	32597	32523	60.52
Met	CAT	32513	32439	36.75
Lys	TTT	32246	32171	62.14
Ala	TGC	31882	31811	56.52
Leu	TAG	31802	31729	50.60
Ser	TGA	31516	31430	22.77
Gln	CTG	30002	29930	61.83
Gln	TTG	29920	29846	62.85
Thr	TGT	29325	29242	65.44
Ile	GAT	28488	28415	68.17
Met	CAT	28315	28243	51.74

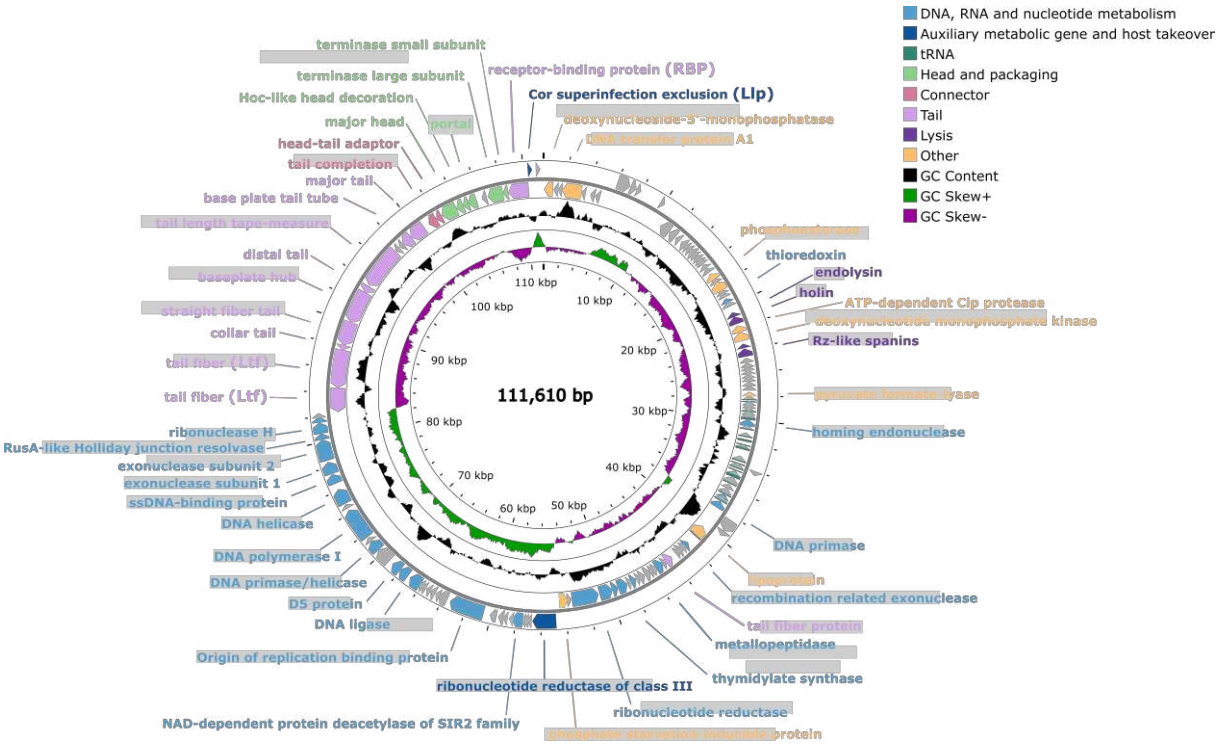

Figure 2. Circular genome map of phage UFVCit2 generated using Proksee, based on functional annotation performed with RAST. Each gene is color-coded according to its predicted functional module. Genes encoding hypothetical proteins with unknown function are shown in gray.

Among the structural genes, proteins involved in host recognition and adsorption—key determinants of host range—were identified. A receptor-binding protein (RBP), commonly responsible for binding to specific bacterial receptors [54], was predicted in ORF 144. ORF 145 encodes an *Llp*-type receptor-blocking protein, which has been associated with superinfection exclusion mechanisms in T5-like phages [55,56]. Two L-shaped tail fiber proteins (Ltf), known to participate in initial adhesion and potential host range expansion [57,58], were annotated in ORFs 124 and 125. No genes related to antibiotic resistance, virulence factors, or lysogeny were detected. A complete list of all predicted ORFs, including their annotations and genomic positions, can be accessed in the GenBank entry for UFVCit2 (accession number: OP745948.1).

3.2.2 Taxonomic assessment and phylogenetics

The BLAST search revealed that the genome of phage UFVCit2 shares high sequence identity with *Salmonella* phage oldekolle (query cover 90%; identity 96.86%; accession number NC_048865.1) and *Salmonella* phage S131 (query cover 92%; identity 96.72%; accession number NC_048009.1 both members of the genus

Tequintavirus (order *Caudovirales*, family *Demerecviridae*, subfamily *Markadamsvirinae*). In the proteomic tree based on genome-wide sequence similarities among members of the *Markadamsvirinae* subfamily, phage UFVCit2 clustered with other phages of the *Tequintavirus* genus (Figure 3), revealing close similarity relationships with members of this group. Consistent with the BLAST and proteomic tree analyses, VIRIDIC analysis (Figure 4) also showed high similarity with *Tequintavirus* phages, with the highest similarity scores obtained for phage NBSal003 (RefSeq accession: NC_048856.1, similarity score: 89.6), *Salmonella* phage S131 (RefSeq accession: NC_048009, similarity score: 89.4), and *Salmonella* phage oldekolle (RefSeq accession: NC_048865.1, similarity score: 88.0). Thus, our phage can be considered a representative of a novel species within the genus *Tequintavirus*.

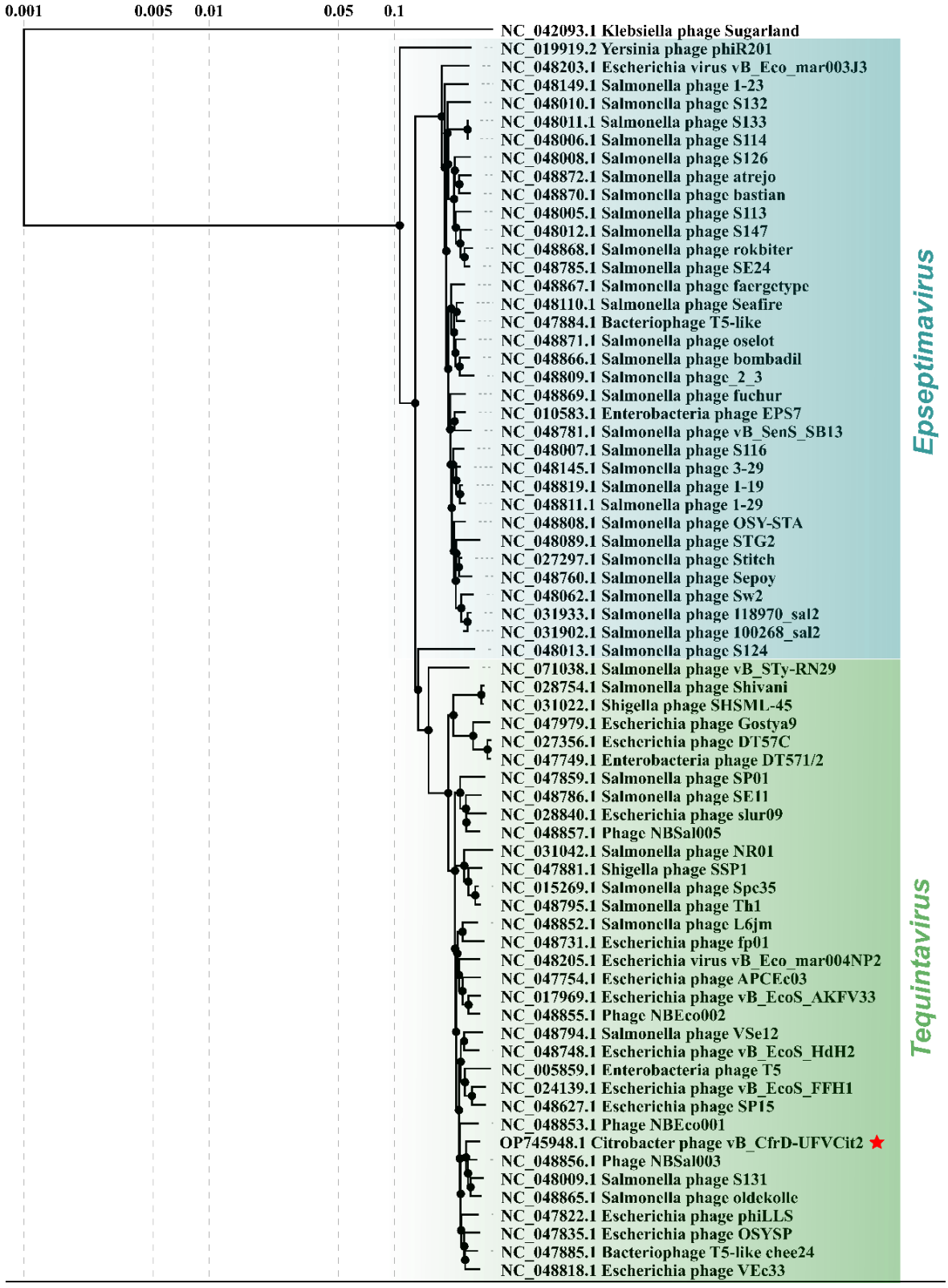

Figure 3. Genome-wide proteomic tree generated using VipTree for phage UFVCit2 (indicated by a red star) and reference genomes (RefSeq) of *Markadamsvirinae* subfamily members. The tree was constructed based on genome-wide amino acid sequence similarities calculated with tBLASTx, using the ViPTree server's default settings.

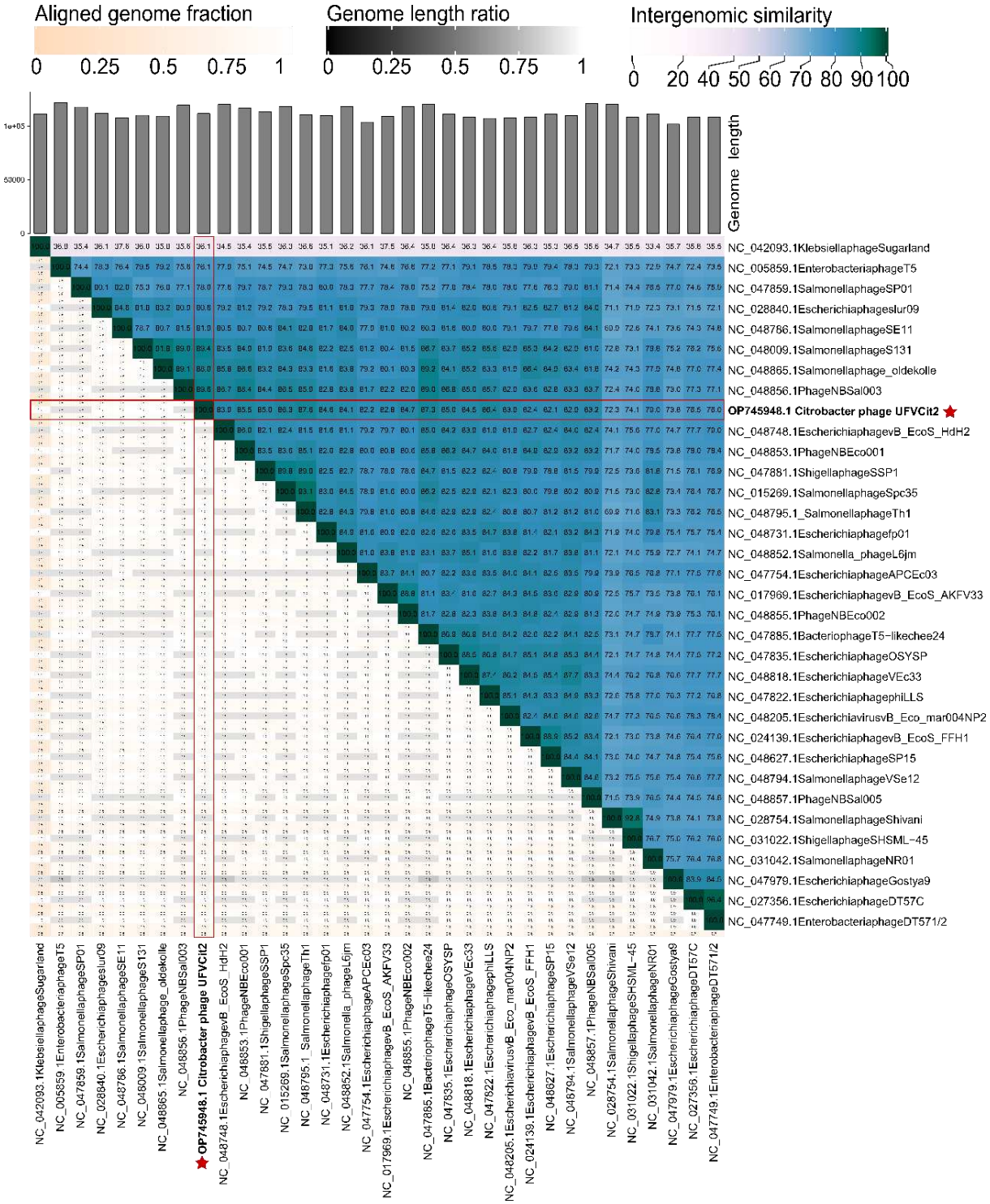

Figura 4. Intergenomic similarity matrix generated using VIRIDIC for phage UFVCit2 (indicated by a red star) and reference genomes (RefSeq) of *Markadamsvirinae* subfamily members. Pairwise nucleotide identity was calculated using BLASTn, and results are presented as a heatmap where darker shades indicate higher similarity.

The Clinker analysis of the complete genome (Figure 5) of UFVCit2, alongside phages from the *Markadamsvirinae* subfamily with known receptor usage was performed to examine genome organization and globally aligned gene clusters. The phages included in the analysis were: *Enterobacteria* phage *T5* (Accession number: NC_005859), *Salmonella* phage *Spc35* (Accession number: NC_015269), *Salmonella* phage S124 (Accession number: NC_048013).

Synteny analysis demonstrated a strong conservation of genes associated with essential biological functions, including DNA replication, virion assembly, and host lysis processes. Notably, almost all predicted structural proteins were highly homologous across the compared genomes, with the exception of host-recognition elements such as the receptor-binding protein (RBP) and the L-shaped tail fibers, which exhibited greater divergence. In contrast, regions enriched in hypothetical proteins and proteins of unknown function displayed considerable variability. These findings indicate that while core functional modules remain conserved among Tequintavirus genomes, variable regions likely represent accessory components contributing to the genomic plasticity observed among closely related *Tequintavirus* isolates [59,60].

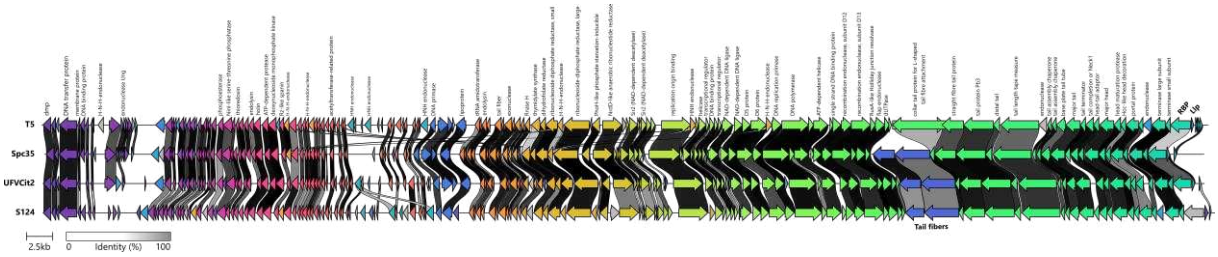

Figure 5. Genomic synteny analysis of phage UFVCit2 and reference genomes from the *Markadamsvirinae* subfamily with known receptor usage, generated using Clinker. Genes are automatically color-coded according to similarity groups. Gray shading between arrows indicates regions of amino acid similarity (threshold ≥30%). GenBank accession numbers: *Enterobacteria* phage T5 – NC_005859, *Salmonella* phage Spc35 – NC_015269, and *Salmonella* phage S124 – NC_048013.

3.2.3 Receptor inference from RBP and LIp clustering

To investigate the probable receptor recognized by UFVCit2, we first analyzed the amino acid identity between its receptor-binding protein (RBP) and those of *Markadamsvirinae* phages with known receptor usage. The RBPs of T5-like phages are typically located at the distal end of a straight tail fiber and are responsible for binding to specific outer membrane receptors. Depending on the phage, these receptors can include ferrichrome (FhuA), vitamin B12 (BtuB), or ferric enterobactin

(FepA) transporters [61–63]. In addition to receptor recognition during initial adsorption, some T5-like phages encode a small lipoprotein (Llp) expressed after genome injection, which binds to the receptor to prevent superinfection and protect progeny phages from being inactivated by infected cells [55,56].

The RBP of UFVCit2 exhibited 96.9% percent identity with the RBP of phage T5, which recognizes FhuA as the bacterial receptor, but only 30.8% identity with the RBP of phage S131, which has also been proposed to target the same receptor [58]. With BtuB-binding phages S126 [58], Spc35 [64], Bf23 [60,61] e DT57C [65], the RBP of UFVCit2 showed 67.0%, 71.8%, 66.7%, and 73.2% identity, respectively. In contrast, percent identity with the RBPs of phages H8 and S124, which recognize FepA [58,62], was only 27.7%.

To further explore these relationships, phylogenetic trees were constructed based on the amino acid sequences of the RBP and the superinfection exclusion protein Llp. In the RBP-based phylogeny (Figure 6A), phages grouped largely according to their experimentally confirmed receptor. BtuB-binding phages—S114, S133, S126, S116, Bf23, Spc35, and DT57C—formed a well-supported clade. Despite being a BtuB-binding phage, DT57C was positioned closer to the FhuA-binding group. UFVCit2 clustered strongly with phage T5 (bootstrap 99%), which uses FhuA as its receptor, supporting the hypothesis that UFVCit2 also recognizes FhuA. In contrast, phages H8 and S124 (FepA-binding) and phage S131—previously proposed to use FhuA—formed separate clades, with S124 and H8 grouping together (bootstrap 100%), and S131 remaining isolated.

The phylogenetic tree based on Llp sequences (Figure 6B) revealed a partially different topology. In this tree, UFVCit2 grouped with the BtuB-binding phages Spc35 and Bf23 (bootstrap values of 79% and 80%, respectively), separating it from the T5/S131 clade (bootstrap 96%), with which it had clustered in the RBP tree. The BtuB-binding phages S114, S133, S126, and S116 formed a well-supported clade (bootstrap values ≥95%), while DT57C and S124 grouped in a closely related branch (bootstrap 99%). Notably, phages T5 and S131, both associated with FhuA recognition, formed a distinct clade (bootstrap 96%), whereas phage H8, which uses FepA as its receptor, was positioned as a distant outgroup.

Together, these results reinforce the inference that UFVCit2 utilizes FhuA as its primary receptor, based on both its close phylogenetic relationship and high sequence identity to T5. The divergence observed in the Llp phylogeny, however, suggest

possible divergence in Llp evolution among *Markadamsvirinae* members and may reflect adaptation to specific receptor-blocking mechanisms across different hosts.

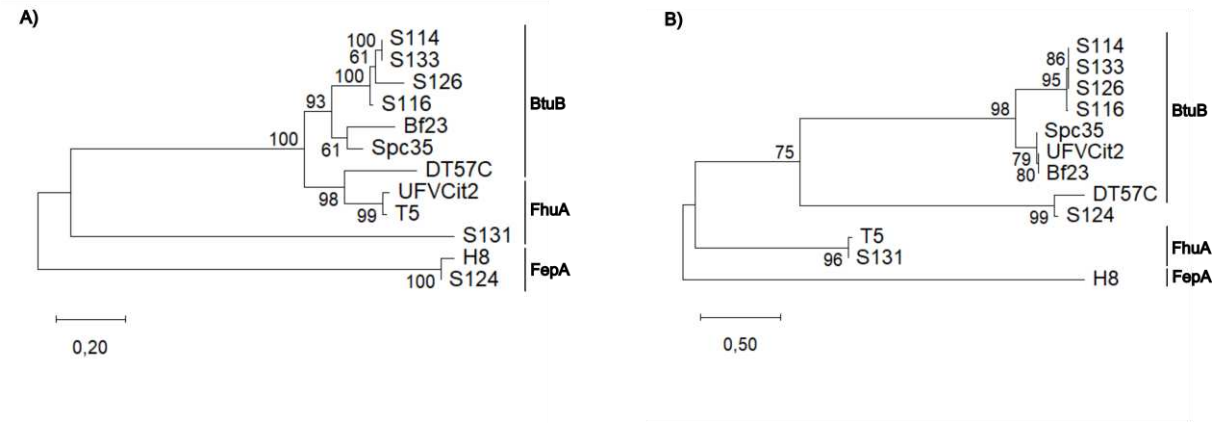

Figure 6. Maximum Likelihood phylogenetic tree based on A) receptor-binding protein (RBP) and B) superinfection exclusion protein (Llp) sequences of UFVCit2 and reference *Markadamsvirinae* phages with experimentally characterized or presumed host receptors. The tree was constructed using MEGA 12 with 1000 bootstrap replicates. Bootstrap values ≥50% are shown. The scale bar represents amino acid substitutions per site. The corresponding GenBank accession numbers were as follows: S114 (NC_048006), S133 (NC_048011), S126 (NC_048008), S116 (NC_048007), Bf23 (OR083247), Spc35 (NC_015269), DT57C (NC_027356), T5 (NC_005859), S131 (NC_048009), H8 (NC_042307), and S124 (NC_048013).

3.3 Multiplicity of Infection (MOI) influence

This and the subsequent assays were conducted using *S*. Enteritidis as a target host to explore the biocontrol potential of phage UFVCit2 against this pathogen. The growth curves of *S. Enteritidis* in the presence of phage UFVCit2 demonstrated the influence of different multiplicities of infection (MOIs) on bacterial proliferation (Figure 7). A statistically significant reduction in bacterial growth ($P < 0.05$) was observed in all phage-challenged groups compared to the phage-free control, regardless of the MOI, confirming the lytic activity of UFVCit2 throughout the 21-hour assay period.

At low MOIs (0.01 and 0.1), initial bacterial growth was detected during the first 1.5 hours of incubation, followed by a sharp decline in optical density (OD). This was succeeded by a partial regrowth phase beginning after approximately 3 hours. The growth curves stabilized around 10 hours (MOI 0.1) and 13 hours (MOI 0.01),

maintaining constant OD values until the end of the experiment. At intermediate to high MOIs (1 to 1000), bacterial growth was initially suppressed, with no increase in OD observed during the early incubation period. However, exponential growth resumed around 7 hours, after which OD values plateaued and remained relatively stable until the experiment concluded. This pattern suggests that phage UFVCit2 effectively restricted bacterial proliferation following an initial adaptation or escape phase.

Despite the early kinetic differences observed between MOIs, statistical analysis revealed no significant difference in final bacterial densities among the phage-treated groups after 21 hours. These findings underscore the complex dynamics of phage-host interactions, in which early suppression is more pronounced at higher MOIs, while long-term outcomes may be modulated by factors such as bacterial regrowth, resistance development, or variability in phage replication efficiency.

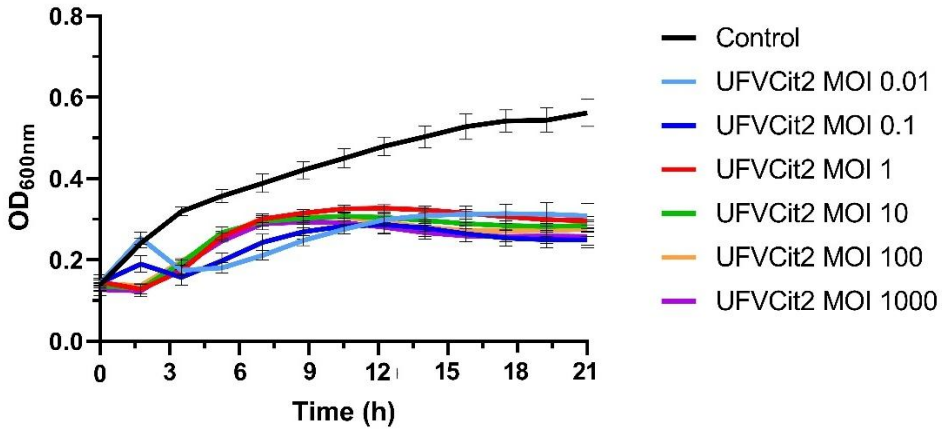

Figure 7. Bacterial growth curves of *S. Enteritidis* over 21 hours in the presence of phage UFVCit2 at different multiplicities of infection (MOIs), ranging from 0.01 to 1000. Optical density (OD_{600}) measurements were taken at regular intervals (15 minutes) to assess the impact of phage infection on bacterial growth dynamics.

3.4 Thermal and pH stability

Aiming at future applications of phage UFVCit2 for the control of *S. enterica*, stability assays were performed using *S. Enteritidis* as the host bacterium. The tests revealed that the phage was highly stable at pH values ranging from 4 to 12 (Figure 8A) and at temperatures up to 60 °C (Figure 8B). However, a reduction of 3.38 $\log_{10}$ PFU/mL was observed at pH 3, and reductions of 0.24, 0.3, 4.46 and 5.90 $\log_{10}$

PFU/mL were recorded at -20 º, 60 ºC, 70 °C and 80 °C, respectively. Complete phage inactivation occurred at pH 2 and at 90 °C.

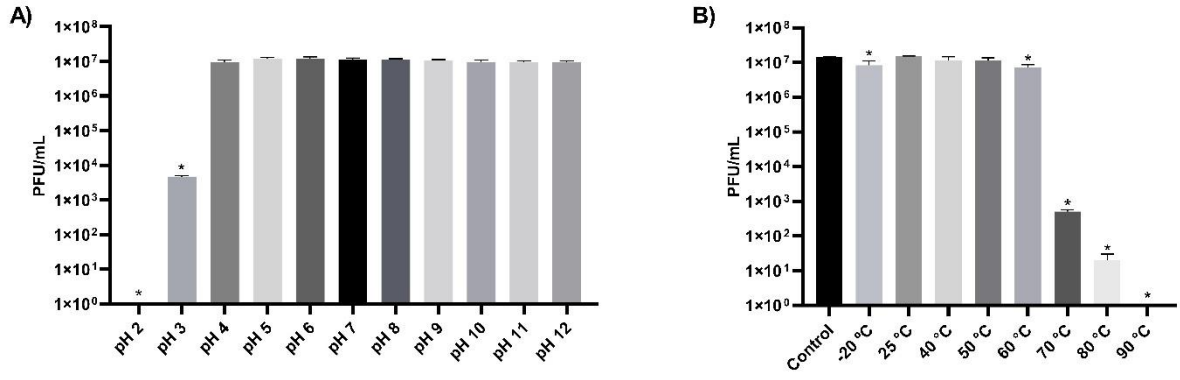

Figure 8. Stability of phage UFVCit2 under different environmental conditions. (A) pH stability assay conducted at room temperature for 1 hour across a pH range of 2 to 12; pH 7 served as the control. (B) Thermal stability assay performed at various temperatures (from 4 °C to 90 °C) for 1 hour; 4 °C was used as the control condition. Phage titers are expressed as $\log_{10}$ PFU/mL. Data represent mean values from independent experiments, with error bars indicating standard deviation. Statistically significant differences ($P < 0.05$) are indicated by asterisks (*).

3.5 In vitro phage challenge at low temperature

This assay was designed to assess whether the phage UFVCit2 is capable of lysing *S. enteritidis* at low temperatures, where bacterial replication—and consequently phage propagation—is strongly limited. To favor the possibility of "lysis from without," in which bacterial cell lysis is induced externally without requiring phage replication inside the host [66], high MOIs (100 and 1000) were used. This strategy increases the chance of multiple phages adsorbing to a single bacterium, promoting direct lysis even in non-permissive conditions for phage replication. Evaluating phage activity at 4 °C is particularly relevant for its potential application as an antibacterial or biocidal agent in refrigerated food products.

Significant bacterial reductions ($P < 0.05$) were observed for both MOIs at all evaluated time points. For MOI 100 (Figure 9A), the reductions relative to the control were 1.13, 1.05, 1.23, 1.16, and 1.07 $\log_{10}$ CFU/mL at 1, 3, 5, 24, and 48 h, respectively. For MOI 1000 (Figure 9B), more pronounced reductions were observed—2.35, 2.24, 2.25, 2.24, and 2.75 $\log_{10}$ CFU/mL at the same time points. These results

indicate that UFVCit2 can effectively reduce *Salmonella* viability under refrigeration conditions, supporting its potential use in food safety applications.

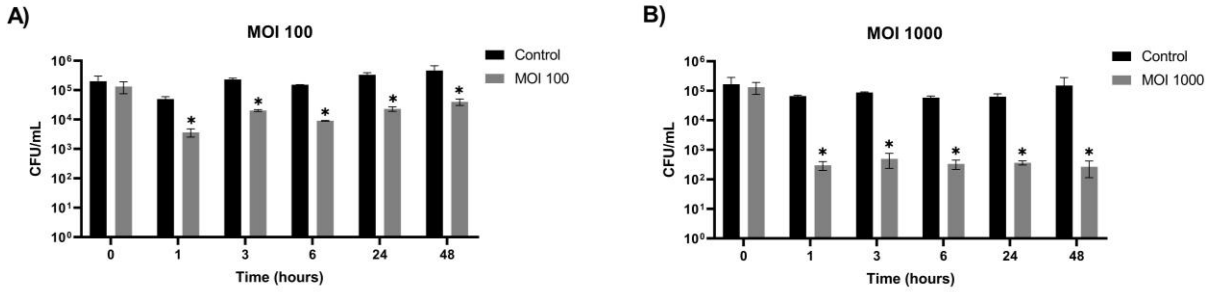

Figure 9. In vitro lytic activity of phage UFVCit2 at low temperature over a 48-hour period. The assay was performed at multiplicities of infection (MOIs) of 100 and 1000, and bacterial growth was monitored to assess phage-mediated inhibition under refrigeration conditions.

3.6 Biocontrol of *S. Enteritidis* in food

Treatment of lettuce leaves was performed at room temperature (~25 °C), which reflects typical conditions used for the storage and transport of fresh produce. The 10-minute phage immersion step was designed to simulate the common household practice of vegetable sanitization. A reduction of 1.83 $\log_{10}$ CFU/mL was observed after 1 hour of phage treatment, followed by 1.84 $\log_{10}$ at 2 hours, and 1.55 $\log_{10}$ at 24 hours, compared to the untreated control (Figure 10A). These results demonstrate that phage UFVCit2 was able to significantly reduce *S. Enteritidis* loads on lettuce surfaces over time, even as bacterial counts increased substantially in the control group.

Chicken meat samples were treated with phage UFVCit2 and subsequently stored at 4 °C for 72 hours to simulate post-processing refrigeration conditions commonly used in the poultry industry. Although phage application is still primarily experimental, this approach was designed to mimic the potential integration of bacteriophage treatment into existing chilling and storage steps in poultry processing workflows. Significant reductions in *S.* Enteritidis counts were observed in the treated group compared to the untreated control (Figure 10B). Reductions of 0.79, 0.84, 0.76, and 0.69 $\log_{10}$ CFU/mL were observed at 1, 6, 24, and 48 hours post-treatment, respectively. These results demonstrate that phage UFVCit2 was effective in maintaining a lower bacterial load during refrigerated storage, with a sustained reduction over the 48-hour period.

Negative control samples (meat pieces not inoculated with *Salmonella* or phage) confirmed the absence of *Salmonella* in the product following immersion in the 50 ppm hypochlorite solution. However, some yellow and translucent colonies were observed on XLD plates, indicating the presence of background microorganisms and suggesting that the disinfection procedure was not fully effective against other bacteria. In *Salmonella*-inoculated samples, these non-black colonies were present but remained scarce up to 48 hours, allowing reliable enumeration of black *Salmonella* colonies. However, by 72 hours, the overgrowth of non-target bacteria rendered accurate quantification of *Salmonella* unfeasible.

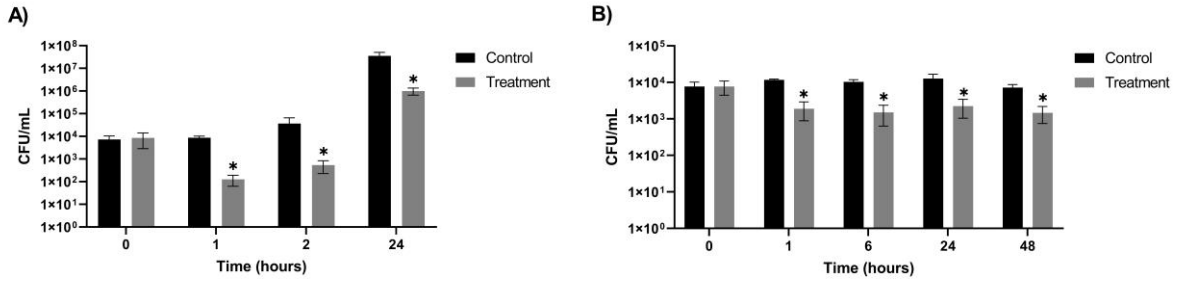

Figure 10. Biocontrol of *S.* Enteritidis using phage UFVCit2 at a multiplicity of infection (MOI) of 1000. (A) Reduction of bacterial counts on lettuce at room temperature. (B) Reduction of bacterial counts on chicken meat at 4 ºC. Statistically significant differences ($P < 0.05$) are indicated by asterisks (*).

4. DISCUSSION

The increasing prevalence of multidrug-resistant (MDR) *S. enterica* serovars in food production chains has prompted the search for sustainable and effective alternatives to traditional antimicrobial agents. In this context, bacteriophages have emerged as promising biocontrol tools due to their specificity, self-replicating nature, and ability to target bacteria even under adverse environmental conditions [33,67–69]. In the present study, we characterized the polyvalent lytic phage UFVCit2 and evaluated its potential application in controlling *S. enterica* in food matrices. Our results collectively highlight its effectiveness, genomic safety, host range breadth, and environmental resilience—key attributes for phage-based biocontrol strategies.

The phage UFVCit2 was isolated from sewage using *C. freundii* ATCC 8090 as the original host and demonstrated the ability to infect a broad spectrum of Enterobacteriaceae, including key pathogenic *S. enterica* serovars (Enteritidis and

Typhimurium), strains isolated from poultry and swine production, and *Shigella flexneri*. Although UFVCit2 did not infect the *E. coli* strains tested in this study, it is important to note that the number of E. coli strains evaluated was limited. Therefore, we cannot rule out the possibility that UFVCit2 is capable of infecting other *E. coli* strains. Future studies should expand the *E. coli* panel in host range analyses to better assess this potential. Notably, high efficiency of plating (EOP ≥ 0.5) was observed in *S*. Enteritidis and *S*. Typhimurium, two of the most prevalent serovars associated with human salmonellosis [8,9]. The ability to infect *S. flexneri* further reinforces its polyvalence—a highly desirable trait for phages intended for use in complex microbial communities such as those found in food-processing environments [31,38]. Additionally, the successful propagation in the non-pathogenic biosafety level 1 strain *C. freundii* further highlights the feasibility of large-scale and safe production of UFVCit2 for industrial applications, minimizing the likelihood of unintentional contamination of production facilities with the target pathogen.

Importantly, UFVCit2's genome lacks identifiable genes related to lysogeny, antibiotic resistance, or virulence—essential criteria for phage safety in food applications [33]. The presence of 21 tRNAs suggests that this phage is equipped to optimize translation of its own proteins during replication, a feature often associated with increased lytic efficiency in large-genome phages [70]. Characterization of UFVCit2 by electron microscopy revealed morphological features typical of the *Tequintavirus* genus within the *Demerecviridae* family, characterized by an isometric capsid and a long, flexible tail. Consistent with T5virus properties, the UFVCit2 genome demonstrated high sequence identity to known *Tequintavirus* genomes, particularly *Salmonella* phages Oldekolle and S131, supporting its taxonomic classification and enabling insights into phage-host interactions and host range determinants. Despite the high conservation of genes involved in virion morphogenesis and lytic functions, synteny and phylogenetic analyses revealed substantial variability in accessory regions and host-recognition modules such as receptor-binding proteins (RBPs) and L-shaped tail fibers (Ltf). This variability likely contributes to the diverse host range observed among related phages and highlights the evolutionary flexibility of this group in adapting to distinct enterobacterial receptors [60,62,65].

Functional inference based on RBP phylogeny suggests that UFVCit2 likely utilizes FhuA, a TonB-dependent outer membrane receptor, as its primary bacterial receptor. This is supported by high amino acid identity (96.9%) and close phylogenetic

clustering with phage T5, a canonical FhuA-binding phage [54,71]. FhuA is involved in both iron uptake and phage adsorption and is broadly conserved among Enterobacteriaceae [39,72,73], which may explain UFVCit2's ability to infect multiple genera. The evolutionary preference of phages for essential or conserved receptors such as FhuA or LPS may provide a selective advantage in accessing hosts [74]. However, even subtle alterations in receptor binding sites can disrupt phage adsorption. Previous studies have shown that small deletions in surface-exposed loops of FhuA, particularly within the gating region, significantly alter phage susceptibility without affecting protein localization [73,75,76]. Although UFVCit2's RBP is highly homologous to that of T5, it failed to infect the tested *E. coli* strains, including *E. coli* K12—a strain typically susceptible to T5 [77]. Structural or conformational differences in the FhuA receptor among strains of *E. coli* and *Salmonella* may account for these discrepancies, restricting UFVCit2's host range despite RBP homology.

Moreover, although a compatible RBP is a prerequisite for infection, successful adsorption, DNA injection, replication, and lysis also depend on the physiological state and genetic background of the bacterial host [75,78]. This aligns with findings by Gencay *et al*. (2019), who showed that receptor identity and phage genus together explain up to 79% of host range variance, leaving the remaining variance likely influenced by other factors such as receptor accessibility, intracellular defense mechanisms (e.g., CRISPR-Cas, RM systems), or replication incompatibilities [58]. The authors also observed that phages that recognize conserved outer membrane proteins—such as T5virus members targeting FhuA or BtuB—tend to have broader host ranges and are commonly isolated from ecologically complex environments like sewage. This correlates with the broad host range and sewage origin of UFVCit2, supporting the notion that ecological niche and receptor specificity co-influence host range.

Lateral tail fibers (Ltfs) in T5-like phages play a critical role in initial reversible adsorption by recognizing O-antigens before irreversible engagement with the primary receptor (e.g., FhuA via Pb5), although are not always essential for infection [57]. Variation in Ltf structure can additionally explain host range differences even among phages that share the same terminal receptor [58]. Moreover, because O-antigen modifications often incur little or no fitness cost, they offer bacteria an efficient means of evading phage infection [79]. The synteny analysis of UFVCit2 revealed substantial variability in Ltf-encoding regions relative to other Tequintaviruses, which may help

explain differences in host specificity. Additionally, the phylogenetic analysis of the suoerinfection exclusion Llp protein from UFVCit2 revealed a divergent clustering pattern, where the UFVCit2 RBP grouped closely with phage T5, while its Llp clustered with phages that typically infect via BtuB. This divergence may reflect functional adaptations in superinfection exclusion systems and suggests a decoupling between RBP-based host recognition and exclusion mechanisms, potentially influencing the host range spectrum [80].

The MOI assay demonstrated that phage UFVCit2 effectively inhibited the growth of *S.* Enteritidis across a range of phage-to-bacteria ratios, supporting its potential as a biocontrol agent. Although all phage-treated groups exhibited significant bacterial suppression, the timing and extent of growth inhibition varied depending on MOI. At lower MOIs (0.01 and 0.1), limited initial phage numbers allowed early bacterial growth before replication-induced lysis triggered a temporary decline, followed by regrowth and eventual stabilization. Higher MOIs (1 to 1000) suppressed bacterial growth immediately, but cultures resumed growth after ~1h30min, stabilizing after 7 hours. Despite these differences, final bacterial densities were statistically similar across all MOIs, highlighting UFVCit2's consistent efficacy and practical utility in settings where precise dosing may be challenging [81]. These findings also align with previous reports indicating that low MOIs can still lead to effective bacterial control over time, provided that the phage can replicate efficiently within the host [82]. Conversely, the transient regrowth observed at higher MOIs may reflect lysis-from-without phenomena or early depletion of susceptible bacterial subpopulations, followed by the expansion of less sensitive clones. Overall, this experiment demonstrates the robustness of UFVCit2 against S. Enteritidis and provides insights into optimizing phage dosage for potential application in food safety strategies.

Stability assays confirmed that UFVCit2 remains infective under a broad range of temperatures and pH values, including pH 4–12 and temperatures up to 60 °C. Its resilience to thermal and pH stress highlights its suitability for food industry applications, where fluctuations in temperature and pH may influence phage stability. Importantly, UFVCit2 retained significant lytic activity at refrigeration temperatures (4 °C), and reduction in *S.* Enteritidis levels was observed at high MOIs, suggesting the occurrence of "lysis from without"—a valuable mechanism in cold-chain scenarios [83]. This phenomenon refers to phage-induced bacterial lysis that occurs without replication, triggered instead by the simultaneous binding of numerous phage particles

to the bacterial surface [66]. The resulting structural damage compromises membrane integrity, leading to cell death even under conditions where phage replication is limited, such as at 4 °C. In refrigerated environments where bacterial metabolic activity is reduced, 'lysis from without' becomes particularly advantageous, enabling immediate reduction of bacterial populations despite the absence of a productive infection cycle.

In food models, UFVCit2 effectively reduced *S.* Enteritidis counts on both lettuce and chicken meat. Reductions were more pronounced at room temperature on lettuce, consistent with previous studies showing that phage efficacy is matrix- and temperature-dependent [47,84]. Several previous studies evaluating *Salmonella* control in food matrices used phage cocktails, often at high MOI. For example, Spricigo et al. (2013) [47] used a cocktail of three phages (UAB_Phi20, UAB_Phi78, and UAB_Phi87) at 4 °C and observed reductions of 2.2 and 0.9 $\log_{10}$ CFU/g for *S.* Typhimurium and *S.* Enteritidis on chicken meat, respectively, after 7 days and up to 3.9 $\log_{10}$ CFU/g on lettuce after 60 minutes. Pelyuntha et al. (2022) [48] also reported reductions in *Salmonella* loads at 4 °C using phage cocktails on chicken meat, employing an MOI of 100 and an evaluation period of 3 days, and observed reductions of 0.3–0.4 log compared to the control between 24 and 72 hours of storage. In contrast, the present study used UFVCit2 as a single phage and achieved comparable reductions after 48 hours at 4 °C—conditions under which both bacterial replication and phage activity are naturally limited.

Although the reductions observed were not as high as those reported for phage cocktails, they are still considered significant, particularly given the complexity of chicken meat as a food matrix. The heterogeneous composition of this substrate, including fat, proteins, and irregular surfaces, can hinder phage diffusion and reduce the likelihood of direct interaction with bacterial cells [85]. This may partially explain the moderate reductions observed. Nonetheless, these findings represent a meaningful impact on the reduction of this pathogen in poultry products and support the potential of UFVCit2 as a viable biocontrol agent. Additionally, the consistent bacterial suppression observed on chicken meat throughout the 48-hour period underscores the phage's robustness in cold-chain applications. Future work should focus on optimizing the multiplicity of infection (MOI) and strategically combining UFVCit2 with complementary phages to potentiate antimicrobial efficacy through synergistic interactions. Importantly, this future cocktail formulations using UFVCit2 should consider the phage genus and receptor specificity of the additional phages, as

superinfection exclusion systems encoded by UFVCit2 may inhibit the activity of genetically similar phages that target the same receptor. Therefore, a rational design based on complementary host recognition profiles is recommended. Moreover, the synergistic potential of such cocktails should be carefully evaluated both in vitro and in different food matrices to ensure efficacy across varied industrial scenarios.

In poultry processing plants in Brazil, immersion chilling is the standard method used to reduce microbial loads on carcasses, as outlined by Portaria nº 210/1998 of the Ministério da Agricultura e do Abastecimento (1998) [86]. This process involves the use of cold potable water (≤4 °C) in countercurrent systems. While effective, it can allow cross-contamination between carcasses. The application of bacteriophages as a post-chilling spray or dip could serve as a complementary strategy, enhancing Salmonella control without altering the sensory properties of the meat or requiring changes to existing workflows. Our results demonstrated that even a short exposure time (10 minutes) to UFVCit2 was sufficient to reduce *S*. Enteritidis levels on chicken meat, likely due to the phage's high adsorption efficiency. This characteristic is particularly advantageous in industrial environments, where carcasses spend limited time in each processing step, making rapid antimicrobial action a key requirement for practical implementation.

Taken together, the findings of this study provide strong evidence supporting the use of UFVCit2 as a versatile and robust biocontrol agent against *Salmonella enterica*, particularly in the context of poultry products. Its broad host range, lytic efficacy, genomic safety, and environmental stability underscore its suitability for integration into food safety protocols, especially during critical control points such as post-chilling stages. While further studies are needed to validate its effectiveness under industrial-scale conditions and in combination with other phages or antimicrobials, the current results establish UFVCit2 as a promising foundation for the development of targeted phage-based interventions in the control of foodborne pathogens.

5. CONCLUSIONS

In this chapter, we isolated and characterized the bacteriophage UFVCit2, a lytic phage belonging to the *Tequintavirus* genus, isolated using *C.r freundii* as a host. Host range analysis confirmed the polyvalent nature of UFVCit2, with lytic activity against *C. freundii*, *S. flexneri*, and different *S. enterica* serovars. This broad host range

highlights its potential for applications in food safety, targeting various enteric pathogens.

Morphological analysis revealed typical features of *Tequintavirus*, with an icosahedral head and a long, flexible tail. Genomic analysis confirmed a genome of 112 kb encoding 146 ORFs and 21 tRNAs, with no genes related to lysogeny, virulence, or antimicrobial resistance, reinforcing its genetic safety for biocontrol applications. Phylogenetic and protein analyses suggested that UFVCit2 likely utilizes FhuA as its primary receptor, similarly to phage T5, while its Llp superinfection exclusion protein clustered with phages that use BtuB, possibly reflecting ecological adaptations to reduce competition with other phages.

One-step growth curve assays revealed a short latency period and a high burst size in *C. freundii*, with slightly lower efficiency in *S. Enteritidis*, reflecting differences in host-phage interaction dynamics. Growth kinetics assays with *S. Enteritidis* further demonstrated that higher MOIs led to faster suppression of bacterial growth, particularly in the early hours, while bacterial regrowth was observed after 6–7 hours regardless of the MOI. This indicates that both phage dose and bacterial physiological factors influence long-term infection dynamics and bacterial control.

Physicochemical stability tests showed that UFVCit2 is highly stable across a wide pH range (4–12) and temperatures up to 60 °C, with reduced activity only under extreme conditions such as pH 3 or temperatures above 70 °C. Biocontrol assays in food models demonstrated that UFVCit2 was able to significantly reduce *S. Enteritidis* counts in both lettuce and chicken meat. Reductions were greater in lettuce at room temperature, while in refrigerated chicken meat the reductions were moderate but sustained over 48 hours. These results highlight the influence of temperature and matrix complexity on phage efficacy.

Altogether, the data presented in this chapter support UFVCit2 as a robust, polyvalent, and genetically safe phage with promising potential for applications in the biocontrol of *Salmonella* and other enteric pathogens in food products.

6. REFERENCES

1. NADI, Z.R.; SALEHI, T.Z.; TAMAI, I.A.; FOROUSHANI, A.R.; SILLANPAA, M.; DALLAL, M.M.S. **Evaluation of Antibiotic Resistance and Prevalence of Common Salmonella Enterica Serovars Isolated from Foodborne Outbreaks.** *Microchemical Journal* **2020**, *155*, 104660, doi:10.1016/j.microc.2020.104660.

2. WORLD HEALTH ORGANIZATION WHO **Estimates of the Global Burden of Foodborne Diseases: Foodborne Disease Burden Epidemiology Reference Group 2007–2015** Available online: https://www.who.int/publications/i/item/9789241565165 (accessed on 1 May 2025).

3. BRASIL. MINISTÉRIO DA SAÚDE. **Secretaria de Vigilância em Saúde Distribuição Temporal Dos Surtos Notificados de Doenças Transmitidas Por Alimentos – Brasil, 2007-2015** Available online: https://www.gov.br/saude/pt-br/centrais-de-conteudo/publicacoes/boletins/epidemiologicos/edicoes/2020/boletim-epidemiologico-svs-32.pdf/view (accessed on 30 April 2025).

4. MARCHELLO, C.S.; BIRKHOLD, M.; CRUMP, J.A.; MARTIN, L.B.; ANSAH, M.O.; BREGHI, G.; CANALS, R.; FIORINO, F.; GORDON, M.A.; KIM, J.-H.; et al. **Complications and Mortality of Non-Typhoidal Salmonella Invasive Disease: A Global Systematic Review and Meta-Analysis.** *Lancet Infect Dis* **2022**, *22*, 692–705, doi:10.1016/S1473-3099(21)00615-0.

5. FOUNOU, L.L.; FOUNOU, R.C.; ESSACK, S.Y. **Antibiotic Resistance in the Food Chain: A Developing Country-Perspective.** *Front Microbiol* **2016**, *7*, doi:10.3389/fmicb.2016.01881.

6. SCHOCH, C.L.; CIUFO, S.; DOMRACHEV, M.; HOTTON, C.L.; KANNAN, S.; KHOVANSKAYA, R.; LEIPE, D.; MCVEIGH, R.; O'NEILL, K.; ROBBERTSE, B.; et al. **NCBI Taxonomy: A Comprehensive Update on Curation, Resources and Tools.** ***Database*** *(Oxford)* **2020**, *2020*, doi:10.1093/database/baaa062.

7. TACK, D.M.; MARDER, E.P.; GRIFFIN, P.M.; CIESLAK, P.R.; DUNN, J.; HURD, S.; SCALLAN, E.; LATHROP, S.; MUSE, A.; RYAN, P.; et al. **Preliminary Incidence and Trends of Infections with Pathogens Transmitted Commonly Through Food — Foodborne Diseases Active Surveillance Network, 10 U.S.** Sites, 2015–2018. *MMWR Morb Mortal Wkly Rep* **2019**, *68*, 369–373, doi:10.15585/mmwr.mm6816a2.

8. FERRARI, R.G.; ROSARIO, D.K.A.; CUNHA-NETO, A.; MANO, S.B.; FIGUEIREDO, E.E.S.; CONTE-JUNIOR, C.A. **Worldwide Epidemiology of** ***Salmonella*** **Serovars in Animal-Based Foods: A Meta-Analysis**. *Appl Environ Microbiol* **2019**, *85*, doi:10.1128/AEM.00591-19.

9. MECHESSO, A.F.; MOON, D.C.; KIM, S.-J.; SONG, H.-J.; KANG, H.Y.; NA, S.H.; CHOI, J.-H.; KIM, H.-Y.; YOON, S.-S.; LIM, S.-K. **Nationwide Surveillance on Serotype Distribution and Antimicrobial Resistance Profiles of Non-Typhoidal Salmonella Serovars Isolated from Food-Producing Animals in South Korea.** *Int J Food Microbiol* **2020**, *335*, 108893, doi:10.1016/j.ijfoodmicro.2020.108893.

10. NAIR, D.V.T.; KOLLANOOR JOHNY, A. **Salmonella in Poultry Meat Production. In** ***Food Safety in Poultry Meat Production***; Springer International Publishing: Cham, 2019; pp. 1–24.

11. WESSELS, K.; RIP, D.; GOUWS, P. **Salmonella in Chicken Meat: Consumption, Outbreaks, Characteristics, Current Control Methods and the Potential of Bacteriophage Use**. *Foods* **2021**, *10*, 1742, doi:10.3390/foods10081742.

12. LU, J.; WU, H.; WU, S.; WANG, S.; FAN, H.; RUAN, H.; QIAO, J.; CAIYIN, Q.; WEN, M. **Salmonella: Infection Mechanism and Control Strategies.** *Microbiol Res* **2025**, *292*, 128013, doi:10.1016/j.micres.2024.128013.

13. GALÁN-RELAÑO, Á.; VALERO DÍAZ, A.; HUERTA LORENZO, B.; GÓMEZ-GASCÓN, L.; MENA RODRÍGUEZ, M.A Á.; CARRASCO JIMÉNEZ, E.; PÉREZ RODRÍGUEZ, F.; Astorga Márquez, R.J. **Salmonella and Salmonellosis: An Update on Public Health Implications and Control Strategies.** *Animals* **2023**, *13*, 3666, doi:10.3390/ani13233666.

14. AGÊNCIA NACIONAL DE VIGILÂNCIA SANITÁRIA - ANVISA **Instrução Normativa - IN Nº 161, de 1º de Julho de 2022** Available online: https://www.in.gov.br/en/web/dou/-/instrucao-normativa-in-n-161-de-1-de-julho-de-2022-413366880 (accessed on 1 May 2025).

15. AGÊNCIA NACIONAL DE VIGILÂNCIA SANITÁRIA - ANVISA **Resolução de Diretoria Colegiada - RDC Nº 724, de 1º de Julho de 2022** Available online: https://www.in.gov.br/en/web/dou/-/resolucao-rdc-n-724-de-1-de-julho-de-2022-413364812 (accessed on 1 May 2025).

16. SORBO, A.; PUCCI, E.; NOBILI, C.; TAGLIERI, I.; PASSERI, D.; ZOANI, C. **Food Safety Assessment: Overview of Metrological Issues and Regulatory Aspects in the European Union.** *Separations* **2022**, *9*, 53, doi:10.3390/separations9020053.

17. WILLIAMS, M.S.; EBEL, E.D.; GOLDEN, N.J.; SAINI, G.; NYIRABAHIZI, E.; CLINCH, N. **Assessing the Effectiveness of Performance Standards for Salmonella Contamination of Chicken Parts.** *Int J Food Microbiol* **2022**, *378*, 109801, doi:10.1016/j.ijfoodmicro.2022.109801.

18. AHN, D.U.; LEE, E.J. **Mechanisms and Prevention of Quality Changes in Meat by Irradiation. In *Food Irradiation Research and Technology***; Wiley, 2012; pp. 209–226.

19. JO, C.; LEE, J.I.; AHN, D.U. **Lipid Oxidation, Color Changes and Volatiles Production in Irradiated Pork Sausage with Different Fat Content and Packaging during Storage.** *Meat Sci* **1999**, *51*, 355–361, doi:10.1016/S0309-1740(98)00134-X.

20. RICHARDSON, S. **Disinfection By-Products and Other Emerging Contaminants in Drinking Water. *TrAC*** *Trends in Analytical Chemistry* **2003**, *22*, 666–684, doi:10.1016/S0165-9936(03)01003-3.

21. YANG, Y.; MIKŠ-KRAJNIK, M.; ZHENG, Q.; LEE, S.-B.; LEE, S.-C.; YUK, H.-G. **Biofilm Formation of Salmonella Enteritidis under Food-Related Environmental Stress Conditions and Its Subsequent Resistance to Chlorine Treatment**. *Food Microbiol* **2016**, *54*, 98–105, doi:10.1016/j.fm.2015.10.010.

22. MOKGATLA, R.M.; BROZEL, V.S.; GOUWS, P.A. **Isolation of Salmonella Resistant to Hypochlorous Acid from a Poultry Abattoir.** *Lett Appl Microbiol* **1998**, *27*, 379–382, doi:10.1046/j.1472-765X.1998.00432.x.

23. HAWKEY, J.; LE HELLO, S.; DOUBLET, B.; GRANIER, S.A.; HENDRIKSEN, R.S.; FRICKE, W.F.; CEYSSENS, P.-J.; GOMART, C.; BILLMAN-JACOBE, H.; HOLT, K.E.; et al. **Global Phylogenomics of Multidrug-Resistant Salmonella Enterica Serotype Kentucky ST198**. *Microb Genom* **2019**, *5*, doi:10.1099/mgen.0.000269.

24. ZHANG, L.; FU, Y.; XIONG, Z.; MA, Y.; WEI, Y.; QU, X.; ZHANG, H.; ZHANG, J.; LIAO, M. **Highly Prevalent Multidrug-Resistant Salmonella From Chicken and Pork Meat at Retail Markets in Guangdong, China.** *Front Microbiol* **2018**, *9*, doi:10.3389/fmicb.2018.02104.

25. MEDALLA, F.; GU, W.; MAHON, B.E.; JUDD, M.; FOLSTER, J.; GRIFFIN, P.M.; HOEKSTRA, R.M. **Estimated Incidence of Antimicrobial Drug–Resistant Nontyphoidal *Salmonella* Infections, United States, 2004–2012.** *Emerg Infect Dis* **2016**, *23*, 29–37, doi:10.3201/eid2301.160771.

26. TACCONELLI, E.; CARRARA, E.; SAVOLDI, A.; HARBARTH, S.; MENDELSON, M.; MONNET, D.L.; PULCINI, C.; KAHLMETER, G.; KLUYTMANS, J.; CARMELI, Y.; et al. **Discovery, Research, and Development of New Antibiotics: The WHO Priority List of Antibiotic-Resistant Bacteria and Tuberculosis.** *Lancet Infect Dis* **2018**, *18*, 318–327, doi:10.1016/S1473-3099(17)30753-3.

27. BECKER, D.; SELBACH, M.; ROLLENHAGEN, C.; BALLMAIER, M.; MEYER, T.F.; MANN, M.; BUMANN, D. **Robust Salmonella Metabolism Limits Possibilities for New Antimicrobials.** *Nature* **2006**, *440*, 303–307, doi:10.1038/nature04616.

28. CLAVIJO, V.; MORALES, T.; VIVES-FLORES, M.J.; REYES MUÑOZ, A. **The Gut Microbiota of Chickens in a Commercial Farm Treated with a Salmonella Phage Cocktail.** *Sci Rep* **2022**, *12*, 991, doi:10.1038/s41598-021-04679-6.

29. NARAYANAN, K.B.; BHASKAR, R.; HAN, S.S. **Bacteriophages: Natural Antimicrobial Bioadditives for Food Preservation in Active Packaging.** *Int J Biol Macromol* **2024**, *276*, 133945, doi:10.1016/j.ijbiomac.2024.133945.

30. COLOM, J.; CANO-SARABIA, M.; OTERO, J.; CORTÉS, P.; MASPOCH, D.; LLAGOSTERA, M. **Liposome-Encapsulated Bacteriophages for Enhanced Oral Phage Therapy against Salmonella Spp**. *Appl Environ Microbiol* **2015**, *81*, 4841–4849, doi:10.1128/AEM.00812-15.

31. SILLANKORVA, S.M.; OLIVEIRA, H.; AZEREDO, J. **BACTERIOPHAGES AND THEIR ROLE IN FOOD SAFETY.** *Int J Microbiol* **2012**, *2012*, 1–13, doi:10.1155/2012/863945.

32. MOSIMANN, S.; DESIREE, K.; EBNER, P. **EFFICACY OF PHAGE THERAPY IN POULTRY: A SYSTEMATIC REVIEW AND META-ANALYSIS.** *Poult Sci* **2021**, *100*, 101472, doi:10.1016/j.psj.2021.101472.

33. GOODRIDGE, L.D.; BISHA, B. **PHAGE-BASED BIOCONTROL STRATEGIES TO REDUCE FOODBORNE PATHOGENS IN FOODS.** *Bacteriophage* **2011**, *1*, 130–137, doi:10.4161/bact.1.3.17629.

34. DUC, H.M.; SON, H.M.; YI, H.P.S.; SATO, J.; NGAN, P.H.; MASUDA, Y.; HONJOH, K.; MIYAMOTO, T. **ISOLATION, CHARACTERIZATION AND APPLICATION OF A POLYVALENT PHAGE CAPABLE OF CONTROLLING SALMONELLA AND ESCHERICHIA COLI O157:H7 IN DIFFERENT FOOD**

MATRICES. *Food Research International* **2020**, *131*, 108977, doi:10.1016/j.foodres.2020.108977.

35. LI, M.; LIN, H.; KHAN, M.N.; WANG, J.; KONG, L. **EFFECTS OF BACTERIOPHAGE ON THE QUALITY AND SHELF LIFE OF *PARALICHTHYS OLIVACEUS* DURING CHILLED STORAGE.** *J Sci Food Agric* **2014**, *94*, 1657–1662, doi:10.1002/jsfa.6475.

36. GUO, Y.; LI, J.; ISLAM, MD.S.; YAN, T.; ZHOU, Y.; LIANG, L.; CONNERTON, I.F.; DENG, K.; LI, J. **APPLICATION OF A NOVEL PHAGE VB_SALS-LPSTLL FOR THE BIOLOGICAL CONTROL OF SALMONELLA IN FOODS.** *Food Research International* **2021**, *147*, 110492, doi:10.1016/j.foodres.2021.110492.

37. YANG, S.; SADEKUZZAMAN, M.; HA, S.-D. **Treatment with Lauric Arginate Ethyl Ester and Commercial Bacteriophage, Alone or in Combination, Inhibits Listeria Monocytogenes in Chicken Breast Tissue.** *Food Control* **2017**, *78*, 57–63, doi:10.1016/j.foodcont.2017.02.021.

38. SUKUMARAN, A.T.; NANNAPANENI, R.; KIESS, A.; SHARMA, C.S. **Reduction of Salmonella on Chicken Meat and Chicken Skin by Combined or Sequential Application of Lytic Bacteriophage with Chemical Antimicrobials.** *Int J Food Microbiol* **2015**, *207*, 8–15, doi:10.1016/j.ijfoodmicro.2015.04.025.

39. VASQUEZ, I.; RETAMALES, J.; PARRA, B.; MACHIMBIRIKE, V.; ROBESON, J.; SANTANDER, J. **Comparative Genomics of a Polyvalent Escherichia-Salmonella Phage Fp01 and In Silico Analysis of Its Receptor Binding Protein and Conserved Enterobacteriaceae Phage Receptor.** *Viruses* **2023**, *15*, 379, doi:10.3390/v15020379.

40. TWEST, R.; KROPINSKI, A.M. **Bacteriophage Enrichment from Water and Soil. In; 2009**; pp. 15–21.

41. TWEST, R.; KROPINSKI, A.M. **Bacteriophage Enrichment from Water and Soil. In; 2009**; pp. 15–21.

42. ADAMS, M.H. ***Bacteriophages*****;** Interscience Publishers, 1959;

43. SAMBROOK, J.; RUSSELL, D.W. ***Molecular Cloning: A Laboratory Manual, Third Edition*****; 3rd edition**.; Cold Spring Harbor Laboratory Press, 2001; Vol. 1;.

44. KHAN MIRZAEI, M.; NILSSON, A.S. **Isolation of Phages for Phage Therapy: A Comparison of Spot Tests and Efficiency of Plating Analyses for Determination of Host Range and Efficacy**. *PLoS One* **2015**, *10*, e0118557, doi:10.1371/journal.pone.0118557.

45. NIU, Y.D.; STANFORD, K.; KROPINSKI, A.M.; ACKERMANN, H.-W.; JOHNSON, R.P.; SHE, Y.-M.; AHMED, R.; VILLEGAS, A.; McAllister, T.A. **Genomic, Proteomic and Physiological Characterization of a T5-like Bacteriophage for Control of Shiga Toxin-Producing Escherichia Coli O157:H7.** *PLoS One* **2012**, *7*, e34585, doi:10.1371/journal.pone.0034585.

46. SVÁB, D.; FALGENHAUER, L.; ROHDE, M.; SZABÓ, J.; CHAKRABORTY, T.; TÓTH, I. **Identification and Characterization of T5-Like Bacteriophages Representing Two Novel Subgroups from** Food Products. *Front Microbiol* **2018**, *9*, doi:10.3389/fmicb.2018.00202.

47. SPRICIGO, D.A.; BARDINA, C.; CORTÉS, P.; LLAGOSTERA, M. **Use of a Bacteriophage Cocktail to Control Salmonella in Food and the Food Industry.** *Int J Food Microbiol* **2013**, *165*, 169–174, doi:10.1016/j.ijfoodmicro.2013.05.009.

48. PELYUNTHA, W.; VONGKAMJAN, K. **Combined Effects of Salmonella Phage Cocktail and Organic Acid for Controlling Salmonella Enteritidis in Chicken Meat.** *Food Control* **2022**, *133*, 108653, doi:10.1016/j.foodcont.2021.108653.

49. CAMACHO, C.; COULOURIS, G.; AVAGYAN, V.; MA, N.; PAPADOPOULOS, J.; BEALER, K.; MADDEN, T.L. **BLAST+: Architecture and Applications.** *BMC Bioinformatics* **2009**, *10*, 421, doi:10.1186/1471-2105-10-421.

50. ZANKARI, E.; ALLESØE, R.; JOENSEN, K.G.; CAVACO, L.M.; LUND, O.; AARESTRUP, F.M. **PointFinder: A Novel Web Tool for WGS-Based Detection of Antimicrobial Resistance Associated with Chromosomal Point Mutations in Bacterial Pathogens.** *Journal of Antimicrobial Chemotherapy* **2017**, *72*, 2764–2768, doi:10.1093/jac/dkx217.

51. BORTOLAIA, V., *et al*. **ResFinder 4.0 for Predictions of Phenotypes from Genotypes.** *Journal of Antimicrobial Chemotherapy* **2020**, *75*, 3491–3500, doi:10.1093/jac/dkaa345.

52. MALBERG TETZSCHNER, A.M.; JOHNSON, J.R.; JOHNSTON, B.D.; LUND, O.; SCHEUTZ, F. ***In Silico*** **Genotyping of Escherichia Coli Isolates for Extraintestinal Virulence Genes by Use of Whole-Genome Sequencing Data.** *J Clin Microbiol* **2020**, *58*, doi:10.1128/JCM.01269-20.

53. JOENSEN, K.G.; SCHEUTZ, F.; LUND, O.; HASMAN, H.; KAAS, R.S.; NIELSEN, E.M.; AARESTRUP, F.M. **Real-Time Whole-Genome Sequencing for Routine Typing, Surveillance, and Outbreak Detection of Verotoxigenic Escherichia Coli.** *J Clin Microbiol* **2014**, *52*, 1501–1510, doi:10.1128/JCM.03617-13.

54. FLAYHAN, A.; WIEN, F.; PATERNOSTRE, M.; BOULANGER, P.; BREYTON, C. **New Insights into Pb5, the Receptor Binding Protein of Bacteriophage T5, and Its Interaction with Its Escherichia Coli Receptor FhuA.** *Biochimie* **2012**, *94*, 1982–1989, doi:10.1016/j.biochi.2012.05.021.

55. BRAUN, V.; KILLMANN, H.; HERRMANN, C. **Inactivation of FhuA at the Cell Surface of Escherichia Coli K-12 by a Phage T5 Lipoprotein at the Periplasmic Face of the Outer Membrane.** *J Bacteriol* **1994**, *176*, 4710–4717, doi:10.1128/jb.176.15.4710-4717.1994.

56. DECKER, K.; KRAUEL, V.; MEESMANN, A.; HELLER, K.J. **Lytic Conversion of *Escherichia Coli* by Bacteriophage T5: Blocking of the FhuA Receptor Protein by a Lipoprotein Expressed Early during Infection.** *Mol Microbiol* **1994**, *12*, 321–332, doi:10.1111/j.1365-2958.1994.tb01020.x.

57. HELLER, K.; BRAUN, V. **Polymannose O-Antigens of Escherichia Coli, the Binding Sites for the Reversible Adsorption of Bacteriophage T5+ via the L-Shaped Tail Fibers.** *J Virol* **1982**, *41*, 222–227, doi:10.1128/jvi.41.1.222-227.1982.

58. GENCAY, Y.E.; GAMBINO, M.; PRÜSSING, T.F.; BRØNDSTED, L. **The Genera of Bacteriophages and Their Receptors Are the Major Determinants of Host Range.** *Environ Microbiol* **2019**, *21*, 2095–2111, doi:10.1111/1462-2920.14597.

59. GOLOMIDOVA, A.K.; KULIKOV, E.E.; PROKHOROV, N.S.; GUERRERO-FERREIRA, R.C.; KSENZENKO, V.N.; TARASYAN, K.K.; LETAROV, A. V. **Complete Genome Sequences of T5-Related Escherichia Coli Bacteriophages DT57C and DT571/2 Isolated from Horse Feces.** *Arch Virol* **2015**, *160*, 3133–3137, doi:10.1007/s00705-015-2582-0.

60. MONDIGLER, M.; AYOUB, A.T.; HELLER, K.J. **The DNA Region of Phage BF23 Encoding Receptor Binding Protein and Receptor Blocking Lipoprotein Lacks Homology to the Corresponding Region of Closely Related Phage T5.** *J Basic Microbiol* **2006**, *46*, 116–125, doi:10.1002/jobm.200510047.

61. BRADBEER, C.; WOODROW, M.L.; KHALIFAH, L.I. **Transport of Vitamin B12 in Escherichia Coli: Common Receptor System for Vitamin B12 and Bacteriophage BF23 on the Outer Membrane of the Cell Envelope.** *J Bacteriol* **1976**, *125*, 1032–1039, doi:10.1128/jb.125.3.1032-1039.1976.

62. RABSCH, W.; MA, L.; WILEY, G.; NAJAR, F.Z.; KASERER, W.; SCHUERCH, D.W.; KLEBBA, J.E.; ROE, B.A.; GOMEZ, J.A.L.; SCHALLMEY, M.; et al. **FepA- and TonB-Dependent Bacteriophage H8: Receptor Binding and Genomic Sequence.** *J Bacteriol* **2007**, *189*, 5658–5674, doi:10.1128/JB.00437-07.

63. BRAUN, V.; SCHALLER, K.; WOLFF, H. **A Common Receptor Protein for Phage T5 and Colicin M in the Outer Membrane of Escherichia Coli B.** *Biochimica et Biophysica Acta (BBA) - Biomembranes* **1973**, *323*, 87–97, doi:10.1016/0005-2736(73)90433-1.

64. KIM, M.; RYU, S. **Characterization of a T5-Like Coliphage, SPC35, and Differential Development of Resistance to SPC35 in *Salmonella Enterica* Serovar Typhimurium and *Escherichia Coli*.** *Appl Environ Microbiol* **2011**, *77*, 2042–2050, doi:10.1128/AEM.02504-10.

65. GOLOMIDOVA, A.; KULIKOV, E.; PROKHOROV, N.; GUERRERO-FERREIRA, R.; KNIREL, Y.; KOSTRYUKOVA, E.; TARASYAN, K.; LETAROV, A. **Branched Lateral Tail Fiber Organization in T5-Like Bacteriophages DT57C and DT571/2 Is Revealed by Genetic and Functional Analysis**. *Viruses* **2016**, *8*, 26, doi:10.3390/v8010026.

66. ABEDON, S.T. Lysis from Without. ***Bacteriophage*** **2011**, *1*, 46–49, doi:10.4161/bact.1.1.13980.

67. SUKJOI, C.; BUDDHASIRI, S.; TANTIBHADRASAPA, A.; KAEWSAKHORN, T.; PHOTHAWORN, P.; NALE, J.Y.; LOPEZ-GARCIA, A. V.; ABUOUN, M.; ANJUM, M.F.; MALIK, D.J.; et al. **Therapeutic Effects of Oral Administration of Lytic Salmonella Phages in a Mouse Model of Non-Typhoidal Salmonellosis.** *Front Microbiol* **2022**, *13*, doi:10.3389/fmicb.2022.955136.

68. MANOHAR, P.; LOH, B.; ATHIRA, S.; NACHIMUTHU, R.; HUA, X.; WELBURN, S.C.; LEPTIHN, S. **Secondary Bacterial Infections During Pulmonary Viral Disease: Phage Therapeutics as Alternatives to Antibiotics?** *Front Microbiol* **2020**, *11*, doi:10.3389/fmicb.2020.01434.

69. COSTA, M.J.; PASTRANA, L.M.; TEIXEIRA, J.A.; SILLANKORVA, S.M.; CERQUEIRA, M.A. **Bacteriophage Delivery Systems for Food Applications: Opportunities and Perspectives.** *Viruses* **2023**, *15*, 1271, doi:10.3390/v15061271.

70. BAILLY-BECHET, M.; VERGASSOLA, M.; ROCHA, E. **Causes for the Intriguing Presence of TRNAs in Phages.** *Genome Res* **2007**, *17*, 1486–1495, doi:10.1101/gr.6649807.

71. BONHIVERS, M.; GHAZI, A.; BOULANGER, P.; LETELLIER, L. **FhuA, a Transporter of the Escherichia Coli Outer Membrane, Is Converted into a Channel upon Binding of Bacteriophage T5.** *EMBO J* **1996**, *15*, 1850–1856, doi:10.1002/j.1460-2075.1996.tb00535.x.

72. WANG, Y.; CHEN, X.; HU, Y.; ZHU, G.; WHITE, A.P.; KÖSTER, W. **Evolution and Sequence Diversity of FhuA in Salmonella and Escherichia.** *Infect Immun* **2018**, *86*, doi:10.1128/IAI.00573-18.

73. KILLMANN, H.; HERRMANN, C.; WOLFF, H.; BRAUN, V. **Identification of a New Site for Ferrichrome Transport by Comparison of the FhuA Proteins of *Escherichia Coli* , *Salmonella Paratyphi* B, *Salmonella Typhimurium* , and *Pantoea Agglomerans*.** *J Bacteriol* **1998**, *180*, 3845–3852, doi:10.1128/JB.180.15.3845-3852.1998.

74. CHATURONGAKUL, S.; OUNJAI, P. **Phage–Host Interplay: Examples from Tailed Phages and Gram-Negative Bacterial Pathogens.** *Front Microbiol* **2014**, *5*, doi:10.3389/fmicb.2014.00442.

75. LABRIE, S.J.; SAMSON, J.E.; MOINEAU, S. **Bacteriophage Resistance Mechanisms.** *Nat Rev Microbiol* 2010, *8*, 317–327.

76. BRAUN, M.; KILLMANN, H.; BRAUN, V. **The B-barrel Domain of FhuAΔ5-160 Is Sufficient for TonB-dependent FhuA Activities of *Escherichia Coli*.** *Mol Microbiol* **1999**, *33*, 1037–1049, doi:10.1046/j.1365-2958.1999.01546.x.

77. CARMEL, G.; COULTON, J.W. **Internal Deletions in the FhuA Receptor of Escherichia Coli K-12 Define Domains of Ligand Interactions.** *J Bacteriol* **1991**, *173*, 4394–4403, doi:10.1128/jb.173.14.4394-4403.1991.

78. EGIDO, J.E.; COSTA, A.R.; APARICIO-MALDONADO, C.; HAAS, P.-J.; BROUNS, S.J.J. **Mechanisms and Clinical Importance of Bacteriophage Resistance.** *FEMS Microbiol Rev* **2022**, *46*, doi:10.1093/femsre/fuab048.

79. KIM, M.; RYU, S. **Spontaneous and Transient Defence against Bacteriophage by Phase-variable Glucosylation of <scp>O</Scp> -antigen in *<scp>S</Scp> Almonella Enterica* Serovar <scp>T</Scp> Yphimurium.** *Mol Microbiol* **2012**, *86*, 411–425, doi:10.1111/j.1365-2958.2012.08202.x.

80. HAGGÅRD-LJUNGQUIST, E.; HALLING, C.; CALENDAR, R. **DNA Sequences of the Tail Fiber Genes of Bacteriophage P2: Evidence for Horizontal Transfer of Tail Fiber Genes among Unrelated Bacteriophages.** *J Bacteriol* **1992**, *174*, 1462–1477, doi:10.1128/jb.174.5.1462-1477.1992.

81. ABEDON, S.T. Phage Therapy Dosing: **The Problem(s) with Multiplicity of Infection (MOI).** *Bacteriophage* **2016**, *6*, e1220348, doi:10.1080/21597081.2016.1220348.

82. HYMAN, P.; ABEDON, S.T. **Bacteriophage Host Range and Bacterial Resistance.** In; 2010; pp. 217–248.

83. AZARI, R.; YOUSEFI, M.H.; TAGHIPOUR, Z.; WAGEMANS, J.; LAVIGNE, R.; HOSSEINZADEH, S.; MAZLOOMI, S.M.; VALLINO, M.; KHALATBARI-LIMAKI, S.; BERIZI, E. **Application of the Lytic Bacteriophage Rostam to Control Salmonella Enteritidis in Eggs**. *Int J Food Microbiol* **2023**, *389*, 110097, doi:10.1016/j.ijfoodmicro.2023.110097.

84. FISTER, S.; ROBBEN, C.; WITTE, A.K.; SCHODER, D.; WAGNER, M.; ROSSMANITH, P. **Influence of Environmental Factors on Phage–Bacteria Interaction and on the Efficacy and Infectivity of Phage P100.** *Front Microbiol* **2016**, *7*, doi:10.3389/fmicb.2016.01152.

85. O'FLYNN, G.; ROSS, R.P.; FITZGERALD, G.F.; COFFEY, A. **Evaluation of a Cocktail of Three Bacteriophages for Biocontrol of *Escherichia Coli* O157:H7.** *Appl Environ Microbiol* **2004**, *70*, 3417–3424, doi:10.1128/AEM.70.6.3417-3424.2004.

86. MINISTÉRIO DA AGRICULTURA E DO ABASTECIMENTO **Portaria Nº 210, de 10 de Novembro de 1998: Aprova o Regulamento Técnico Da Inspeção Tecnológica e Higiênico-Sanitária de Carne de Aves** Available online: https://www.gov.br/agricultura/pt-br/assuntos/inspecao/produtos-animal/arquivos-portal-carne-aves/PORTARIA210.pdf (accessed on 21 April 2025).

CHAPTER 2

Characterization of newly isolated *Rosenblumvirus* phage infecting *Staphylococcus aureus* from different sources

Paloma Cavalcante Cunha [1,†], Pedro Samuel de Souza [2,†], Ana Julia Dill Rosseto [2], Isabella Ribeiro Rodrigues[2], Roberto Sousa Dias [2], Vinícius da Silva Duarte [3], Davide Porcellato [3], Cynthia Canêdo da Silva [1] and Sérgio Oliveira de Paula [2,*]

[1]Department of Microbiology, Federal University of Viçosa, Avenida Peter Henry Rolfs, s/n, Viçosa 36570-900, Minas Gerais, Brazil; paloma.cavalcante@ufv.br (P.C.C.); ccanedosilva@gmail.com (C.C.d.S.)

[2]Department of General Biology, Federal University of Viçosa, Avenida Peter Henry Rolfs, s/n, Viçosa 36570-900, Minas Gerais, Brazil; samuelhomero59@gmail.com (P.S.d.S.); ana.rosseto@ufv.br (A.J.D.R.); isabella.r.rodrigues@ufv.br (I.R.R.); rosousa318@gmail.com (R.S.D.)

[3]Faculty of Chemistry, Biotechnology and Food Science, The Norwegian University of Life Sciences, P.O. Box 5003, 1432 Ås, Norway; vinicius.da.silva.duarte@nmbu.no (V.d.S.D.); davide.porcellato@nmbu.no (D.P.)

† These authors contributed equally to this work.

* Correspondence author: depaula@ufv.br

Paper published in *Microorganisms* journal on 15 March 2025
https://doi.org/10.3390/microorganisms13030664

ABSTRACT

Staphylococcus aureus is a globally significant pathogen associated with severe infections, foodborne illnesses, and animal diseases. Its control has become increasingly challenging due to the spread of antibiotic-resistant strains, highlighting the urgent need for effective alternatives. In this context, bacteriophages have emerged as promising biocontrol agents. This study aimed to characterize the newly isolated *Staphylococcus* phage CapO46 and evaluate its efficacy in reducing *S. aureus* in milk. Identified as a new species within the *Rosenblumvirus* genus, CapO46 exhibited a podovirus-like structure and a small linear dsDNA genome (17,107 bp), with no lysogeny-related, antimicrobial resistance, or virulence genes. Host range assays demonstrated its ability to infect all 31 *S. aureus* isolates from two different countries and in diverse environmental contexts, achieving high efficiency of plating (EOP > 0.5) in 64.5% of cases. Kinetic analyses revealed rapid adsorption and a short latent period, with a burst size of approximately 30 PFU/cell. In UHT whole-fat milk, CapO46 achieved a maximum reduction of 7.2 log10 CFU/mL in bacterial load after 12 h, maintaining significant suppression (1.6 log10 CFU/mL) after 48 h. Due to its genetic safety, high infectivity across multiple isolates, and antimicrobial activity in milk, CapO46 can be considered a promising candidate for *S. aureus* biocontrol applications

Keywords: *Staphylococcus* phage; *Rosenblumvirus*; biocontrol; host range

1. INTRODUCTION

Staphylococcus aureus is a bacterium of great global significance, with a substantial impact on public health, food safety, and animal health. This pathogen is responsible for a wide range of infections in humans, ranging from mild conditions, such as skin infections, to severe and potentially fatal diseases, such as pneumonia, sepsis, and endocarditis [1]. In food, *S. aureus* is one of the leading causes of foodborne intoxication due to its production of heat-stable enterotoxins [2,3]. In animal health, it stands out as the main causative agent of bovine mastitis, a disease that compromises milk quality, reduces productivity, and causes significant economic losses in the dairy production chain [4,5]. The control of *S. aureus* is challenging due to its ability to form biofilms, which protect bacterial cells from the immune system and antimicrobials, as well as its increasing resistance to conventional antibiotics, such as beta-lactams, which has given rise to the well-known methicillin-resistant strains (MRSA—methicillin-resistant *Staphylococcus aureus*) [1,2]. These features underscore the urgent need to develop alternative strategies for controlling this pathogen in diverse settings.

Bacteriophages (phages) have emerged as promising tools for bacterial biocontrol due to their high specificity, lytic efficacy, and environmental safety [6–8]. These viruses selectively target and destroy bacteria, offering a significant advantage over antibiotics. Additionally, phages can degrade biofilms using specific enzymes such as depolymerizes and endolysins, enhancing their effectiveness in environments where biofilms protect bacteria or contribute to resistance [9,10]. In the agro-food industry, phages have been used as food biopreservatives, biopesticides to mitigate disease loads in crops, feed additives to manage bacterial infections in animals, and surface sanitizers in livestock facilities and food processing industries [11,12]. Phage application can reduce pathogens without harming beneficial microorganisms thus improving animal health, preserving product quality, and ensuring consumer safety [13–15]. Moreover, introducing phages as a natural alternative could promote more sustainable agricultural practices by reducing antibiotic use and minimizing pharmaceutical residues in the environment.

For safe and effective use in commercial agro-food applications, phages must exhibit several desirable characteristics [12]. These include the absence of genes associated with antibiotic resistance or virulence, as well as the absence of lysogeny-

related genes (i.e., they must be strictly lytic). Additionally, they should be highly specific to the target bacterium to prevent disruptions to the beneficial microbiota, and they must be stable to maintain efficacy under varying environmental conditions, such as temperature and pH fluctuations. Moreover, phages should be easily producible on a large scale to ensure commercial viability. Thus, the use of phages requires not only their isolation but also their biological and genomic characterization to enable a full exploration of their practical applications [16].

In this study, we report the isolation of the phage CapO46, obtained from effluents of a goat farm in Brazil, and evaluate its host range in *S. aureus* isolates from two different countries and diverse environmental contexts. Through genomic analyses, we determine the taxonomic classification of this novel phage and its genetic safety. Finally, we investigate the antimicrobial efficacy of CapO46 in *S. aureus*-contaminated ultra-high-temperature (UHT) whole-fat milk, highlighting its potential as a biocontrol agent under practical conditions.

2. MATERIALS AND METHODS

2.1 Bacterial strains and growth conditions

The *S. aureus* O46, isolated from an ewe with mild mastitis [17,18], was used as the host for phage isolation and propagation. For the host range investigation, *S. aureus* isolates from animals, humans, and cow milk were selected from the various bacterial libraries of collaborating research laboratories (Supplementary Table S1). Some isolates, including those kindly provided by EMBRAPA Gado de Leite (Juiz de Fora, MG, Brazil), had been previously characterized [19–23]. The Norwegian isolates were obtained from the SciFood Lab at the Norwegian University of Life Sciences (NMBU), Norwegian city, Norway, and there was no information regarding genetic variability. The *S. aureus* strain NCTC 8325-4 was kindly provided by Professor Morten Kjos from NMBU.

Isolates were routinely cultured in Brain Heart Infusion (BHI) broth (Kasvi, São Paulo, SP, Brazil) and BHI agar (1.5% agar *w/v*), then incubated at 37 °C. Optical density was measured using a spectrophotometer (Shanghai Spectrum SP-1105, Shanghai, China) at 600 nm (OD_{600}) to determine the phase of bacterial growth.

2.2 Phage isolation and propagation

For phage isolation, a sample was collected from the goat farm wastewater at UFV, processed, and then enriched following the method of Van Twest and Kropinski [24]. Briefly, the sample was centrifuged at 10,000× *g* for 15 minutes at 4 °C, and the supernatant was filtered through a 0.45 µm PES membrane (Millipore, Billerica, MA, USA). Next, 10 mL of sterile double-strength BHI broth was inoculated with 0.1 mL of *S. aureus* O46 culture (Table S1) in the logarithmic growth phase (OD_{600} = 0.4) and mixed with 10 mL of the filtered wastewater sample. The mixture was incubated at 37 °C with shaking at 100 rpm for 24 hours.

Following incubation, the mixture was centrifuged at 10,000× *g* for 10 minutes at 4 °C, and the supernatant (lysate) was filtered through a 0.22 µm PES membrane (Millipore, Billerica, MA, USA). The lysate was then diluted in SM buffer (5.8 g/L NaCl, 2.0 g/L $MgSO_4 \cdot 7H_2O$, 50.0 mL/L Tris-HCl 1M, 5.0 mL/L 2% *w/v* gelatin, pH 7.5) and plated using the double-layer agar (DLA) technique [24,25]. The plates were incubated overnight at 37 °C. Among the resulting lysis plaques, one was selected, excised, and replated. This process was repeated at least three times to ensure the isolation of a single phage. Finally, the phage was propagated in BHI broth as described by Sambrook *et al*. [26], filtered through a 0.22 µm PES membrane, titrated, and stored at 4 °C.

2.3 Transmission electron microscopy

For the viral morphology analysis, transmission electron microscopy (TEM) was performed. Briefly, 5 µL of a high-titer viral suspension (>10^{10} PFU/mL) was applied to Formvar®-coated grids with 200-mesh support for 5 minutes, followed by negative staining with 5 µL of 3% (*w/v*) uranyl acetate for 15 seconds. The grids were then dried in a vacuum chamber for approximately 24 hours and analyzed using a Zeiss EM 109 transmission electron microscope (Zeiss, Oberkochen, Germany) at the Center for Microscopy and Microanalysis (UFV). The acquired images were analyzed for capsid and tail dimensions using the ImageJ v1.54g software (National Institutes of Health, Bethesda, MD, USA). Measurements were obtained from three separate images to ensure accuracy and consistency.

2.4 Host range

The ability of the phage to infect different bacterial strains was initially assessed by spotting 10 µL of the phage suspension onto the surface of a double-layer agar plate inoculated with the test bacterium (Table S1). The plates were incubated overnight at 37 °C. Bacteria that exhibited clear spots or plaques at the inoculation site were recorded as sensitive to the phage and subsequently used in the efficiency of plating (EOP) assay to evaluate productive infection [27]. For the EOP assay, the phage lysate was serially diluted in SM buffer and spot-plated onto double-layer agar containing the sensitive bacteria. The plates were incubated overnight at 37 °C, and the PFU/mL was calculated the following day. All experiments were performed in triplicate.

To determine the EOP, the mean PFU/mL of the test bacterium was divided by the mean PFU/mL of the original host bacterium. The EOP for a specific phage–bacterium combination was classified as “high production” when the ratio was 0.5 or higher, meaning that productive infection in the target bacterium resulted in at least 50% of the PFU/mL observed in the original host. It was considered “medium production” when the EOP ranged from 0.1 to less than 0.5, “low production” when it ranged from 0.001 to less than 0.1, and “inefficient” when it was greater than 0 but less than or equal to 0.001. If no lysis plaques were observed, the EOP was classified as “no production”.

2.5 Adsorption and one-step growth curve

To evaluate the kinetics of viral infection, adsorption and one-step growth curve assays were performed in triplicate. For both assays, the isolate *S. aureus* O46 was grown in a BHI medium until reaching the mid-exponential phase (OD_{600} = 0.4).

The adsorption assay was conducted as described by Hyman and Abedon [28] but with modifications. The bacterial culture was infected with the phage at a multiplicity of infection (MOI) of 0.01 and incubated at 37 °C for 14 minutes. Samples were collected immediately and at 2 minutes intervals, post-infection, then centrifuged at 13,000× *g* for 1 minute. The supernatants were diluted and plated using the DLA method to determine the titers of non-adsorbed phages. The adsorption curve was expressed as relative adsorption (%), calculated as follows:

100 × [1 − (titer of non-adsorbed phages at each time point/initial titer of phages)]. (1)

The one-step growth curve assay was performed as reported by Sharifi *et al*. [29] but with some modifications. Briefly, 10 mL of bacterial culture was mixed with 100 µL of phage suspension to achieve an MOI of 0.01. The mixture was incubated for 10 minutes at 37 °C to allow for viral adsorption, then centrifuged (10,000× *g*, 5 minutes) to remove non-adsorbed phages. The supernatant was discarded, and the pellet was resuspended in 10 mL of pre-warmed BHI broth and incubated again at 37 °C with shaking at 100 rpm. Samples were collected immediately after resuspension (T0) and at 5 minutes intervals for 60 minutes and then plated using the DLA method. The latent period was defined as the time interval between adsorption and the onset of the first burst, as indicated by the initial rise in phage titer. The burst size was calculated by dividing the mean titer observed after the first burst by the average initial titer before the burst.

2.6 Genome sequencing and bioinformatics analysis

For phage genome extraction, the phage lysate was first treated with 5 µL/mL of DNase I (Thermo Fisher Scientific, Waltham, MA, USA) at 37 °C for 60 minutes to eliminate free host DNA contamination. DNase I was inactivated with 50 mM EDTA by incubation at 65 °C for 10 minutes, and the viral DNA was subsequently extracted using the mag™ Midi DNA Purification Kit (LGC Biosearch Technologies, Teddington, UK), following the manufacturer's instructions. The sequencing library was prepared using 1 ng of input DNA with the Illumina Nextera XT DNA Kit (Illumina, San Diego, CA, EUA), and normalization was performed using the SequalPrep™ Normalization Kit (Thermo Fisher Scientific). Whole-genome sequencing was conducted by Novogene (Cambridge, UK) using the Illumina NovaSeq X Plus 2 × 150 bp paired-end.

Raw reads were quality-filtered and assembled into contigs and scaffolds using SPAdes v3.13.0 through the Bacterial and Viral Bioinformatics Resource Center (BV-BRC) (https://www.bv-brc.org/, accessed on 7 May 2024), with read trimming (TrimGalore) and normalization enabled in the 'True' mode. The minimum contig length and coverage thresholds were set to 1000 and 5, respectively. The obtained CapO46 genome sequence was analyzed using the BLASTn tool in the NCBI database (https://blast.ncbi.nlm.nih.gov/Blast.cgi, accessed on 7 May 2024) to identify the

closest related sequences and their corresponding subfamily. All RefSeq genomes of the members of the identified subfamily were retrieved from the NCBI Virus database (https://www.ncbi.nlm.nih.gov/labs/virus/vssi/#/, accessed on 7 May 2024). The CapO46 genome was then incorporated into the subfamily genome dataset and analyzed using the Viral Proteomic Tree (ViPTree) server [30] (https://www.genome.jp/viptree/, accessed on 7 May 2024) to determine the phylogenetic relationships and generate a proteomic tree. Intergenomic comparisons were performed via the VIRIDIC web server [31] (http://rhea.icbm.uni-oldenburg.de/viridic/, accessed on 7 May 2024) following the International Committee on Taxonomy of Viruses (ICTV) guidelines, which define species and genus boundaries at similarity thresholds of 95% and 70%, respectively [32].

Gene prediction for the CapO46 genome was performed using Prokka v1.14.6+galaxy1 on the Phage Galaxy web platform (https://phage.usegalaxy.eu/, accessed on 7 January 2025). Automatic annotations were manually curated using the BLASTp tool in NCBI and the InterProScan web service (https://www.ebi.ac.uk/interpro/, accessed on 7 January 2025) to generate the final consensus annotation table. The phage genomic map was constructed using the Proksee platform [33] (https://proksee.ca/, accessed on 7 January 2025). Antimicrobial resistance genes and virulence factors were identified using ResFinder 4.5.0 [34] and VirulenceFinder 2.0.5 [35,36] on the CGE platform (https://www.genomicepidemiology.org/, accessed on 7 January 2025).

The complete CapO46 genome sequence has been deposited in the NCBI GenBank under accession number PV007823.

2.7 Phage bactericidal activity in UHT whole-fat milk

The bactericidal activity of the phage in UHT whole-fat milk (3% fat) was evaluated as described by García *et al*. [37], with modifications. The bacterial culture was grown to the mid-exponential phase (OD_{600} = 0.4) and subsequently diluted in phosphate-buffered saline (PBS). Aliquots of 50 µL of the diluted bacterial culture and 50 µL of the phage suspension, also diluted in PBS, were added to tubes containing 5 mL of UHT whole-fat milk to achieve a multiplicity of infection (MOI) of 1000. Positive control tubes, inoculated with bacteria only, received 50 µL of sterile PBS instead of phage. Negative control tubes, containing only sterile PBS and without bacterial or

phage inoculation, were used to check for milk contamination. The tubes were incubated at 37 °C, and aliquots were collected at 0, 3, 6, 12, 24, and 48 hours. The aliquots were diluted in PBS, and the bacterial concentrations (CFU/mL) were determined using the spread-plate method. The phage concentrations (PFU/mL) were determined by the DLA method. The entire experiment was conducted in triplicate.

2.8 Statistical analysis

The statistical significance of the means was assessed using GraphPad Prism software v 8.3.0 (538). First, the normality of the data was evaluated. If the data were normally distributed, an independent t-test was used to compare the means of the control and CapO46-treated groups at each time point (0, 3, 6, 12, 24, and 48 hours). If the data were not normally distributed, the Mann–Whitney test was applied. Significant differences were considered for p-values < 0.05.

3. RESULTS

3.1 Isolation and morphology of CapO46 phage

The lytic *Staphylococcus* phage CapO46, hereafter referred to as CapO46, was isolated from goat farm (*caprinocultura* in Brazilian Portuguese) wastewater using an *S. aureus* strain (O46) obtained from an ewe with mild mastitis [17,18]. The phage readily achieves high titers (>10^{10} PFU/mL) when routinely propagated in its isolation host. In the BHI medium, the phage produces clear, round lysis plaques approximately 1 mm in diameter, surrounded by a translucent halo of about 3 mm in diameter (Figure 1A). Electron micrographs reveal that the phage has a podovirus morphology, with an icosahedral head approximately 40 nm in diameter (n = 3) and a short, non-contractile tail about 23 nm in length (Figure 1B).

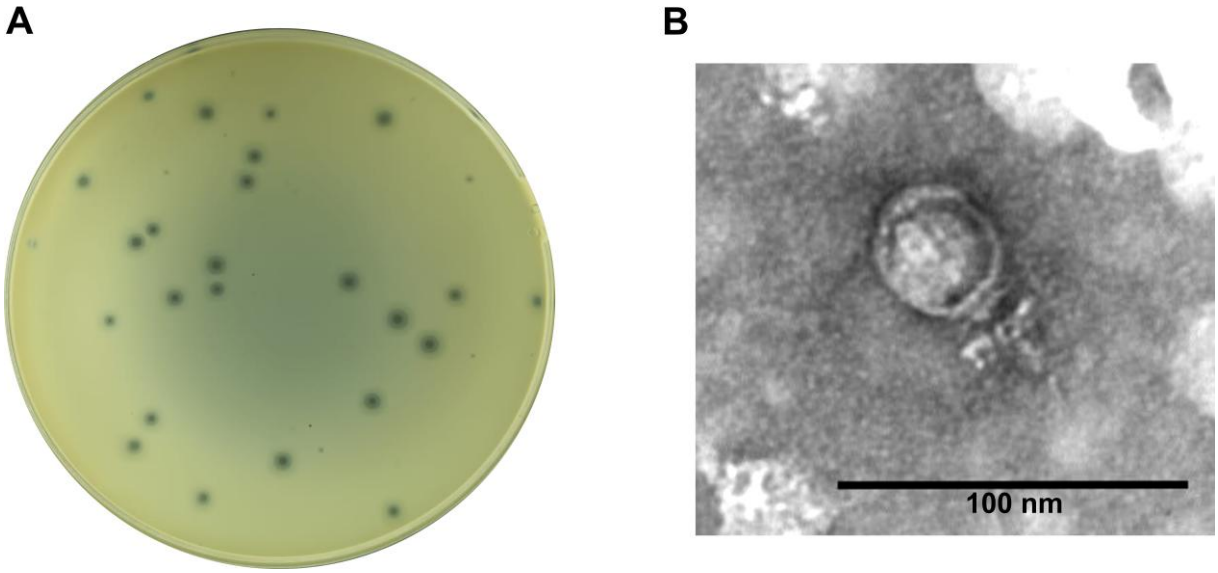

Figure 1. CapO46 phage A) Plaque morphology on BHI medium and B) Transmission electron micrograph of negatively stained phage particle.

3.2 CapO46 genome annotation and phylogenetic analysis

CapO46 is a virulent phage with a small dsDNA genome of 17,107 bp and a G + C content of 29.08%. Of the 19 putative open reading frames (ORFs) identified, 12 were predicted to be functional, and 7 were annotated as hypothetical proteins of unknown function (Figure 2). The functional ORFs were categorized into the following four modules: DNA and nucleotide metabolism (two ORFs), head and packaging (two ORFs), tail and connector (four ORFs), and lysis (three ORFs). No genes encoding tRNA, virulence factors, or antibiotic resistance genes were identified in the phage genome.

Regarding the taxonomic analyses, CapO46 was grouped in the same clade of the proteomic tree as representatives of the *Rosenblumvirus* genus (*Rakietenvirinae* subfamily, *Rountreeviridae* family), alongside a clade formed by members of the same subfamily (*Andhravirus* genus) (Figure 3A). In the VIRIDIC analysis (Figure 3B), the highest similarity score obtained was with *Staphylococcus* phage SA46-CL1 (RefSeq accession: NC_055802.1, similarity score: 92.9), indicating that CapO46 represents a new species within the *Rosenblumvirus* genus, according to ICTV criteria.

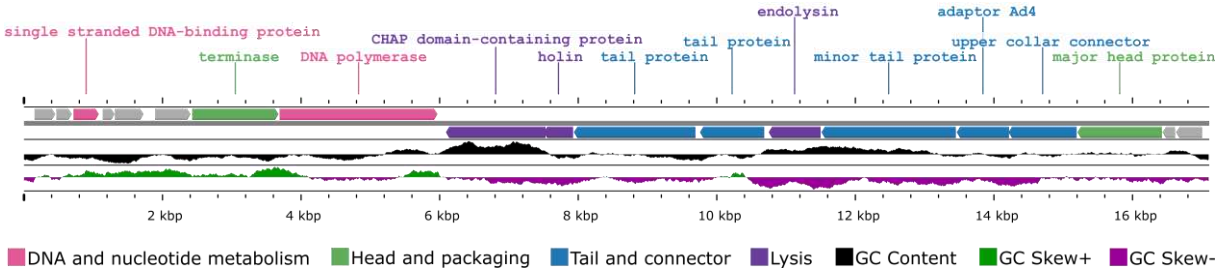

Figure 2. Genome map of phage CapO46 generated by Proksee based on ORF annotations from Prokka. The genes are color-coded based on their predicted functionality, and the GC content is represented by different colors using CGView v1.0.2.

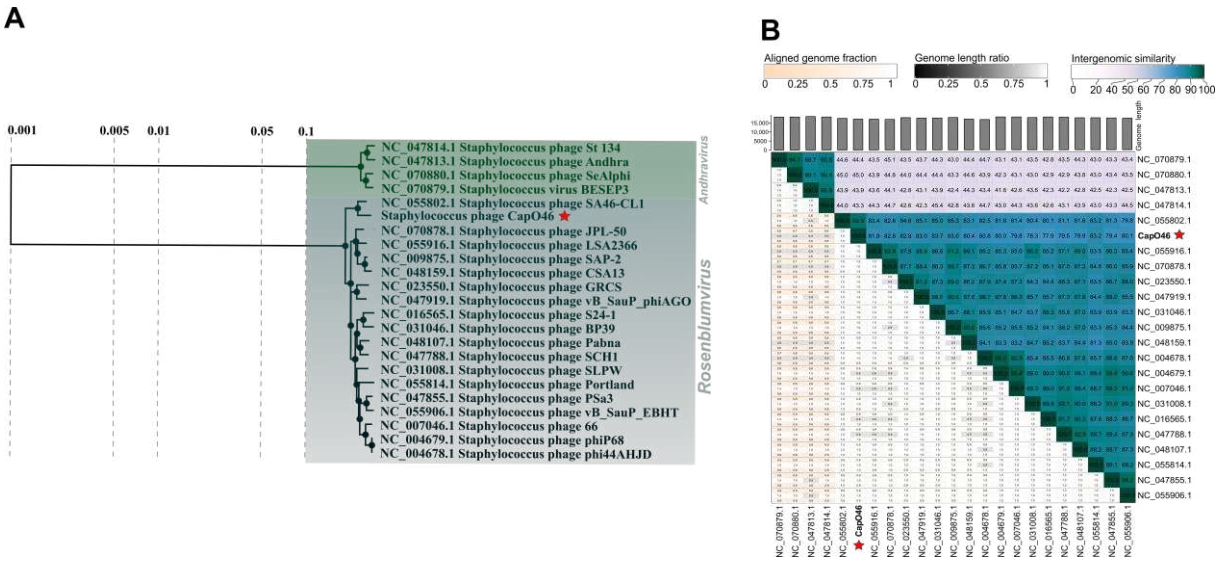

Figure 3. CapO46 phage (**A**) Phylogenetic tree and (**B**) Intergenomic similarity scores, showing its relationship with RefSeq genomes of members of the *Rakietenvirinae* subfamily. The CapO46 phage is highlighted with a red star in both images.

3.3 CapO46 host range

The CapO46 phage exhibited a wide strain specificity, being capable of infecting various *S. aureus* isolates from both Brazil and Norway, additionally of its Franch isolation strain. All 31 *S. aureus* isolates tested were lysed to some extent by the phage (Table 1). The EOP assays revealed that the phage was able to infect 64.5% of the isolates with high EOP (20/31), 9.7% with medium EOP (3/31), and 25.8% with inefficient EOP (8/31). Notably, the majority of the isolates classified as having high EOP (14/20) were Norwegian *S. aureus* strains. The phage did not infect any strain of non-aureus staphylococci.

Table 1. Host range of CapO46 phage and its efficiency of plating (EOP) on different bacterial hosts.

Bacterial Isolate	Source of Isolation	Spot-Test	EOP		
			Average Titer	EOP Value	Production
Staphylococcus aureus					
S. aureus O46 *	A (Fr)	+		1.0	High
S. aureus St 10	H (Br)	+	3.4×10^{3}	1.68×10^{-8}	Inefficient
S. aureus St 67	H (Br)	+	3.2×10^{3}	1.62×10^{-8}	Inefficient
S. aureus St 112	H (Br)	+	5.0×10^{3}	2.5×10^{-8}	Inefficient
S. aureus 222	A (Br)	+	8.7×10^{9}	1.225	High
S. aureus St 261	H (Br)	+	2.0×10^{5}	8.6×10^{-6}	Inefficient
S. aureus 1334	A (Br)	+	7.6×10^{7}	0.10	Medium
S. aureus UFV2030RH1	A (Br)	+	4.0×10^{9}	0.53	High
S. aureus 3059	A (Br)	+	5.0×10^{9}	0.791	High
S. aureus 3212	A (Br)	+	8.0×10^{9}	1.076	High
S. aureus 3906	A (Br)	+	7.3×10^{4}	3.6×10^{-7}	Inefficient
S. aureus 3907	A (Br)	+	9.0×10^{5}	4.5×10^{-6}	Inefficient
S. aureus 4081	A (Br)	+	1.3×10^{6}	0.0002	Inefficient
S. aureus 4182	A (Br)	+	1.1×10^{10}	1.476	High
S. aureus ATCC33591	TC	+	1.0×10^{6}	5×10^{-6}	Inefficient
S. aureus BO169-1	CM (No)	+	8.0×10^{9}	0.714	High
S. aureus B172-1	CM (No)	+	1.9×10^{9}	0.169	Medium
S. aureus H69Col2	CM (No)	+	1.0×10^{10}	0.948	High
S. aureus H90Col1	CM (No)	+	1.0×10^{10}	0.951	High
S. aureus H90Col2	CM (No)	+	1.3×10^{10}	1.163	High
S. aureus H90Col3	CM (No)	+	1.2×10^{10}	1.045	High
S. aureus H182Col1	CM (No)	+	6.1×10^{9}	0.547	High
S. aureus H249Col1	CM (No)	+	6.1×10^{9}	0.540	High
S. aureus H250Col1	CM (No)	+	7.9×10^{9}	0.710	High
S. aureus H288Col2	CM (No)	+	5.9×10^{9}	0.532	High
S. aureus H297Col1	CM (No)	+	9.9×10^{9}	0.884	High
S. aureus H295Col2	CM (No)	+	6.3×10^{9}	0.562	High
S. aureus H349Col1	CM (No)	+	1.1×10^{10}	0.944	High
S. aureus H350Col1	CM (No)	+	4.1×10^{9}	0.369	Medium

S. aureus H361Col1	CM (No)	+	1.4×10^{10}	1.281	High
S. aureus NCTC8325-4	TC	+	8.3×10^{9}	0.737	High
Non-aureus staphylococci					
S. chromogenes BO226-1	CM (No)	−			
S. epidermidis BO5-3	CM (No)	−			
S. equorum BO53-1	CM (No)	−			
S. gallinarum BO63-3	CM (No)	−			
S. haemolyticus BO28-3	CM (No)	−			
S. sciuri BO63-2	CM (No)	−			
S. warneri BO64-1	CM (No)	−			
S. xylosus BO186-3	CM (No)	−			

* CapO46 isolation and propagation host. A (Fr) = Animal (France); A (Br) = Animals (Brazil); H (Br) = Humans (Brazil); CM (No) = Raw cow milk (Norway); TC = Type collections. + = positive

e for lysis; − = no lysis

3.4 CapO46 adsorption and one-step growth curve

The adsorption of CapO46 phage occurs rapidly, with approximately 50% (50.3% ± 1.5%) of the phage particles adsorbed to bacterial cells in just 2 minutes and nearly 100% (98.3% ± 1.1%) adsorbed within 10 minutes (Figure 4A). The one-step growth curve shows that the phage's latent period at an MOI of 0.01 is 20 minutes, and the burst size, which occurs at 30 minutes, is on average 30 (30.7 ± 3.8) PFU/cell (Figure 4B).

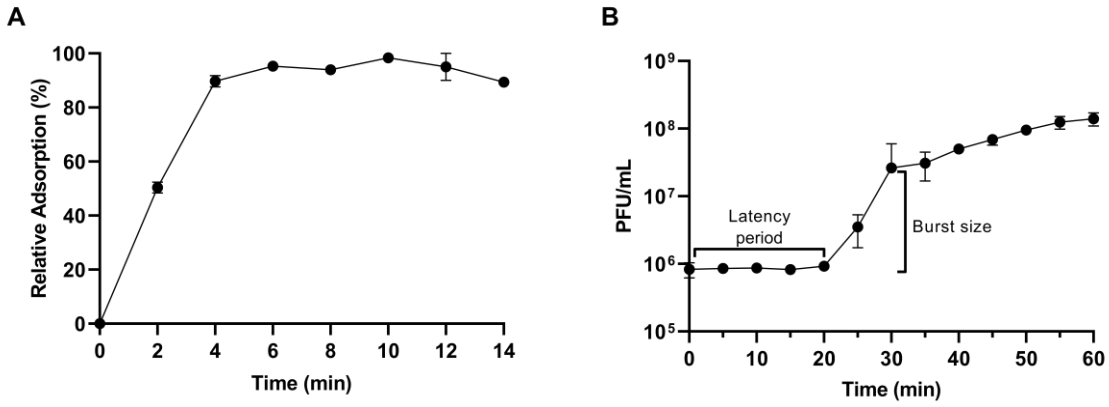

Figure 4. A) Relative adsorption and B) One-step growth curve of CapO46 phage at an MOI of 0.01.

3.5 Capo46 bactericidal activity in UHT whole-fat milk

The potential of phage CapO46 to inhibit *S. aureus* growth in UHT whole-fat milk was evaluated over 48 h at 37 °C (Figure 5). Treatment with the phage at an MOI of 1000 demonstrated a significant reduction (p-value < 0.05) in bacterial load, starting at 6 hours of incubation. By 6 hours, the bacterial counts had decreased by 5.2 log10 CFU/mL, reaching a peak reduction of 7.2 log10 CFU/mL at 12 hours. Although the bacterial population began to regrow after 24 hours of incubation, its concentration remained lower in the phage-treated samples compared to the control, with bacterial loads reduced by 3.5 log10 CFU/mL at 24 hours and 1.6 log10 CFU/mL at 48 hours relative to the untreated control.

The phage titers were also assessed at different time points, demonstrating the effective replication of phage CapO46 in the milk (Figure 5). After 3 hours of incubation, a slight increase of 0.23 log10 PFU/mL was observed, indicating limited initial activity. However, a substantial increase was recorded at 6 hours, with the mean phage titer reaching 8.13 log10 PFU/mL, representing a 2.08 log10 increase compared to the

initial time. Between 6 and 12 hours, the phage titers remained stable, with a mean value of 8.12 log10 PFU/mL at 12 hours. A further increase was observed at 24 hours, with a mean titer of 8.65 log10 PFU/mL, corresponding to a 0.53 log10 PFU/mL rise from 12 h. At the final time point (48 hours), the mean phage titer reached 9.60 log10 PFU/mL, representing the highest titer observed and an overall increase of 3.78 log10 PFU/mL from the initial time.

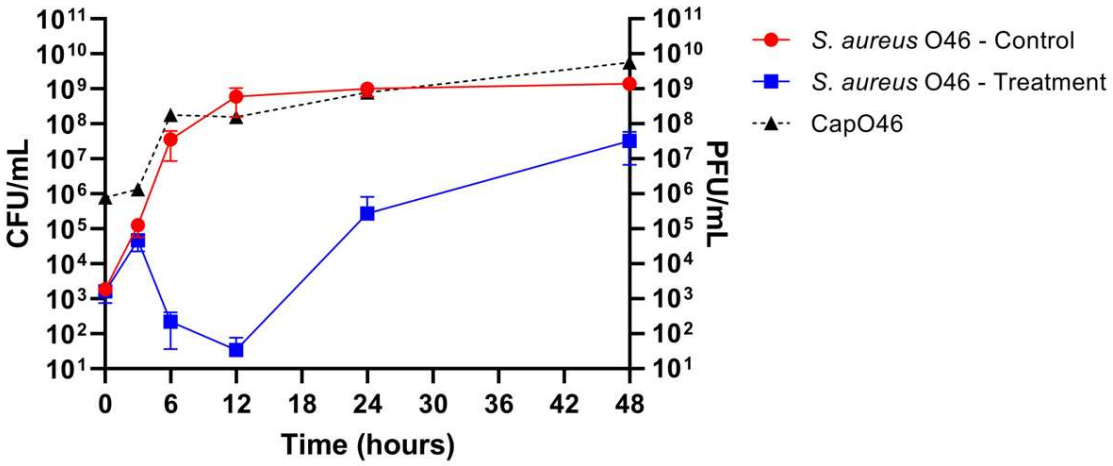

Figure 5. Bactericidal activity of phage CapO46 against *S. aureus* O46 in UHT whole-fat milk over 48 h. The graph illustrates the bacterial load (*S. aureus* O46 CFU/mL) in untreated samples (red line, "*S. aureus* O46—Control") and the reduction in bacterial counts following phage treatment (blue line, "*S. aureus* O46—Treatment"). Phage replication is represented by titers in PFU/mL (dotted black line, "CapO46").

4. DISCUSSION

The findings of this study highlight the potential of the phage CapO46 as a promising candidate for *S. aureus* biocontrol applications. The successful isolation of CapO46 from farm wastewater underscores the effectiveness of bacterium-enrichment methodologies for recovering lytic phages and emphasizes the importance of such environments as sources for discovering novel viruses [24,38]. Morphological characterization revealed a podovirus-like structure, which is consistent with the genomic and taxonomic analyses that classify CapO46 as a member of the genus *Rosenblumvirus*. Furthermore, the absence of lysogeny-related and tRNA-encoding genes aligns with the observations of phages in the subfamily *Rakietenvirinae* [39,40]. For phage therapy or biocontrol applications, strictly lytic phages are preferable, as they immediately lyse their host cells. Additionally, since some phages can carry virulence, toxin, or antibiotic resistance genes—thus contributing to the pathogenicity

of their bacterial hosts—such characteristics must be avoided [41]. Therefore, the absence of these genes in the CapO46 genome strengthens its genetic safety profile for therapeutic applications.

The host range assay revealed that CapO46 is capable of infecting a wide variety of *S. aureus* isolates from different environmental origins and unrelated countries. The phage isolation host, *S. aureus* O46, is a French isolate obtained from an ewe with mild mastitis, isolated by Vautor et al. (2009) [17] and sequenced by Le Maréchal et al. (2011) [18]. The Brazilian isolates obtained from EMBRAPA dairy cattle have already been evaluated for genetic diversity along with the key virulence factors [20]. Among the isolates analyzed by the authors, those used in our study were clustered into different groups based on a dissimilarity index of 30% using the UPGMA clustering method. Genetic comparisons were also performed between isolates 3059 and UFV2030RH1, revealing significant differences in the categories related to nucleotide, carbohydrate, amino acid, and cofactor metabolism, as well as cell regulation, signaling, and bacteriophages [19]. Furthermore, the antimicrobial susceptibility analysis of these two isolates showed resistance to aztreonam and bacitracin. The isolates obtained from humans (St 10, St 67, St 112, and St 261) are multidrug resistant and have also been genetically analyzed for their similarities [22]. The dendrogram based on PFGE patterns post-digestion with SmaI, associated with the One Health sector and Multidrug Efflux System genes, indicates that isolates St 112 and St 261 were grouped within the same cluster, while St10 and St67 formed a separate cluster. These data indicate considerable genetic differences regarding the Brazilian isolates. As for the Norwegian isolates, we currently lack information on their genotype and antimicrobial susceptibility. Since they were obtained from the same farm, with some originating from the same animal, it is possible that some may be clones. However, considering the geographic distance, substantial environmental differences, and variations in antibiotic therapy between Brazil and Norway [42,43], it is plausible that significant differences also exist between the Brazilian and Norwegian isolates.

Notably, 100% of the *S. aureus* isolates tested were sensitive to the phage, outperforming the previously reported phages in the literature [9,44–47]. Additionally, high efficiency of plating (EOP > 0.5) was observed in 64.5% of the sensitive isolates. While some isolates exhibited medium or inefficient EOP, this can be attributed to the phage's exceptionally high efficiency in its isolation host, resulting in elevated titers in that host. In comparison, the relative infection efficiency appears lower in other hosts,

but significant phage titers (>10^6 PFU/mL) were still achieved, even in hosts with inefficient EOP. Moreover, the high EOP observed in almost all the Norwegian isolates may indicate genetic similarities between them, as well as the genetic or environmental factors that render these isolates more susceptible. This raises the possibility of comparative genomic studies between the Brazilian and Norwegian *S. aureus* isolates to identify the genetic determinants of susceptibility.

The kinetic data revealed rapid adsorption, with nearly 100% of the phage particles adsorbed within 10 min, a short latent period of 20 min, and a small burst size of approximately 30 particles per cell. These results are consistent with findings for the phage vB_SauP_phiAGO1.3, another member of the genus *Rosenblumvirus*, which also adsorbs quickly to its host cells, has a short latent period (30 min), and produces a burst size very similar to that of CapO46 (about 35 PFU/cell) [48]. The rapid adsorption and short latent period of CapO46, combined with its ability to easily reach high titers (>10^{10} PFU/mL), underscore its strong replicative potential—a highly desirable trait for phages intended for biocontrol. Moreover, in industrial applications, achieving high phage titers is advantageous as it facilitates both large-scale production and application, optimizing costs and operational efficiency [16,49].

The performance of CapO46 in UHT whole-fat milk contaminated with *S. aureus* demonstrated its effectiveness in reducing bacterial load under practical conditions. The maximum reduction of 7.2 log CFU/mL observed after 12 h highlights the phage's strong bactericidal effect in a nutrient-rich environment that favors bacterial growth. Even after 48 h of incubation, the phage's lytic activity persisted, maintaining the host concentration 1.6 logs below that of the control—a 97% reduction. This demonstrates the phage's strong bactericidal potential, even several hours post-treatment. Previous studies have suggested that heat treatment (UHT > pasteurized) and milk skimming enhances the bactericidal activity of phages by minimizing the inhibitory effects of components found in raw milk [37,50,51]. These raw milk components, including a more complex lipid and protein composition that may inhibit phage binding to host cells, as well as the presence of a microbiota that can slow *S. aureus* growth, could lead to reduced phage propagation in raw milk and, consequently, diminished bactericidal activity. Nevertheless, several studies have already demonstrated the ability of phages to reduce bacterial growth even in raw milk [9,52–54].

Evaluating the lytic activity of the CapO46 phage in raw milk will be crucial to further assess its potential for controlling *S. aureus* in more complex contexts, such as

those related to bovine mastitis. The phage could be applied, for example, through an intramammary infusion system to treat *S. aureus* infections, as previously demonstrated in preliminary trials using phage-derived endolysins [55]. This approach could not only reduce the costs associated with antibiotic use and the loss of contaminated milk but also lead to improvements in both milk productivity and quality, as prompt mastitis treatment may minimize damage to mammary tissues and enhance the production of healthy milk.

Future studies should also focus on stability assays of the CapO46 phage under different temperature and pH conditions to ensure its viability in varied environments. Additionally, the formulation of phage cocktails, including new phages with diverse specificities, represents a promising perspective to expand the spectrum of action and enhance efficacy in combating *S. aureus*. This approach may also help mitigate the risk of bacterial resistance development, further strengthening the biotechnological potential of phages for industrial and public health applications.

Finally, the results of this study demonstrate that the ability of the phage CapO46 to infect a wide range of *S. aureus* isolates, coupled with its specificity for this species, highlights CapO46 as a promising tool for various applications, particularly in managing infections related to animal health and ensuring food safety in the industry. Its specificity allows for targeted action against the pathogen of interest without affecting beneficial microorganisms, providing a significant biotechnological advantage. Additionally, its ability to reach high titers offers a highly desirable practicality for large-scale application. Lastly, this study provides new insights into the phage's ability to infect strains from geographically distant, unrelated countries with distinct environmental conditions.

5. CONCLUSIONS

The results of this study highlight the promising potential of the bacteriophage CapO46 as a biocontrol agent against *S. aureus*. Its high infectivity across multiple isolates, high lytic efficiency, and favorable genomic profile position it as a viable candidate for applications in food safety and animal health. The ability of CapO46 to significantly reduce *S. aureus* populations in UHT whole-fat milk illustrates its lytic efficacy in complex environments. While the phage maintained substantial bactericidal activity for 48 h, the eventual regrowth of *S. aureus* underscores the need for further

optimization, such as phage cocktail formulations. Future research should also explore the stability of CapO46 under varying environmental conditions and its performance in more complex contexts, like raw milk. Collectively, these findings support the promotion of phage CapO46 as an innovative and sustainable solution for combating *S. aureus* in critical settings.

6. SUPPLEMENTARY MATERIALS

Table S1. *Staphylococcus* spp. isolates used for phage host range investigation and their sources of isolation.

Source	Isolate	Source description	Sampling location	Reference
Animal (France)	*S. aureus* O46	Ewe with mild mastitis, from a dairy sheep farm	Southeast of France	[17,18]
Animals (Brazil)	*S. aureus* 222	-	-	-
	S. aureus 1334	-	-	-
	S. aureus 3059 *	Dairy cow with clinical mastitis	Brazil	[19]
	S. aureus 3906 *	Dairy cow with subclinical mastitis	Rio de Janeiro, RJ, Brazil	[20]
	S. aureus 3907 *	Dairy cow with subclinical mast19itis	Rio de Janeiro, RJ, Brazil	[20]
	S. aureus 3212 *	Dairy cow with subclinical mastitis	Rio de Janeiro, RJ, Brazil	[20]
	S. aureus 4081 *	Dairy cow with subclinical mastitis	Juíz de Fora, MG, Brazil	[20]
	S. aureus 4182 *	Dairy cow with subclinical mastitis	Patrocínio, MG, Brazil	[21]
	S. aureus UFV2030RH1	Raw cow milk of a dairy cow at drying-off period	Viçosa, MG, Brazil	[19]
Humans (Brazil)	*S. aureus* St 10	Orthopedic screw	-	[22]
	S. aureus St 67	Blood culture	-	[22]
	S. aureus St 112	Tracheal secretion	-	[22]
	S. aureus St 261	Skull bone	-	[22]
Type collections	*S. aureus* ATCC 33591	-	-	-
	S. aureus NCTC 8325-4 **	-	-	[23]
	S. aureus BO169-1	Isolated 2018, Farm 2	Ås, Norway	-

Raw cow milk (Norway)	*S. aureus* B172-1	Isolated 2018, Farm 1	Ås, Norway	-
	S. aureus H69Col2	Farm 1, Cow1, isolated on 15/11/2022	Ås, Norway	-
	S. aureus H90Col1	Farm 1, Cow2, isolated 15/11/2022	Ås, Norway	-
	S. aureus H90Col2	Farm 1, Cow2, isolated 15/11/2022	Ås, Norway	-
	S. aureus H90Col3	Farm 1, Cow2, isolated 15/11/2022	Ås, Norway	-
	S. aureus H182Col1	Farm 1, Cow2, isolated 16/02/2023	Ås, Norway	-
	S. aureus H249Col1	Farm 1, Cow1, isolated 09/05/2023	Ås, Norway	-
	S. aureus H250Col1	Farm 1, Cow1, isolated 09/05/2023	Ås, Norway	-
	S. aureus H288Col2	Farm 1, Cow2, isolated 30/05/2023	Ås, Norway	-
	S. aureus H297Col1	Farm 1, Cow3, isolated 08/06/2023	Ås, Norway	-
	S. aureus H295Col2	Farm 1, Cow4, isolated 08/06/2023	Ås, Norway	-
	S. aureus H349Col1	Farm 1, Cow1, isolated 29/08/2023	Ås, Norway	-
	S. aureus H350Col1	Farm 1, Cow1, isolated 29/08/2023	Ås, Norway	-
	S. aureus H361Col1	Farm 1, Cow5, isolated 29/08/2023	Ås, Norway	-
	S. chromogenes BO226-1	-	Ås, Norway	-
	S. epidermidis BO5-3	-	Ås, Norway	-
	S. equorum BO53-1	-	Ås, Norway	-
	S. gallinarum BO63-3	-	Ås, Norway	-
	S. haemolyticus BO28-3	-	Ås, Norway	-
	S. sciuri BO63-2	-	Ås, Norway	-

S. warneri BO64-1	-	Ås, Norway	-
S. xylosus BO186-3	-	Ås, Norway	-

* Kindly provided by EMBRAPA Dairy Cattle (Juiz de Fora, MG, Brazil).
** Kindly provided by Professor Morten Kjos, NMBU (Norway).

7. REFERENCES

1. CHEUNG, G.Y.C.; BAE, J.S.; OTTO, M. **Pathogenicity and Virulence of *Staphylococcus Aureus*.** *Virulence* **2021**, *12*, 547–569. https://doi.org/10.1080/21505594.2021.1878688.

2. LIM, K.L.; KHOR, W.C.; ONG, K.H.; TIMOTHY, L.; AUNG, K.T. **Occurrence and Patterns of Enterotoxin Genes, Spa Types and Antimicrobial Resistance Patterns in Staphylococcus Aureus in Food and Food Contact Surfaces in Singapore.** *Microorganisms* **2023**, *11*, 1785. https://doi.org/10.3390/microorganisms11071785.

3. LÉGUILLIER, V.; PINAMONTI, D.; CHANG, C.-M.; GUNJAN; MUKHERJEE, R.; HIMANSHU; COSSETINI, A.; MANZANO, M.; ANBA-MONDOLONI, J.; MALET-VILLEMAGNE, J.; et al. **A Review and Meta-Analysis of *Staphylococcus Aureus* Prevalence in Foods.** *Microbe* **2024**, *4*, 100131. https://doi.org/10.1016/j.microb.2024.100131.

4. CHENG, W.N.; HAN, S.G. Bovine Mastitis: Risk Factors, Therapeutic Strategies, and Alternative Treatments—A Review. *Asian-Australas. J. Anim. Sci.* **2020**, *33*, 1699–1713. https://doi.org/10.5713/ajas.20.0156.

5. GONÇALVES, J.L.; KAMPHUIS, C.; MARTINS, C.M.M.R.; BARREIRO, J.R.; TOMAZI, T.; GAMEIRO, A.H.; HOGEVEEN, H.; DOS SANTOS, M.V. **Bovine Subclinical Mastitis Reduces Milk Yield and Economic Return.** *Livest. Sci.* **2018**, *210*, 25–32. https://doi.org/10.1016/j.livsci.2018.01.016.

6. MELO, L.D.R.; OLIVEIRA, H.; PIRES, D.P.; DABROWSKA, K.; AZEREDO, J. Phage Therapy Efficacy: **A Review of the Last 10 Years of Preclinical Studies.** *Crit. Rev. Microbiol.* **2020**, *46*, 78–99. https://doi.org/10.1080/1040841X.2020.1729695.

7. ANGELOPOULOU, A.; WARDA, A.K.; HILL, C.; ROSS, R.P**. Non-Antibiotic Microbial Solutions for Bovine Mastitis—Live Biotherapeutics, Bacteriophage, and Phage Lysins.** *Crit. Rev. Microbiol.* **2019**, *45*, 564–580. https://doi.org/10.1080/1040841X.2019.1648381.
8. BREYNE, K.; HONAKER, R.W.; HOBBS, Z.; RICHTER, M.; ŻACZEK, M.; SPANGLER, T.; STEENBRUGGE, J.; LU, R.; KINKHABWALA, A.; MARCHON, B.; et al. **Efficacy and Safety of a Bovine-Associated *Staphylococcus Aureus* Phage Cocktail in a Murine Model of Mastitis.** *Front. Microbiol.* **2017**, *8*, 2348. https://doi.org/10.3389/fmicb.2017.02348.

9. MOHAMMADIAN, F.; RAHMANI, H.K.; BIDARIAN, B.; KHORAMIAN, B**. Isolation and Evaluation of the Efficacy of Bacteriophages against Multidrug-Resistant (MDR), Methicillin-Resistant (MRSA) and Biofilm-Producing Strains of *Staphylococcus Aureus* Recovered from Bovine Mastitis.** *BMC Vet. Res.* **2022**, *18*, 406. https://doi.org/10.1186/s12917-022-03501-3.

10. TOPKA-BIELECKA, G.; DYDECKA, A.; NECEL, A.; BLOCH, S.; NEJMAN-FALEŃCZYK, B.; WĘGRZYN, G.; WĘGRZYN, A. **Bacteriophage-Derived**

Depolymerases against Bacterial Biofilm. *Antibiotics* **2021**, *10*, 175. https://doi.org/10.3390/antibiotics10020175.

11. FERNÁNDEZ, L.; GUTIÉRREZ, D.; RODRÍGUEZ, A.; GARCÍA, P. **Application of Bacteriophages in the Agro-Food Sector: A Long Way Toward Approval.** *Front. Cell. Infect. Microbiol.* **2018**, *8*, 296. https://doi.org/10.3389/fcimb.2018.00296.

12. SIYANBOLA, K.F.; EJIOHUO, O.; ADE-ADEKUNLE, O.A.; ADEKUNLE, F.O.; ONYEAKA, H.; FURR, C.-L.L.; HODGES, F.E.; CARVALHO, P.; OLADIPO, E.K. **Bacteriophages: Sustainable and Effective Solution for Climate-Resilient Agriculture.** *Sustain. Microbiol.* **2024**, *1*, qvae025. https://doi.org/10.1093/sumbio/qvae025.

13. FERNÁNDEZ, L.; DUARTE, A.C.; RODRÍGUEZ, A.; GARCÍA, P. **The Relationship between the Phageome and Human Health: Are Bacteriophages Beneficial or Harmful Microbes?** *Benef. Microbes* **2021**, *12*, 107–120. https://doi.org/10.3920/BM2020.0132.

14. CLAVIJO, V.; MORALES, T.; VIVES-FLORES, M.J.; REYES MUÑOZ, A**. The Gut Microbiota of Chickens in a Commercial Farm Treated with a *Salmonella* Phage Cocktail.** *Sci. Rep.* **2022**, *12*, 991. https://doi.org/10.1038/s41598-021-04679-6.

15. NARAYANAN, K.B.; BHASKAR, R.; HAN, S.S. Bacteriophages: **Natural Antimicrobial Bioadditives for Food Preservation in Active Packaging.** *Int. J. Biol. Macromol.* **2024**, *276*, 133945. https://doi.org/10.1016/j.ijbiomac.2024.133945.

16. CASEY, E.; VAN SINDEREN, D.; MAHONY, J. **In Vitro Characteristics of Phages to Guide 'Real Life' Phage Therapy Suitability.** *Viruses* **2018**, *10*, 163. https://doi.org/10.3390/v10040163.

17. VAUTOR, E.; COCKFIELD, J.; LE MARECHAL, C.; LE LOIR, Y.; CHEVALIER, M.; ROBINSON, D.A.; THIERY, R.; LINDSAY, J. **Difference in Virulence between *Staphylococcus Aureus* Isolates Causing Gangrenous Mastitis versus Subclinical Mastitis in a Dairy Sheep Flock.** *Vet. Res.* **2009**, *40*, 56. https://doi.org/10.1051/vetres/2009039.

18. LE MARÉCHAL, C.; HERNANDEZ, D.; SCHRENZEL, J.; EVEN, S.; BERKOVA, N.; THIÉRY, R.; VAUTOR, E.; FITZGERALD, J.R.; FRANÇOIS, P.; LE LOIR, Y. **Genome Sequences of Two Staphylococcus Aureus Ovine Strains That Induce Severe (Strain O11) and Mild (Strain O46) Mastitis.** *J. Bacteriol.* **2011**, *193*, 2353–2354. https://doi.org/10.1128/JB.00045-11.

19. DA SILVA DUARTE, V.; TREU, L.; SARTORI, C.; DIAS, R.S.; DA SILVA PAES, I.; VIEIRA, M.S.; SANTANA, G.R.; MARCONDES, M.I.; GIACOMINI, A.; CORICH, V.; et al. **Milk Microbial Composition of Brazilian Dairy Cows Entering the Dry Period and Genomic Comparison between *Staphylococcus Aureus* Strains Susceptible to the Bacteriophage VB_SauM-UFV_DC4.** *Sci. Rep.* **2020**, *10*, 5520. https://doi.org/10.1038/s41598-020-62499-6.

20. KLEIN, R.C.; FABRES-KLEIN, M.H.; BRITO, M.A.V.P.; FIETTO, L.G.; RIBON, A. DE O.B. ***Staphylococcus Aureus* of Bovine Origin: Genetic Diversity, Prevalence and the Expression of Adhesin-Encoding Genes.** *Vet. Microbiol.* **2012**, *160*, 183–188. https://doi.org/10.1016/j.vetmic.2012.05.025.

21. ROCHA, L.S. ***Estudo Da Variabilidade e Organização de Genes Que Codificam Proteínas de Superfície de Cepas de Staphylococcus Aureus Associadas à Mastite Bovina***; Universidade Federal de Viçosa: Viçosa, Brazil, 2021.

22. DE BARROS, M.; DA SILVA LOPES, I.; MOREIRA, A.J.; DOS SANTOS OLIVEIRA ALMEIDA, R.; MATIUZZI DA COSTA, M.; MOTA, R.A.; NERO, L.A.; **Scatamburlo Moreira, M.A. Multidrug Efflux System-Mediated Resistance in *Staphylococcus Aureus* under a One Health Approach.** *World J. Microbiol. Biotechnol.* **2024**, *40*, 9. https://doi.org/10.1007/s11274-023-03793-z.

23. BÆK, K.T.; FREES, D.; RENZONI, A.; BARRAS, C.; RODRIGUEZ, N.; MANZANO, C.; KELLEY, W.L. **Genetic Variation in the *Staphylococcus Aureus* 8325 Strain Lineage Revealed by Whole-Genome Sequencing.** *PLoS ONE* **2013**, *8*, e77122. https://doi.org/10.1371/journal.pone.0077122.

24. TWEST, R.; KROPINSKI, A.M. **Bacteriophage Enrichment from Water and Soil.** In *Bacteriophages*; Humana: Totowa, NJ, USA, 2009; pp. 15–21.

25. ADAMS, M.H. ***Bacteriophages***; Interscience Publishers: Geneva, Switzerland, 1959.

26. SAMBROOK, J.; RUSSELL, D.W. ***Molecular Cloning: A Laboratory Manual***, 3rd ed.; Cold Spring Harbor Laboratory Press: New York, NY, USA, 2001; Volume 1.

27. KHAN MIRZAEI, M.; NILSSON, A.S**. Isolation of Phages for Phage Therapy: A Comparison of Spot Tests and Efficiency of Plating Analyses for Determination of Host Range and Efficacy.** *PLoS ONE* **2015**, *10*, e0118557. https://doi.org/10.1371/journal.pone.0118557.

28. HYMAN, P.; ABEDON, S.T. **Practical Methods for Determining Phage Growth Parameters**. In *Bacteriophages*; Humana: Totowa, NJ, USA, 2009; pp. 175–202.

29. SHARIFI, F.; MONTASERI, M.; YOUSEFI, M.H.; SHEKARFOROUSH, S.S.; BERIZI, E.; WAGEMANS, J.; VALLINO, M.; HOSSEINZADEH, S. **Isolation and Characterization of Two Staphylococcus Aureus Lytic Bacteriophages "Huma" and "Simurgh".** *Virology* **2024**, *595*, 110090. https://doi.org/10.1016/j.virol.2024.110090.

30. NISHIMURA, Y.; YOSHIDA, T.; KURONISHI, M.; UEHARA, H.; OGATA, H.; GOTO, S. **ViPTree: The Viral Proteomic Tree Server.** *Bioinformatics* **2017**, *33*, 2379–2380. https://doi.org/10.1093/bioinformatics/btx157.

31. MORARU, C.; VARSANI, A.; KROPINSKI, A.M. **VIRIDIC—A Novel Tool to Calculate the Intergenomic Similarities of Prokaryote-Infecting Viruses**. *Viruses* **2020**, *12*, 1268. https://doi.org/10.3390/v12111268.

32. TURNER, D.; ADRIAENSSENS, E.M.; TOLSTOY, I.; KROPINSKI, A.M. **Phage Annotation Guide: Guidelines for Assembly and High-Quality Annotation.** *Phage* **2021**, *2*, 170–182. https://doi.org/10.1089/phage.2021.0013.

33. GRANT, J.R.; ENNS, E.; MARINIER, E.; MANDAL, A.; HERMAN, E.K.; CHEN, C.; GRAHAM, M.; VAN DOMSELAAR, G.; STOTHARD, P. Proksee: In-Depth **Characterization and Visualization of Bacterial Genomes.** *Nucleic Acids Res.* **2023**, *51*, W484–W492. https://doi.org/10.1093/nar/gkad326.

34. BORTOLAIA, V.; KAAS, R.S.; RUPPE, E.; ROBERTS, M.C.; SCHWARZ, S.; CATTOIR, V.; PHILIPPON, A.; ALLESOE, R.L.; REBELO, A.R.; FLORENSA, A.F.; et al. **ResFinder 4.0 for Predictions of Phenotypes from Genotypes.** *J. Antimicrob. Chemother.* **2020**, *75*, 3491–3500. https://doi.org/10.1093/jac/dkaa345.

35. MALBERG TETZSCHNER, A.M.; JOHNSON, J.R.; JOHNSTON, B.D.; LUND, O.; SCHEUTZ, F. **In Silico Genotyping of Escherichia Coli Isolates for Extraintestinal Virulence Genes by Use of Whole-Genome Sequencing Data.** *J. Clin. Microbiol.* **2020**, *58*, e01269-20. https://doi.org/10.1128/JCM.01269-20.

36. JOENSEN, K.G.; SCHEUTZ, F.; LUND, O.; HASMAN, H.; KAAS, R.S.; NIELSEN, E.M.; AARESTRUP, F.M**. Real-Time Whole-Genome Sequencing for Routine Typing, Surveillance, and Outbreak Detection of Verotoxigenic Escherichia Coli.** *J. Clin. Microbiol.* **2014**, *52*, 1501–1510. https://doi.org/10.1128/JCM.03617-13.

37. GARCÍA, P.; MADERA, C.; MARTÍNEZ, B.; RODRÍGUEZ, A.; EVARISTO SUÁREZ, J. **Prevalence of Bacteriophages Infecting *Staphylococcus Aureus* in Dairy Samples and Their Potential as Biocontrol Agents.** *J. Dairy. Sci.* **2009**, *92*, 3019–3026. https://doi.org/10.3168/jds.2008-1744.

38. CAO, S.; YANG, W.; ZHU, X.; LIU, C.; LU, J.; SI, Z.; PEI, L.; ZHANG, L.; HU, W.; LI, Y.; et al**. Isolation and Identification of the Broad-Spectrum High-Efficiency Phage VB_SalP_LDW16 and Its Therapeutic Application in Chickens.** *BMC Vet. Res.* **2022**, *18*, 386. https://doi.org/10.1186/s12917-022-03490-3.

39. HUA, Y.; AN, X.; PEI, G.; LI, S.; WANG, W.; XU, X.; FAN, H.; HUANG, Y.; ZHANG, Z.; MI, Z.; et al. **Characterization of the Morphology and Genome of an *Escherichia Coli* Podovirus.** *Arch. Virol.* **2014**, *159*, 3249–3256. https://doi.org/10.1007/s00705-014-2189-x.

40. PARK, S.Y.; KWON, H.; KIM, S.G.; PARK, S.C.; KIM, J.H.; SEO, S. **Characterization of Two Lytic Bacteriophages, Infecting *Streptococcus Bovis*/*Equinus* Complex (SBSEC) from Korean Ruminant.** *Sci. Rep.* **2023**, *13*, 9110. https://doi.org/10.1038/s41598-023-36306-x.

41. JIANG, T.; GUO, C.; WANG, M.; WANG, M.; ZHANG, X.; LIU, Y.; LIANG, Y.; JIANG, Y.; HE, H.; SHAO, H.; et al. **Genome Analysis of Two Novel *Synechococcus* Phages That Lack Common Auxiliary Metabolic Genes: Possible Reasons and Ecological Insights by Comparative Analysis of Cyanomyoviruses.** *Viruses* **2020**, *12*, 800. https://doi.org/10.3390/v12080800.

42. RAJALA-SCHULTZ, P.; NØDTVEDT, A.; HALASA, T.; PERSSON WALLER, K. **Prudent Use of Antibiotics in Dairy Cows: The Nordic Approach to Udder Health.** *Front. Vet. Sci.* **2021**, *8*, 623998. https://doi.org/10.3389/fvets.2021.623998.

43. ANDRETTA, M.; CALL, D.R.; NERO, L.A**. Insights into Antibiotic Use in Brazilian Dairy Production.** *Int. J. Dairy. Technol.* **2023**, *76*, 28–37. https://doi.org/10.1111/1471-0307.12914.

44. WANG, Z.; ZHENG, P.; JI, W.; FU, Q.; WANG, H.; YAN, Y.; SUN, J. SLPW: A **Virulent Bacteriophage Targeting Methicillin-Resistant *Staphylococcus Aureus* In Vitro and In Vivo.** *Front. Microbiol.* **2016**, *7*, 934. https://doi.org/10.3389/fmicb.2016.00934.

45. JI, J.; LIU, Q.; WANG, R.; LUO, T.; GUO, X.; XU, M.; YIN, Q.; WANG, X.; ZHOU, M.; LI, M.; et al**. Identification of a Novel Phage Targeting Methicillin-Resistant *Staphylococcus Aureus* In Vitro and In Vivo**. *Microb. Pathog.* **2020**, *149*, 104317. https://doi.org/10.1016/j.micpath.2020.104317.

46. TITZE, I.; LEHNHERR, T.; LEHNHERR, H.; KRÖMKER, V. **Efficacy of Bacteriophages Against *Staphylococcus Aureus* Isolates from Bovine Mastitis.** *Pharmaceuticals* **2020**, *13*, 35. https://doi.org/10.3390/ph13030035.

47. KOLENDA, C.; MEDINA, M.; BONHOMME, M.; LAUMAY, F.; ROUSSEL-GAILLARD, T.; MARTINS-SIMOES, P.; TRISTAN, A.; PIROT, F.; FERRY, T.; LAURENT, F. **Phage Therapy against *Staphylococcus Aureus*: Selection and Optimization of Production Protocols of Novel Broad-Spectrum Silviavirus Phages**. *Pharmaceutics* **2022**, *14*, 1885. https://doi.org/10.3390/pharmaceutics14091885.

48. GŁOWACKA-RUTKOWSKA, A.; GOZDEK, A.; EMPEL, J.; GAWOR, J.; ŻUCHNIEWICZ, K.; KOZIŃSKA, A.; DĘBSKI, J.; GROMADKA, R.; ŁOBOCKA, M. The Ability of Lytic **Staphylococcal Podovirus VB_SauP_phiAGO1.3 to Coexist in Equilibrium With Its Host Facilitates the Selection of Host Mutants of Attenuated Virulence but Does Not Preclude the Phage Antistaphylococcal Activity in a Nematode Infection Model.** *Front. Microbiol.* **2019**, *9*, 3227. https://doi.org/10.3389/fmicb.2018.03227.

49. GILL, J.; HYMAN, P. **Phage Choice, Isolation, and Preparation for Phage Therapy.** *Curr. Pharm. Biotechnol.* **2010**, *11*, 2–14. https://doi.org/10.2174/138920110790725311.

50. O'FLAHERTY, S.; COFFEY, A.; MEANEY, W.J.; FITZGERALD, G.F.; ROSS, R.P. **Inhibition of Bacteriophage K Proliferation on *Staphylococcus Aureus* in Raw Bovine Milk**. *Lett. Appl. Microbiol.* **2005**, *41*, 274–279. https://doi.org/10.1111/j.1472-765X.2005.01762.x.

51. GILL, J.J.; SABOUR, P.M.; LESLIE, K.E.; GRIFFITHS, M.W. **Bovine Whey Proteins Inhibit the Interaction of *Staphylococcus Aureus* and Bacteriophage K.** ***J.*** *Appl. Microbiol.* **2006**, *101*, 377–386. https://doi.org/10.1111/j.1365-2672.2006.02918.x.

52. SON, H.M.; DUC, H.M. **Prevalence and Phage-Based Biocontrol of Methicillin-Resistant Staphylococcus Aureus Isolated from Raw Milk of Cows with Subclinical Mastitis in Vietnam**. *Antibiotics* **2024**, *13*, 638. https://doi.org/10.3390/antibiotics13070638.

53. BADIYAL, A.; DHIAL, K.; SINGH, G.; DHAR, P.; SHARMA, M.; VERMA, S. **Isolation, Characterization and In Vitro Evaluation of Novel Lytic Phages Active Against Staphylococcus Aureus and Escherichia Coli of Bovine Mastitis Origin.** *Proc. Natl. Acad. Sci. India Sect. B Biol. Sci.* **2024**, *95*, 37–45. https://doi.org/10.1007/s40011-024-01621-4.

54. MCLEAN, S.K.; DUNN, L.A.; PALOMBO, E.A. **Phage Inhibition of *Escherichia Coli* in Ultrahigh-Temperature-Treated and Raw Milk**. *Foodborne Pathog. Dis.* **2013**, *10*, 956–962. https://doi.org/10.1089/fpd.2012.1473.

55. FAN, J.; ZENG, Z.; MAI, K.; YANG, Y.; FENG, J.; BAI, Y.; SUN, B.; XIE, Q.; TONG, Y.; MA, J**. Preliminary Treatment of Bovine Mastitis Caused by *Staphylococcus Aureus*, with Trx-SA1, Recombinant Endolysin of *S. Aureus* Bacteriophage IME-SA1**. *Vet. Microbiol.* **2016**, *191*, 65–71. https://doi.org/10.1016/j.vetmic.2016.06.001.

CHAPTER 3

Genome-wide CRISPRi screening reveals host factors required for CapO46 phage infection in *Staphylococcus aureus*

ABSTRACT

The rise of multidrug-resistant *Staphylococcus aureus* strains has renewed interest in bacteriophage therapy as an alternative antimicrobial strategy. However, bacterial resistance to phage infection remains a major obstacle, and the genetic determinants that modulate susceptibility or resistance in *S. aureus* are not fully understood—particularly those involving essential genes. In this study, we applied a genome-wide CRISPR interference (CRISPRi) approach to systematically identify *S. aureus* host factors involved in the infection by the lytic phage CapO46. Using a pooled CRISPRi-seq screen in the prophage-cured strain NCTC8325-4, we identified genes whose repression either impaired or enhanced bacterial survival during phage challenge. Among the hits, *mgrA*, *sarZ*, and SAOUHSC_00695 were classified as “costly” (repression conferred resistance), while *rpiRc* and others were classified as “essential” (repression increased susceptibility). Phenotypic validation of selected targets through growth curves, CFU and PFU quantification, adhesion assays, and biofilm analysis confirmed the CRISPRi-seq results. Silencing of *mgrA* or SAOUHSC_00695 led to complete resistance to CapO46, likely by affecting wall teichoic acid (WTA) glycosylation. In contrast, *rpiRc* repression impaired bacterial fitness and increased phage susceptibility, possibly due to metabolic deregulation and altered cell surface properties. Biofilm and adhesion assays revealed that gene silencing also affects surface-associated phenotypes, further linking phage resistance to virulence modulation. Our findings demonstrate the power and efficiency of CRISPRi-seq to uncover novel, functionally relevant host factors, including essential genes, in a high-throughput and practical manner. This study provides a foundation for understanding phage-host dynamics in *S. aureus* and highlights potential targets for phage therapy optimization.

Keywords: *Staphylococcus aureus*; Bacteriophage; CRISPRi; Host factors; Phage resistance; *mgrA*; sarZ; rpiRc.

1. INTRODUCTION

Despite significant advances in recent decades, infections caused by antibiotic-resistant bacteria, such as methicillin-resistant Staphylococcus aureus (MRSA), remain a major clinical challenge worldwide, leading to severe healthcare complications and increased mortality rates [1,2]. In this context, bacteriophages (phages), viruses capable of specifically infecting bacteria, have emerged as a promising therapeutic alternative. As predators responsible for host bacterial mortality and horizontal gene transfer, phages significantly influence the dynamics, activity, and evolution of bacterial communities [3,4]. Since their discovery in the early 20th century, phages have been utilized as microbiological control agents [5]. However, the increasing concern regarding antibiotic resistance has revitalized interest in phage therapy [6,7]. Beyond their proven effectiveness in controlling various pathogens, phages are considered safe, causing no adverse effects when administered orally, intravenously, topically, or subcutaneously [8–13]. Nonetheless, bacterial resistance to phages remains a critical limitation, prompting research into the mechanisms underlying bacterial susceptibility and resistance to phage infection [14].

In *Staphylococcus* species, documented resistance mechanisms predominantly act at the stages of phage adsorption, biosynthesis, and assembly [15,16]. Structural modifications of bacterial surface receptors, especially cell wall teichoic acids (WTAs), are key defense mechanisms [17–20]. These ribitol phosphate polymers, characteristic of Gram-positive bacteria, can be modified with residues such as α-O-N-acetylglucosamine (α-O-GlcNAc), β-O-N-acetylglucosamine (β-O-GlcNAc), or D-alanine by glycosyltransferase enzymes TarM (α-O-GlcNAc) and TarS (β-O-GlcNAc) [21,22]. Different phage types recognize specific glycosylation patterns: siphoviruses interact with α-O-GlcNAc or β-O-GlcNAc, podoviruses specifically require β-O-GlcNAc, while myoviruses recognize both unmodified and β-O-GlcNAc-decorated WTAs [18–20,23,24]. Although genes responsible for WTA biosynthesis are conserved across the species, occasional inactivation or absence of *tarM* increases susceptibility to podovirus [19,20]. Additionally, occlusion of receptors by large surface proteins and polysaccharide capsules can physically block phage access to their specific receptors [25,26]. Other resistance mechanisms include viral DNA restriction-modification systems, interference in viral assembly mediated by staphylococcal pathogenicity

islands, as well as sporadic mechanisms such as superinfection immunity and CRISPR-Cas systems [27–31].

Although classical genetic techniques such as transposon-based mutagenesis [32] have contributed to identifying genetic determinants in phage-host interactions, these methods have important limitations, particularly for essential genes whose deletion is lethal to the bacterium. Therefore, high-throughput experimental approaches are necessary to facilitate and improve the characterization of the largely unexplored genetic landscape of these interactions [33]. Over the last decade, genome-wide depletion of gene expression using CRISPR interference (CRISPRi) has emerged as an effective strategy for identifying genetic determinants involved in antibiotic susceptibility [34–36], pathogenesis-related genes [37], and host factors required for phage infection [33,38]. CRISPRi employs a catalytically inactive Cas9 endonuclease (dCas9) guided by a single-guide RNA (sgRNA) to block transcription at targeted genomic loci, thereby allowing reversible and efficient gene silencing without permanent genetic modifications [39,40]. This strategy enables repression of both the targeted gene and downstream co-transcribed genes. Using pooled sgRNA libraries, CRISPRi can be scaled to genome-wide screens in bacteria through established high-throughput sequencing methods (CRISPRi-seq) [33,34,41].

Phage-host interactions have increasingly been explored using CRISPRi-based approaches. For example, Harding *et al.* [42] used CRISPRi to validate *Serratia* genes involved in infection by a jumbo nucleus-forming phage, following an initial Tn-seq screen. Similarly, Rousset *et al*. [33] applied genome-wide CRISPR-dCas9 screening in *E. coli* to identify host factors required for infection by three distinct phages, including lambda (λ), revealing both known and novel genes involved in susceptibility. Mutalik *et al*. [38] further expanded this approach, identifying essential *E. coli* genes responsible for resistance to 14 different phages. Collectively, these studies demonstrate the power of CRISPRi for dissecting genetic determinants of phage-host dynamics.

To date, no genome-wide CRISPRi studies have investigated *S. aureus* host factors required for bacteriophage infection. In this study, we addressed this gap by using a previously developed genome-wide inducible CRISPRi library in *S. aureus* strain NCTC8325-4 [34] to perform CRISPRi-seq screens that quantify gene fitness during infection with the lytic phage CapO46 [43], followed by functional validation of selected targets. This approach allowed us to investigate the role of essential genes

and regulatory elements in shaping the phage-host interaction, providing novel insights into the genetic basis of phage susceptibility in *S. aureus*.

2. MATERIALS AND METHODS

2.1 Bacterial strains, culture conditions, and bacteriophage

The genome-wide CRISPRi library for *S. aureus* was kindly provided by Professor Morten Kjos (Norwegian University of Life Sciences, NMBU, Norway). This library was constructed from the commonly used laboratory strain *S. aureus* NCTC8325-4, a prophage-cured derivative of NCTC8325, as described previously [34], and is hereafter referred to as MM267LG. A control version of the CRISPRi system, carrying a non-targeting sgRNA and named MM268, was used in experiments where gene silencing was not intended (controls). Additionally, specific strains carrying gene-targeted sgRNAs, constructed as described previously [34], were also kindly provided by Professor Kjos.

CRISPRi strains were recovered from frozen glycerol stocks (25% v/v) and grown in Brain Heart Infusion (BHI) broth (Kasvi, São Paulo, SP, Brazil) or BHI agar (1.5%) supplemented with 10 µg/mL chloramphenicol (CAM). Cultures were incubated at 37 °C with shaking at 180 rpm. Expression of the CRISPRi system was induced by adding 30 ng/mL of anhydrotetracycline (aTc) to the medium. The propagation host of the phage, *S. aureus* O46 [43], was obtained from the Molecular Immunovirology Laboratory at the Federal University of Viçosa (UFV), Brazil, and cultured under the same conditions, except without the addition of antibiotics. The optical density of the cultures was measured at a wavelength of 600 nm (OD_{600nm}) using a spectrophotometer (Shanghai Spectrum SP-1105, Shanghai, China) to monitor bacterial growth phase.

The lytic *Staphylococcus* phage CapO46 was routinely propagated as described elsewhere [43].

2.2 Efficiency of Plating (EOP)

To evaluate the infection capacity of CapO46 phage in the CRISPRi library, the efficiency of plating (EOP) assay was carried out as previously described [44] using the MM268 strain. For that, both *S. aureus* MM268 and *S. aureus* O46 cultures were plated with dilutions of CapO46 phage using the standard double-layer agar (DLA)

method [45,46]. The plates were incubated overnight at 37 ºC, and the phage titer noted in the following day. The EOP was calculated by dividing the average plaque forming unit number (PFU/mL) found on target bacteria (*S. aureus* MM268) by the average PFU/mL found on host bacteria (*S. aureus* O46). The EOP evaluation was defined as: “high production”, if the ratio is 0.5 or more, that is, when the productive infection in the target bacteria resulted in at least 50% of the PFU found for the original host; “medium production”, when the EOP is from 0.2 to <0.5; “low production”, when the EOP is from 0.001 to <0.2; and “inefficient” if the EOP is equal to or less than 0.001.

2.3 Adsorption and one-step growth curve

To evaluate the kinetics of viral infection in the CRISPRi library, adsorption and one-step growth curve assays were performed in triplicate using the *S. aureus* MM268 strain. For both assays, the strain was grown in BHI broth (10 µg/mL CAM) until reaching mid-exponential-phase (OD_{600nm} = 0.4, approximately 10^8 CFU/mL).

The adsorption assay was conducted following a modified protocol described by Hyman and Abedon [47]. Cultures were infected with the CapO46 phage at a multiplicity of infection (MOI) of 0.01 and incubated for 0, 1, 3, 5, 7, 9, 12, 15, 18, 21, 24, 27, and 30 minutes. At each time point, samples were collected and centrifuged at 15,000 ×g for 1 minute. The supernatant was diluted in SM buffer (100 mM NaCl, 8 mM $MgSO_4$, 50 mM Tris-HCl, 0.01% gelatin [w/v], pH 7.5), and serial dilutions were plated using the DLA method to quantify non-adsorbed phages. Relative adsorption (RA%) was calculated as the percentage of phages adsorbed at each time point using the formula:

RA (%) = 100 × [1 − (titer of non-adsorbed phages at each time point / initial phage titer)].

The one-step growth curve assay was adapted from Hamza *et al*. [46]. Ten milliliters of a mid-exponential-phase bacterial culture were mixed with 100 µL of the phage suspension to achieve an MOI of 1 and incubated for 10 minutes at 37 °C to allow phage adsorption. The mixture was centrifuged (10,000 ×g for 5 minutes) to remove non-adsorbed phages; the supernatant was discarded, and the pellet was resuspended in 10 mL of pre-warmed BHI broth (supplemented with 10 µg/mL CAM). The culture was incubated at 37 °C with shaking at 100 rpm. Samples were collected immediately after pellet resuspension (T0) and at 10-minute intervals up to 100

minutes. Each sample was centrifuged (15,000 ×g for 1 minute), and the supernatant was plated by the DLA method.

Latent period and burst size were calculated from the one-step growth curve. The latent period was defined as the time interval between the adsorption and the beginning of the first burst (indicated by the initial rise in phage titer), and the burst size as number of virions produced per phage-infected bacterium calculated by the formula: (Nf – N0)/N0, where Nf corresponds to the mean titers of viral particles released after the first burst (plateau after the titer increase), and N0 corresponds to the mean titers of free viral particles before the first burst.

2.4 *In silico* analysis of phage receptor

To investigate the putative receptor-binding protein (RBP) of the CapO46 phage and infer its potential receptor on the bacterial surface, we performed an *in silico* comparative analysis using BLASTp. The amino acid sequence of the CapO46 minor tail protein (GenBank accession: XPO54741.1), previously predicted to function as an RBP, was aligned against known RBPs of *Rosenblumvirus* phages S13′ (BAL42324.1) and S24-1 (BAL42303.1), both of which have experimentally validated receptor specificities [20,24]. Sequence alignments were carried out using NCBI's BLASTp tool (https://blast.ncbi.nlm.nih.gov/Blast.cgi) with default parameters. Percent identity and query coverage were recorded to assess sequence similarity and potential functional conservation.

2.5 Phage challenge of the genome-wide CRISPRi library

2.5.1 Infectivity assay with CapO46 phage

To determine optimal collection time points for the CRISPRi-seq experiment with the CapO46 phage, a pilot infectivity assay was performed in duplicate. The MM267LG strain was grown at 37 °C in BHI broth (10 µg/mL CAM), either with (induced, I) or without (non-induced, NI) 30 ng/mL of anhydrotetracycline (aTc). Once cultures reached an OD_{600} of 0.8, they were diluted 1:100 in fresh BHI broth (10 µg/mL CAM) containing the same induction condition as before and incubated until reaching an OD_{600} of 0.4. At this point, treatment groups (+P) were infected with 100 µL of CapO46 phage suspension to achieve an MOI of 1, ensuring a high infection rate while minimizing the likelihood of multiple infections per cell. Control groups (−P) received

100 µL of SM buffer in place of the phage. Samples were taken at time 0 (before phage addition) and at 1, 2, 3, and 4 hours post-infection to determine bacterial viability (CFU/mL) and phage concentration (PFU/mL). For each time point, 100 µL aliquots were collected, serially diluted, and 10 µL of each dilution was spot-plated.

2.5.2 CRISPRi-seq assay

Based on differences in CFU/mL between the induced (+aTc) and non-induced (−aTc) phage-challenged groups observed in the pilot assay, three collection time points were selected for the CRISPRi-seq experiment: T0 (before phage addition), T1 (1 hour after phage addition), and T2 (3 hours after phage addition). The assay was conducted following the same experimental setup described above, but in quadruplicate. Instead of 100 µL aliquots, 10 mL of culture was collected at each time point. The full experimental design is illustrated in Figure 1.

Collected samples were centrifuged at 13,000 ×g for 5 minutes at 4 °C. Supernatants were discarded, and the resulting pellets were washed twice with phosphate-buffered saline (PBS; 137 mM NaCl, 2.7 mM KCl, 10 mM Na_2HPO_4, 1.8 mM KH_2PO_4, pH 7.4), and immediately frozen at −20 °C. For plasmid library extraction, pellets were resuspended in 250 µL of Solution I from the E.Z.N.A.® Plasmid DNA Midi Kit (Omega Bio-Tek, Norcross, GA, USA), followed by the addition of 1 µL lysostaphin (40 µg/mL) and 20 µL lysozyme (800 µg/mL). The mixture was incubated at 37 °C for 1 hour, and subsequent steps were carried out according to the kit manufacturer's protocol. Plasmid DNA concentration was quantified using the Qubit® dsDNA High Sensitivity Assay Kit (Invitrogen, Carlsbad, CA, USA).

For sequencing library preparation, Illumina indexing PCR was performed using indexed primers. PCR products were normalized and purified using the SequalPrep™ Normalization Kit (Thermo Scientific, Waltham, MA, USA) and the GenElute PCR Clean-Up Kit (Sigma-Aldrich, St. Louis, MO, USA), respectively, following the manufacturers' instructions. Sequencing was performed by Novogene (Cambridge, UK), using the Miseq platform.

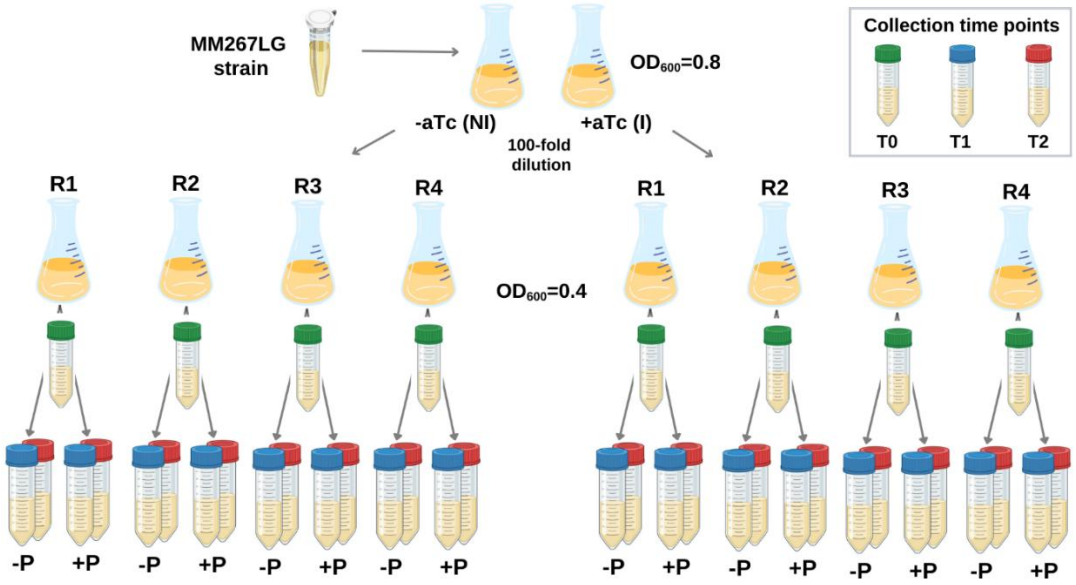

Figure 1. Experimental design of the CRISPRi-seq assay. −aTc = non-induced condition; +aTc = induced condition; R1–R4 = biological replicates 1 to 4; −P = control group (no phage added); +P = phage-challenged group; T0 = before phage infection; T1 = first post-infection time point; T2 = second post-infection time point.

2.5.3 Data analysis

The methodology for CRISPRi-seq data analysis was conducted according to Liu *et al*. [34], with specific adjustments tailored to the quantification of the effects of gene silencing and phage CapO46 infection at 1-hour and 3-hour time points. Briefly, paired-end sequencing data obtained from the genome-wide CRISPRi MM267LG library and the original plasmid pool were initially merged using PEAR (v0.9.11) to generate single continuous sequences. Subsequently, sgRNA counts were extracted from these merged sequences using 2FAST2Q (v2.5.0). Given the lower sequencing quality observed at the extremities of single-end sequencing datasets, alignment parameters in 2FAST2Q were specifically set to use nucleotides 2–17 of the sgRNA sequences, with all other parameters remaining at their default values. Differential enrichment analyses to assess significant changes in sgRNA abundance following induction and phage exposure were performed using DESeq2 in the R statistical environment (v4.1.1). Significant enrichment or depletion was determined by considering an absolute log2 fold-change (log2FC) greater than 1 and an adjusted p-value (Padj) less than 0.05.

For principal component analysis (PCA), sgRNA counts were normalized using DESeq2's blind regularized-logarithm (rlog) transformation to identify global sample

differences. During data validation, replicates exhibiting abnormal read count patterns or poor correlation with corresponding experimental replicates were excluded from subsequent analyses. Log2 fold-change values from 1-hour and 3-hour time point experiments were scaled for comparative analysis using the R function scale(), which divides by the root mean square of the values within each dataset, enabling accurate fitness quantifications across experimental conditions.

2.6 Phage challenge of CRISPRi-targeted strains

2.6.1 Growth curve and quantification of CFU and PFU

CRISPRi-targeted strains were evaluated under phage challenge to assess whether gene silencing affected the growth dynamics of infected bacteria. Briefly, cultures were grown in BHI broth (supplemented with 10 µg/mL CAM), with (I) or without (NI) aTc induction, until reaching OD_{600} = 0.8. Cultures were then diluted 1:100 in fresh medium as described previously. Once OD_{600} = 0.4 was reached, 180 µL of induced or non-induced bacterial culture and 20 µL of phage suspension were added to the wells of a 96-well polystyrene microplate (Kasvi, Brazil), achieving an MOI of 1. Control wells received 20 µL of SM buffer instead of phage. The microplate was incubated at 37 °C for 4 hours in a Multiskan™ GO spectrophotometer (Thermo Scientific, Waltham, MA, USA), with optical density measurements (OD_{600}) taken every 15 minutes.

At the end of the growth curve assay, 100 µL was collected from each well for viable cell count (CFU/mL), and another 100 µL was used for phage quantification (PFU/mL), to evaluate phage replication in the induced and non-induced conditions. For CFU determination, cultures were serially diluted in PBS and spread-plated onto BHI agar. For phage titration, cultures from phage-challenged wells were transferred to microcentrifuge tubes and centrifuged at 15,000 ×g for 1 minute. The supernatant was recovered, diluted in SM buffer, and titrated using the double-layer agar (DLA) method. Plates were incubated at 37 °C, and CFU/mL and PFU/mL values were recorded the following day.

2.6.2 Adhered cells count

To determine whether phage infection altered cell adhesion in the induced and non-induced cultures, an adhesion assay was performed using MBEC plates

(Innovotech Inc., Edmonton, AB, Canada) as described by Rice *et al*. [48], with some modifications. The 96-well base plate was prepared with 180 µL of bacterial suspension and 20 µL of phage suspension (MOI 1) or SM buffer. The MBEC lid with pegs was placed onto the base plate and incubated at 37 °C for 4 hours.

After incubation, the pegs were rinsed twice by immersing the MBEC lid in a fresh 96-well plate containing 250 µL PBS for 10 seconds. The pegs were then removed using sterilized pliers, transferred to microcentrifuge tubes containing 200 µL PBS, and placed in a sonication bath (Cristófoli, Brazil) for 10 minutes to detach adhered cells. The resulting suspensions were serially diluted in PBS, plated, and CFU/mL was determined the next day.

2.6.3 Crystal violet biofilm quantification assay

To assess whether phage infection influenced early biofilm formation in cells with or without gene silencing, a total biofilm biomass quantification assay using crystal violet (CV) staining was performed. A 96-well microtiter plate was set up and incubated under the same conditions previously described for the growth curve assay. After a 4-hour incubation period, the culture medium was removed, and the wells were rinsed three times with 0.9% (w/v) saline solution and allowed to air-dry at room temperature for one hour. The adherent cells were then fixed using methanol for 15 minutes, followed by staining with 0.1% (w/v) crystal violet solution for 20 minutes. Excess stain was removed by washing the wells three times with saline, and the plate was again air-dried for one hour. To solubilize the bound dye, 250 µL of an 80:20 (v/v) ethanol-acetone solution was added to each well and incubated for 15 minutes at room temperature. Absorbance was measured at 590 nm using a Multiskan GO spectrophotometer (Thermo Scientific, Waltham, MA, USA). Higher absorbance values correlate with increased biofilm biomass.

2.7 Statistical Analysis

Unless otherwise stated, all experiments were performed in triplicate, and statistical analyses were conducted using GraphPad Prism (GraphPad Software, La Jolla, CA, USA). Data normality was assessed using the Shapiro–Wilk test. For datasets with normal distribution, parametric tests such as the unpaired *t*-test and one-

way ANOVA were applied. For non-normally distributed data, the non-parametric Wilcoxon rank-sum test (Mann–Whitney) was used.

For growth curve analyses, statistical significance was determined using multiple *t*-tests with the Holm–Sidak method, and an alpha level of 0.05. Each time point was analyzed independently, without assuming equal standard deviation.

3. RESULTS

3.1 EOP, adsorption and one-step growth

The efficiency of plating (EOP) for CapO46 phage in *S. aureus* MM268 was 0.88, demonstrating that it can infect this strain in a highly productive manner (EOP≥0.5) [44]. The adsorption rate and one-step growth curve are shown in Figure 2. After 10 minutes, around 80% of the viral particles were adsorbed to the host cells, and more than 90% adsorption was only achieved with 30 minutes of incubation (Fig. 2A). Regarding the one-step growth curve, it demonstrates that CapO46 phage's latency period in the *S. aureus* MM268 was 30 minutes, and the burst size was around 103 PFU per infected cell (Fig. 2B).

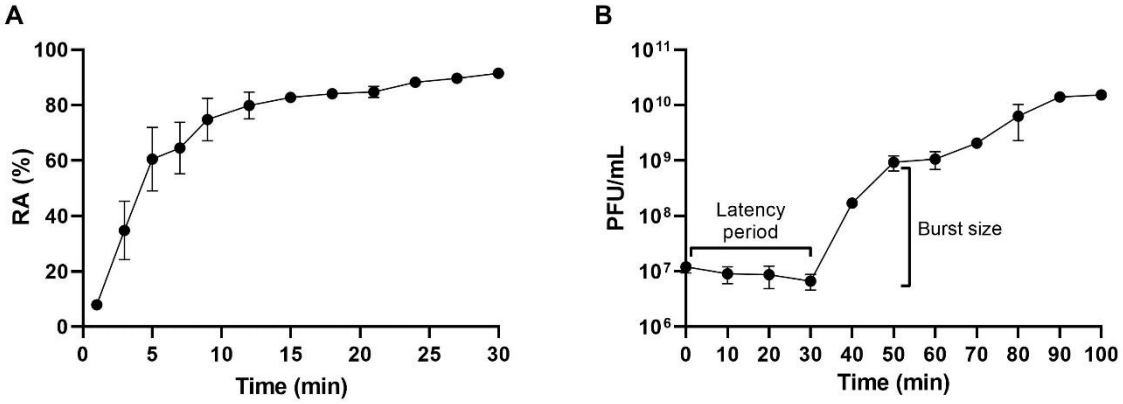

Figure 2. CapO46 phage A) Relative adsorption (RA%) and B) One-step growth curve in the *S. aureus* MM268.

3.2 *In silico* analysis of phage receptor

Bacteriophages that infect *S. aureus* typically use wall teichoic acids (WTAs) as receptors [18,23]. The interaction with WTAs is mediated by receptor-binding proteins (RBPs) that enable phage adsorption and subsequent infection [20]. To identify the putative RBP of the CapO46 phage, we conducted a BLASTp analysis of its predicted

proteins against the RBPs of *Rosenblumvirus* phages S13′ and S24-1, whose adsorption to *S. aureus* has been previously characterized using strains with modified WTA glycosidic linkages [20,24].

The analysis revealed that the minor tail protein (XPO54741.1) of CapO46 shows complete query coverage (100%) and high sequence identity (91.77%) with the RBP of phage S13′ (BAL42324.1), but only moderate identity (66.46%) with the RBP of phage S24-1 (BAL42303.1). These results suggest that CapO46, like S13′, may require β-O-GlcNAc-modified WTAs for host binding.

3.3 Phage challenge of the genome-wide CRISPRi library

3.3.1 Infectivity assay with CapO46 phage

A 4-hour infectivity assay was conducted using the MM267LG strain, which harbors the genome-wide CRISPRi system, to determine the optimal time points for sample collection in the CRISPRi-seq experiment. The 4-hour timeframe was based on findings by Liu *et al*. [34], who demonstrated that approximately 12 generations of bacterial growth are sufficient to identify most genes with fitness effects under their test conditions. We hypothesized that differences in bacterial concentration (CFU/mL) between the induced and non-induced phage-challenged groups (I +P vs. NI +P) could indicate fitness changes, i.e., increased susceptibility or resistance to phage infection.

MM267LG cultures were grown to stationary phase (OD_{600} = 0.8) to allow expression of dCas9 and depletion of the target gene products in the induced group. Cultures were then diluted 1:100 and grown to mid-exponential phase, followed by infection with CapO46 at an MOI of 1. CFU/mL and PFU/mL were quantified hourly over 4 hours to maximize lysis of susceptible cells and minimize the emergence of resistant mutants.

As shown in Figure 3, significant differences in CFU/mL were observed between the I +P and NI +P groups after 1 and 3 hours of infection ($p < 0.05$). At 1 hour, the CFU/mL decreased by 0.21 $\log_{10}$ (39.5%) in the induced group compared to the non-induced one. In contrast, at 3 hours post-infection, the CFU/mL increased by 0.27 $\log_{10}$ (46.3%) in I +P compared to NI +P. No significant differences were observed at 2 or 4 hours. Additionally, phage titers (PFU/mL) remained similar between groups at all time points, and no changes were detected in bacterial concentrations in control groups (NI −P and I −P). Although the changes in CFU/mL at 1 and 3 hours were modest, they

were statistically significant. Therefore, these time points were selected for CRISPRi-seq sample collection.

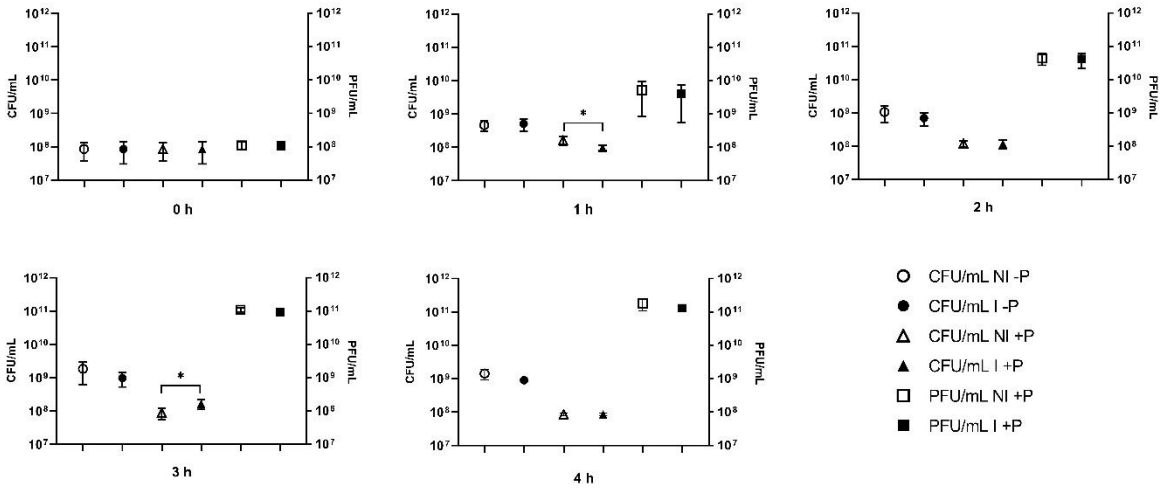

Figure 3. Infectivity assay of CapO46 phage in *S. aureus* MM267LG library. Bacterial CFU/mL was measured in both control (−P, no phage) and phage-challenged (+P, with phage) groups, under non-induced (NI) and induced (I) conditions. Phage PFU/mL was measured in the phage-challenged group (+P), for both NI and I conditions. Asterisks (*) indicate statistically significant differences ($p < 0.05$).

3.3.2 CRISPRi-seq

We used CRISPRi-seq to investigate bacterial host factors involved in susceptibility or resistance to phage infection. To this end, the sgRNA pool was sequenced before and after 1 and 3 hours of phage challenge, and analyzed to identify sgRNAs that were significantly over- or under-represented after infection ($|L2FC| > 1$, $P_{adj} < 0.05$). Genes were classified as essential when sgRNA abundance significantly decreased ($L2FC < -1$), neutral when sgRNA abundance remained stable ($-1 \leq L2FC \leq 1$), and costly when sgRNA abundance increased ($L2FC > 1$). Here, “essential” indicates that gene repression reduced bacterial fitness under the tested condition, while “costly” implies that silencing the gene improved bacterial fitness. A full list of results is presented in Supplementary Table S1.

From the global dataset, we observed that induction alone (without phage) identified 261 essential genes and 1 costly gene at 1 hour, and 260 essential genes and 1 costly gene at 3 hours. This analysis identifies genes whose sgRNA abundance changes due to induction alone, i.e., the genes that are essential for growth in BHI. In

the presence of phage, fewer genes were classified as essential (245 at 1 hour, 244 at 3 hours), but the number of costly genes increased (3 at 3 hours). This comparison aims to reveal genes whose sgRNA abundance changes due to induction in response to the phage, highlighting how phage presence alters gene fitness. Genes classified as costly specifically at the 3-hour time point with phage (SAOUHSC_00695 and *sarZ)* emerged as particularly interesting targets for further study due to their clear association with enhanced bacterial fitness under phage pressure.

Principal Component Analysis (PCA) (Figure 4) illustrated that the primary variance (PC1) was explained largely by induction with aTc, which activates dCas9 expression and gene silencing, thus significantly impacting bacterial growth and fitness profiles, whereas phage presence contributed to secondary variance (PC2), particularly evident at 3 hours, likely reflecting accumulated biological changes in bacterial populations exposed to phage pressure over time. This visualization confirmed that the CRISPRi-seq system effectively distinguished conditions based primarily on induction and secondarily on phage exposure, validating the robustness of the assay.

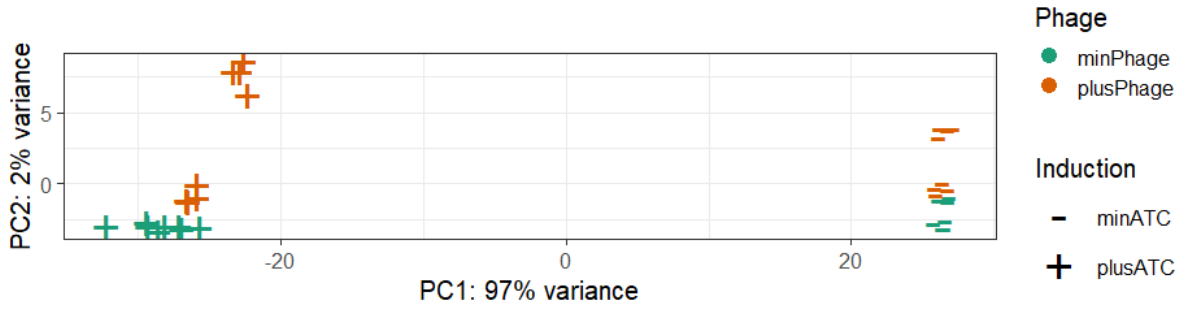

Figure 4. Principal Component Analysis (PCA) of rlog-transformed sgRNA counts across all experimental conditions and time points. Each point represents a biological replicate under different experimental conditions: induced (+aTc) or non-induced (-aTc), in the presence (plusPhage) or absence (minPhage) of CapO46 phage.

A total of five genes were classified as essential under phage challenge (but not in its absence), suggesting that their repression increased bacterial sensitivity to phage. In contrast, two genes were classified as costly under this condition (but not without phage), suggesting that their silencing may contribute to resistance (Table 1). At the 1-hour time point, only SAOUHSC_00551 shifted from neutral (in the absence of phage) to essential (in the presence of phage), a classification that persisted at 3 hours. Additionally, at 3 hours, four more genes were classified as essential—

SAOUHSC_00003, SAOUHSC_00473, SAOUHSC_02355, and *rpiRc* (SAOUHSC_02589)—while two others, SAOUHSC_00695 and *sarZ* (SAOUHSC_02669), were classified as costly.

SAOUHSC_00551 encodes a hypothetical protein of unknown function and is the first gene in an operon that includes *bshB2* and *folE2*. SAOUHSC_00003 also encodes a hypothetical protein, but contains a known S4 domain (protein YaaA), and is the first gene in an operon involved in DNA metabolism (downstream genes include *recF*, *gyrB*, and *gyrA*). SAOUHSC_00473 encodes a hypothetical protein with no predicted domain or polycistronic organization. SAOUHSC_02355 is predicted to encode an acetyltransferase, while *rpiRc* is a metabolic regulator linked to carbon flux and virulence gene expression. *sarZ* encodes a redox-sensitive transcriptional regulator involved in adhesion and biofilm formation, and SAOUHSC_00695 is predicted to function as a metal chaperone, possibly involved in zinc homeostasis.

An additional gene, *mgrA* (SAOUHSC_00694), stood out as costly across all tested conditions (with and without phage, at both 1 and 3 hours). Notably, *mgrA* displayed the highest L2FC observed under any condition at 3 hours with phage (L2FC = 2.39, Padj = 1.7E-70). This gene encodes a global regulator controlling clumping, virulence, surface protein expression, and biofilm formation through repression of adhesins [49].

Since phage adsorption in *S. aureus* is often dependent on specific glycosylation patterns of wall teichoic acids (WTAs), particularly the presence of α-O-GlcNAc and β-O-GlcNAc residues that serve as receptors for some phages [19], we sought to evaluate the expression of the glycosyltransferase genes *tarS* and *tarM*, responsible for these modifications. Although the MM267LG CRISPRi library does not include sgRNAs directly targeting *tarS* or *tarM* due to their location within operons [182], we assessed the abundance of sgRNAs targeting the first genes of the respective operons—*ispD (tarI)* for the *tarS* operon and *SAOUHSC_00972* for the *tarM* operon—as a proxy, considering the polar effect of CRISPRi. Our results showed that the sgRNA targeting *ispD (tarI)* had an L2FC < −1 under all conditions, classifying it as essential, with no significant variation across treatments. In contrast, *SAOUHSC_00972* was classified as neutral in all conditions, with a slight, non-significant reduction in sgRNA abundance at 3 hours post-phage challenge (Table S1).

Table 1. Genes influencing *S. aureus* susceptibility to CapO46 phage infection identified through genome-wide CRISPRi-seq screening.

Target locus	Target genes	Function	log_2FC	P_{adj}	Time
SAOUHSC_00551	_00551	Unknown	-1,31	6,1E-05	1 h
SAOUHSC_00003	_00003	Unknown	-1,86	1,3E-15	3 h
SAOUHSC_00473	_00473	Unknown	-1,39	7,5E-06	
SAOUHSC_00551	_00551	Unknown	-1,83	3,0E-16	
SAOUHSC_02355	_02355	Unknown	-2,09	1,0E-10	
SAOUHSC_02589	***rpiRc***	**Phosphosugar-binding transcriptional regulator**	**-1,42**	**3,8E-09**	
SAOUHSC_02669	***sarZ***	**Transcriptional regulator**	**1,84**	**1,7E-42**	
SAOUHSC_00695	**_00695**	**Unknown**	**1,87**	**2,6E-47**	
SAOUHSC_00694*	***mgrA***	**Transcriptional regulator**	**2,39**	**1,7E-70**	

* The only “costly” gene under all tested conditions. The L2FC value shown corresponds to the highest observed among all conditions.
Experimentally verified hits are highlighted in bold.

3.4 Functional validation of CRISPRi-targeted strains under phage challenge

To validate the CRISPRi-seq findings, we used CRISPRi strains targeting genes that were predicted to confer either resistance or increased susceptibility to phage infection. The selected targets included two genes classified as "costly" at 3 hours post-infection (*sarZ* and *SAOUHSC_00695*), the only gene classified as costly across all tested conditions (*mgrA*), and one gene classified as essential in the presence of phage and showing a significant interaction effect (*rpiRc*). We also constructed double-target CRISPRi strains (*sarZ/mgrA*, *sarZ/SAOUHSC_00695*, and *SAOUHSC_00695/mgrA*) to assess whether simultaneous gene silencing enhances the resistance phenotype.

We assessed the susceptibility of induced and non-induced strains to phage CapO46 by analyzing bacterial growth curves, quantifying viable planktonic cells (CFU/mL), and measuring phage titers (PFU/mL) after 4 hours of infection. Additionally, the effect of phage on early biofilm development was evaluated through adhered cell quantification using the MBEC assay and total biofilm biomass via crystal

violet staining. Although the CRISPRi-seq was performed over a 3-hour period, we extended the assays to 4 hours to match approximately 12 bacterial generations and better capture early biofilm dynamics.

As in previous assays, four conditions were tested for each strain: non-induced cultures without phage (NI −P), induced cultures without phage (I −P), non-induced cultures with phage (NI +P), and induced cultures with phage (I +P).

3.4.1 Effect of gene silencing on bacterial growth and phage replication

Bacterial growth curves, planktonic cell counts (CFU/mL), and phage titers (PFU/mL) at 4 hours are shown in Figure 5. For all strains, a significant ($P < 0.05$) reduction in OD was observed in the NI +P group compared to NI −P, demonstrating the efficient lysis of *S. aureus* cultures by CapO46 under standard growth conditions. In these same groups, phage titers increased by approximately 2.8 $\log_{10}$ PFU/mL over the initial inoculum.

In the control strain MM268 (Fig. 5A), no differences were observed between NI −P and I −P or between NI +P and I +P, indicating that aTc induction alone does not affect bacterial growth or phage infectivity. Phage titers confirmed this, with both NI +P and I +P groups exhibiting a similar increase (~2.85 $\log_{10}$ PFU/mL).

In the growth curve of the single-target strain MK2137 (Fig. 5B), which carries an sgRNA targeting the sarZ gene, no significant differences were observed between induced and non-induced cultures without phage (NI −P vs. I −P) or between those with phage (NI +P vs. I +P). However, CFU/mL counts at the 4-hour mark revealed a significant increase of 1.23 $\log_{10}$ viable cells in the I +P group compared to the NI +P group. At the same time, phage titration at the end of the experiment showed that the phage concentration in the I +P group was significantly lower (by 0.56 $\log_{10}$) than in the NI +P group. These results are consistent with the CRISPRi-seq findings and indicate that silencing sarZ reduces bacterial susceptibility to phage infection.

In strains MK2138 (Fig. 5C) and MK2139 (Fig. 5D), targeting *SAOUHSC_00695* and *mgrA*, respectively, I −P cultures showed slightly but significantly lower OD compared to NI −P throughout the experiment. However, CFU/mL counts were not significantly different at 4 hours. In both strains, I +P groups exhibited increased growth and higher CFU/mL (2.1 and 1.8 $\log_{10}$, respectively) compared to NI +P, suggesting resistance to phage infection upon gene silencing. This was confirmed by phage

titration, as PFU/mL in the I +P group for both strains remained comparable to the initial inoculum, indicating that phage replication was blocked.

For strain MK2140 (Fig. 5E), targeting *rpiRc*, a significant reduction in the growth curve of the I −P group compared to NI −P was detected as early as 30 minutes post-incubation and persisted throughout the 4-hour assay. A similar trend was seen in the CFU/mL count at 4 hours, with a 0.3 $\log_{10}$ reduction in the I −P group, suggesting that *rpiRc* silencing impairs bacterial growth. In the presence of phage, a further reduction in the I +P growth curve compared to the NI +P group was noted starting at 3 hours post-infection, continuing to the end of the experiment. This aligns with the CRISPRi-seq results, where *rpiRc* showed a significant drop in L2FC only at the 3-hour time point. The increased susceptibility to phage observed in I +P was further supported by a 0.43 $\log_{10}$ CFU/mL decrease compared to NI +P. Despite these findings, phage titration at the end of the experiment showed no significant difference in PFU/mL between the I +P and NI +P groups.

In double-target strains MK2155 (Fig. 5F) and MK2157 (Fig. 5 H), I −P cultures showed slight OD reduction compared to NI −P, but CFU/mL counts were unchanged. In MK2156 (Fig. 5G) (*sarZ/SAOUHSC_00695*), no differences were seen in growth or CFU/mL between NI −P and I −P. However, in all three double-target strains, the I +P groups showed significantly higher OD and CFU/mL compared to NI +P—1.8, 4.0, and 2.35 $\log_{10}$ CFU/mL for MK2155, MK2156, and MK2157, respectively—reaching levels comparable to the I −P condition. This indicates that combined gene silencing conferred resistance to phage infection. In MK2156, phage titration showed no increase in PFU/mL, indicating a complete block in viral replication. This result corroborates the CFU/mL data and suggests that silencing *sarZ* and *SAOUHSC_00695* together conferred full resistance to phage infection. In contrast, in MK2155 and MK2157, phage titers in the I +P groups increased by 0.55 and 0.80 $\log_{10}$ PFU/mL, respectively. Although the CFU/mL profiles for these strains indicated phage resistance, the observed increase in PFU/mL demonstrates that this resistance was not complete, as phage replication still occurred. Notably, silencing *sarZ* or *SAOUHSC_00695* together with *mgrA* partially restored phage replication, which was otherwise fully suppressed in the *mgrA*-only silenced strain MK2139. These results suggest that MgrA's role in phage susceptibility may be mediated through downstream targets. Moreover, phage replication was reduced by 1.56 $\log_{10}$ PFU/mL in *sarZ/mgrA* double mutants compared to *sarZ* alone, while *SAOUHSC_00695/mgrA* mutants

showed ~0.7 $\log_{10}$ increase in replication compared to the single-gene silencing conditions.

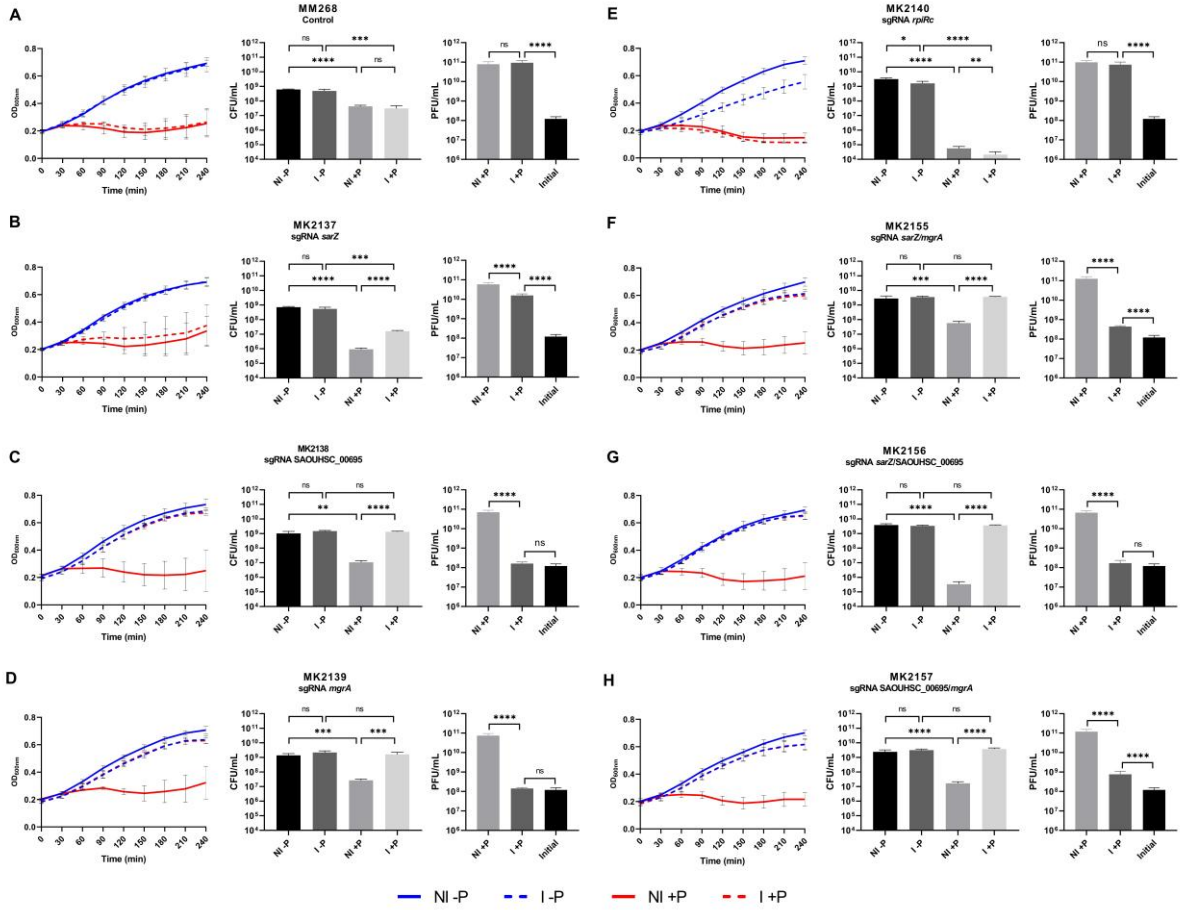

Figure 5. Bacterial growth curves and endpoint analyses of CRISPRi-targeted *S. aureus* strains under phage challenge. Growth curves were monitored over 4 hours (240 min) for each strain in the absence (−P, blue lines) and presence (+P, red lines) of phage CapO46, under non-induced (NI, solid lines) and induced (I, dashed lines) conditions. Standard deviations (black bars) are shown at the 30-minute time point. Adjacent bar graphs represent planktonic bacterial quantification (CFU/mL) after 4 hours and phage titration (PFU/mL) at the start (initial) and after 4 hours (NI +P and I +P). Error bars indicate standard deviation. Statistically significant differences between groups are denoted as follows: P < 0.05 (), P < 0.0001 (***), and ns indicates no significant difference.

3.4.2 Effect of gene silencing on cell adhesion

To evaluate the impact of target gene silencing on cell adhesion in the presence or absence of phage, we quantified the number of adhered cells on MBEC pegs after 4 hours of incubation. Results, expressed as CFU/mL, are shown in Figure 6. As expected, all strains exhibited a significant reduction (P < 0.05) in the NI +P group compared to NI −P (not annotated in the figure to avoid visual overload), confirming

phage lytic activity against adhered cells under normal conditions. Reductions of 2.2, 2.7, 1.8, 3.4, 1.9, 1.8, and 3.1 $\log_{10}$ CFU/mL were observed for strains MM268, MK2137, MK2138, MK2139, MK2155, MK2156, and MK2157, respectively. For strain MK2140, adhered cells were undetectable in phage-exposed groups (NI +P and I +P).

In the control strain MM268 (Fig. 6A) and in MK2137 (Fig. 6B), no significant differences were observed between NI −P and I −P or between NI +P and I +P, indicating that neither aTc induction nor *sarZ* silencing affected adhesion at 4 hours. For strains MK2138 (Fig. 6C), MK2139 (Fig. 6D), MK2140 (Fig. 6E), MK2155 (Fig. 6F), and MK2156 (Fig. 6G), significant reductions of 1.2, 0.7, 1.8, 0.6, and 1.4 $\log_{10}$ CFU/mL, respectively, were observed in the I −P groups compared to NI −P. However, CFU/mL measurements in the previous section showed no significant reduction in planktonic bacterial counts for these strains, indicating that the decrease in adhered cells was not due to impaired bacterial growth. This suggests a more direct impact of gene silencing on the adhesion capacity itself. In contrast, MK2157 (Fig. 6H) showed no significant difference in adhesion between NI −P and I −P, consistent with the unchanged CFU/mL previously observed under the same conditions.

Comparing I +P to NI +P groups, significantly higher adhesion was observed in I +P for MK2138, MK2139, MK2155, MK2156, and MK2157, with increases of 1.5, 2.7, 1.3, 2.9, and 1.2 $\log_{10}$ CFU/mL, respectively. These findings are consistent with the CFU/mL results from the previous assay, which showed increased viable planktonic cell counts in the I +P groups for these strains. This suggests that although gene silencing may impair adhesion—as indicated by reductions in the I −P groups—the greater bacterial survival in the I +P groups compared to NI +P was sufficient to result in higher adhered cell numbers despite potentially reduced adhesion capacity.

For MM268 and MK2137, significant differences were observed only between phage-exposed and unexposed groups (NI −P vs. NI +P and I −P vs. I +P), indicating that phage activity alone influenced adhesion. Reductions in I +P vs. I −P were 2.0 $\log_{10}$ for MM268 and 2.4 $\log_{10}$ for MK2137; MK2140 showed a ~3 $\log_{10}$ reduction but could not be precisely quantified due to undetectable levels. Conversely, MK2138 and MK2156 showed increased adhesion in I +P vs. I −P (1.0 and 2.5 $\log_{10}$, respectively), while no significant differences were observed for MK2139 and MK2155.

In MM268, MK2137, and MK2140, reduced adhesion in I +P vs. I −P aligned with planktonic CFU/mL reductions reported previously. In MK2157, however, there was no difference in adhered cell counts between NI −P and I −P, indicating that silencing

SAOUHSC_00695 together with *mgrA* does not affect adhesion in the absence of phage. Yet, under phage challenge, a reduction in adhesion was observed in I +P compared to I −P, despite equivalent planktonic CFU/mL values between these two groups. This suggests that the silencing of *SAOUHSC_00695* together with *mgrA* specifically impairs adhesion when phage is present. Conversely, in MK2138 and MK2156, phage exposure appeared to slightly enhance adhesion when *SAOUHSC_00695* was silenced alone or in combination with *sarZ*.

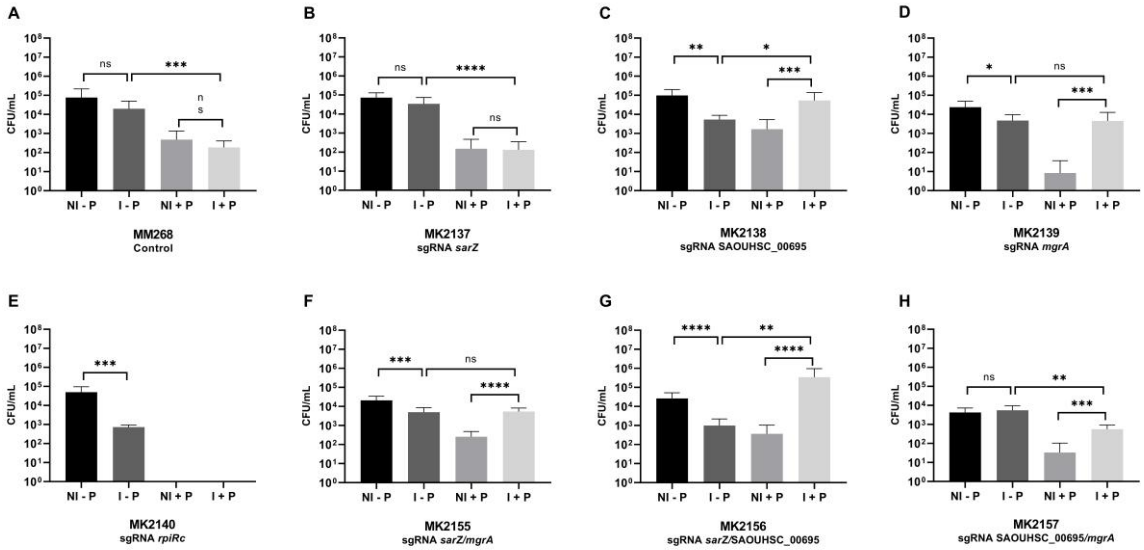

Figure 6. Adhered cell counts of CRISPRi-targeted *S. aureus* strains on MBEC pegs after a 4-hour incubation period. Bars represent the mean CFU/mL of three replicates, with error bars indicating standard deviation. NI −P = non-induced, no phage; I −P = induced, no phage; NI +P = non-induced, with phage; I +P = induced, with phage. Statistically significant differences ($P < 0.05$) between groups are indicated by asterisks: $P < 0.05$ (*), $P < 0.01$ (**), $P < 0.001$ (***), and $P < 0.0001$ (****). "ns" indicates no significant difference.

3.4.3 Effect of gene silencing on biofilm biomass

To evaluate whether gene silencing affected total biofilm biomass, we quantified biofilm formation after 4 hours using a crystal violet assay (Figure 7). Biofilm biomass is expressed as absorbance at 590 nm (Abs 590nm), and significant differences ($P < 0.05$) between groups are indicated with asterisks.

In the control strain MM268 (Fig. 7A), no significant differences were observed between NI −P and I −P or between NI +P and I +P, confirming that aTc induction alone had no impact on biofilm biomass. However, biofilm was significantly reduced in

phage-challenged groups (NI +P and I +P) compared to their respective controls, consistent with the reductions in planktonic population observed previously.

For the MK2137 strain (sarZ silencing, (Fig. 7B), biofilm biomass was significantly reduced in I −P compared to NI −P, despite no difference in planktonic CFU/mL, suggesting that *sarZ* contributes to biofilm formation independently of cell density. In the presence of phage, I +P produced slightly more biofilm than I −P, even though CFU/mL was lower in I +P. This may reflect phage-related stress or DNA release from cell lysis, which can enhance biofilm production by contributing to the extracellular matrix [183,184]. Nonetheless, both I +P and NI +P produced significantly less biofilm than NI −P, indicating that *sarZ* silencing and phage infection both reduce total biomass.

In MK2138 (SAOUHSC_00695 silencing, (Fig. 7C), biofilm biomass was significantly reduced in I −P versus NI −P, with no significant changes in CFU/mL. Although I +P had higher planktonic CFU/mL than NI +P, both groups showed similar biofilm levels, suggesting that silencing this gene suppresses biofilm even when cell numbers increase under phage resistance.

In MK2139 (mgrA silencing, (Fig. 7D), biofilm biomass was significantly reduced in I −P versus NI −P, and also in I +P compared to NI +P. Despite a 1.8 $\log_{10}$ increase in CFU/mL in I +P versus NI +P, biofilm remained lower in I +P, reinforcing *mgrA*'s role in biofilm regulation regardless of population size.

MK2140 (rpiRc silencing, Figure 7E) showed no significant differences in biofilm biomass between groups, even though CFU/mL was reduced in I −P and I +P compared to NI −P. These results indicate that *rpiRc* silencing does not significantly affect early biofilm formation under the tested conditions.

In MK2155 (sarZ/mgrA silencing, Figure 7F), biofilm biomass was significantly reduced in I −P and I +P compared to their respective non-induced controls, indicating that simultaneous silencing of *sarZ* and *mgrA* impairs biofilm formation. No difference was observed between NI −P and NI +P, despite NI +P showing a lower CFU/mL, suggesting that biofilm production was maintained even under phage pressure when the genes were not silenced.

In MK2156 (sarZ/SAOUHSC_00695 silencing, Figure 7G), biofilm biomass was significantly reduced in I −P and NI +P compared to NI −P, indicating that both gene silencing and phage infection impaired biofilm formation. No significant difference was observed between I −P and I +P or between NI +P and I +P, even though CFU/mL was

higher in the I +P group. This suggests that silencing *sarZ* and *SAOUHSC_00695* compromises biofilm production regardless of increased bacterial survival under phage challenge.

In MK2157 (SAOUHSC_00695/mgrA silencing, Figure 7H), a significant reduction in biofilm biomass was observed in I −P compared to NI −P, with no differences in CFU/mL. No significant changes were found between NI +P and I +P or between I −P and I +P, even though CFU/mL was higher in the I +P group. These results suggest that silencing *SAOUHSC_00695* and *mgrA* reduces biofilm formation independently of bacterial population density.

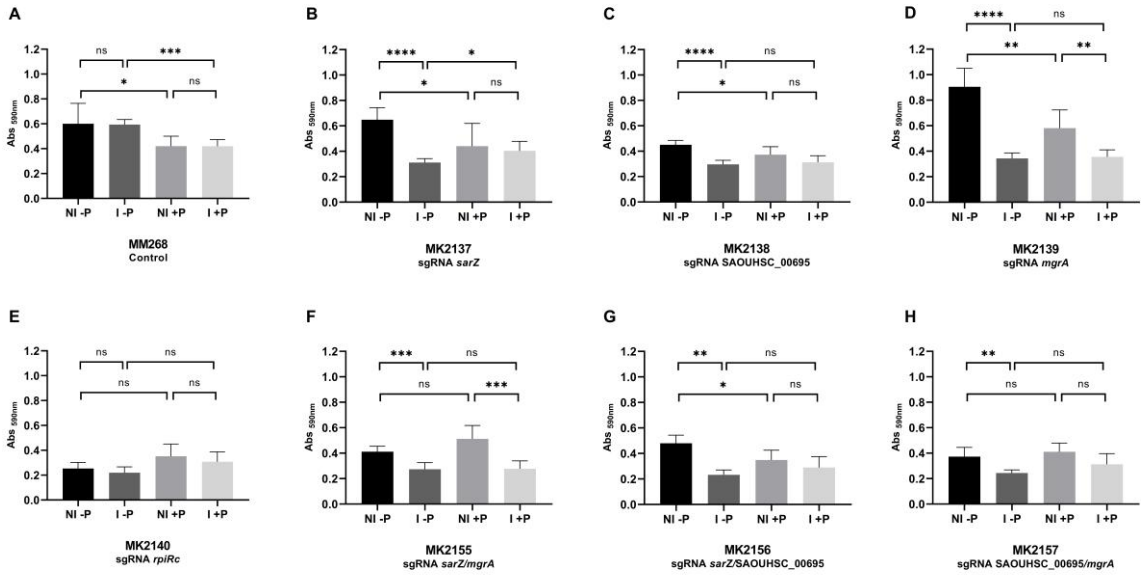

Figure 7. Total biofilm biomass of CRISPRi-targeted *S. aureus* strains after a 4-hour incubation period, quantified using the crystal violet assay. Bars represent the mean CFU/mL of three replicates, with error bars indicating standard deviation. NI −P = non-induced, no phage; I −P = induced, no phage; NI +P = non-induced, with phage; I +P = induced, with phage. Statistically significant differences ($P < 0.05$) between groups are indicated by asterisks: $P < 0.05$ (*), $P < 0.01$ (**), $P < 0.001$ (***), and $P < 0.0001$ (****). "ns" indicates no significant difference.

4. DISCUSSION

CapO46 infection in strain MM268, a prophage-free derivative of S. aureus 8325-4, exhibited significant differences compared to its original host (S. aureus O46), including slower adsorption (30 min to reach 90% vs. 5 min in the original host) and a higher burst size (103 vs. 30 PFU/cell). Strains derived from 8325 are known to have reduced activity of the alternative sigma factor SigB, due to deletions in the rsbU

regulatory gene [53]. Since SigB plays an important role in environmental stress responses [54–56], we hypothesize that diminished SigB activity may impair bacterial responses to phage infection. On the other hand, the higher burst size observed in MM268 may be attributed to the absence of prophages in this strain, eliminating possible superinfection exclusion mechanisms and metabolic competition [15]. Similarly, Finstrlová *et al*. [57], also reported increased burst sizes in prophage-free strains compared to their lysogenic counterparts. Despite these kinetic differences, phage CapO46 was still able to productively infect MM268 with high efficiency (EOP = 0.88).

Following this initial infectivity assessment in the genome-wide CRISPRi strain, we aimed to identify ideal timepoints for CRISPRi-seq that would reveal host factors involved in phage susceptibility or resistance. The strategy of quantifying CFU/mL at various timepoints was based on the hypothesis that the proportion of costly and essential gene knockdowns would change over time as infection progressed. Indeed, differences were observed between the 1-hour and 3-hour timepoints. However, at 1 hour, only one essential gene showed a significant reduction in sgRNA abundance, suggesting increased susceptibility upon silencing. Although unlikely, it cannot be ruled out that the drop in CFU/mL was caused solely by this one gene. At 3 hours, six essential genes showed decreased sgRNA abundance, compared to only three costly genes, suggesting that adaptation of the bacterial population—via silencing of resistance-favoring genes—may have outweighed cell death caused by silencing of essential ones.

The genome-wide CRISPRi-seq assay revealed essential genes required for bacterial survival during phage infection, previously undescribed for *S. aureus* phages. The essential gene SAOUHSC_00551 is part of an operon that encodes proteins involved in bacillithiol and folate biosynthesis (*bshB2* and *folE2*), which are important for oxidative stress resistance, immune evasion, and folate metabolism under stress conditions [58–61]. Another essential gene, SAOUHSC_00473, has an unknown function but is located downstream of *rplY*, which encodes ribosomal protein L25—associated with stress adaptation in *B. subtilis* [62,63]. SAOUHSC_00003 encodes a protein with an RNA-binding S4 domain related to YaaA, which in *B. subtilis* is involved in ribosome assembly and possibly in coordinating DNA replication with ribosome biogenesis, especially under stress [64].

The uncharacterized gene SAOUHSC_02355, also essential, is the first in an operon that includes *glyA*, *upp*, and *mnaA*, all involved in essential metabolic functions. *glyA* is linked to folate metabolism and serine-to-glycine conversion, and plays a role in lysostaphin resistance and bacterial virulence [65,66]. *upp* is involved in nucleotide recycling and is induced by acid shock, indicating a role in pH stress adaptatio [67,68]. *mnaA* is required for wall teichoic acid (WTA) biosynthesis and has been proposed as an antibiotic target [69,70]. SAOUHSC_02355 also contains an IPR028345 domain associated with aminoglycoside resistance (e.g., gentamicin, kanamycin) [71]. Thus, this operon may integrate metabolic, stress response, and antimicrobial resistance functions. The gene *rpiRc*, discussed later, is a metabolic regulator that modulates virulence via the agr system [72,73]. Together, these findings suggest that metabolic processes, stress responses, and virulence regulation are fundamental for *S. aureus* survival during phage infection.

Phenotypic confirmation of CRISPRi-seq results—via 4-hour growth curves and endpoint CFU/mL and PFU/mL counts—demonstrated that silencing *sarZ*, SAOUHSC_00695, *mgrA*, and *rpiRc* significantly impacted phage susceptibility in ways consistent with CRISPRi-seq findings. Silencing the costly gene *sarZ* reduced bacterial susceptibility to CapO46, while silencing the costly genes SAOUHSC_00695 and *mgrA* led to complete resistance, suggesting these genes are necessary for productive infection. Conversely, silencing the essential gene rpiRc increases bacterial susceptibility to phage infection after 3 hours. Since changes in growth curves became more evident after the first hour of incubation, it explains why these genes—except *mgrA*—were classified as essential or costly only at the 3-hour CRISPRi-seq, while being neutral at 1 hour. This supports that the phenotypic effects of gene silencing became more pronounced over longer infection periods.

Previous studies have shown that MgrA, a global regulator in *S. aureus*, participates in WTA glycosylation via the ArlRS two-component system, which activates *mgrA* to repress *tarM*, allowing *TarS* to add β1,4-GlcNAc to WTA [74]. In *mgrA*-deficient mutants, β1,4-GlcNAc is absent, though α1,4-GlcNAc levels remain unchanged. As CapO46 likely depends on β1,4-GlcNAc for adsorption, complete *mgrA* silencing in strain MK2139 may have removed this glycopolymer from the cell surface, blocking phage infection. A similar effect may have occurred in *sarZ*-silenced strain MK2137, since *sarZ* and *mgrA* regulate each other [75,76], and *sarZ* silencing may have indirectly reduced β1,4-GlcNAc levels. Moreover, *sarZ* also modulates virulence

factors, biofilm formation, and stress responses [75–77], and its deletion has been associated with decreased *mgrA*, *hla*, and *sspA* expression, and increased spa expression [75]. Since Protein A overexpression can physically block phage binding sites [25], increased spa expression may have contributed to reduced phage replication in both *sarZ*- and *mgrA*-silenced strains, as these mutants are known to upregulate spa [78,79]. To determine whether resistance stems from β1,4-GlcNAc loss or Protein A overexpression, additional experiments such as RNA-seq, RT-qPCR, or assays using β1,4-GlcNAc-deficient mutants are required.

Besides *mgrA*, *sarZ*, and SAOUHSC_00695, other WTA glycosylation-related genes like *tarS* and *tarM* could also affect phage susceptibility. However, their direct effects could not be evaluated, as they belong to operons where only the first gene was targeted by sgRNA—*ispD* (*tarI*) and SAOUHSC_00972, respectively. Since *tarI* and *tarJ* are essential and form a duplicated cluster whose backup copy cannot fully compensate for loss of the main genes [80–83], silencing them is lethal. Our CRISPRi-seq data confirmed this, as *ispD* (*tarI*) was essential under all conditions. Therefore, it remains unclear whether *tarS* loss affects phage infection. Regarding *tarM*, its absence is known to favor binding of phages that recognize β-O-GlcNAc-modified WTAs [29]. However, SAOUHSC_00972 was classified as neutral. Although the CRISPRi-seq approach proved robust in identifying and validating host factors, the technique's ability to evaluate genes such as *tarS* and *tarM* was limited by their genomic context. To overcome this limitation, future studies should design gene-specific sgRNAs targeting *tarS* and *tarM* directly, enabling a more precise dissection of their individual contributions.

Given that *sarZ* and *mgrA* directly influence biofilm formation in *S. aureus* [75,84], we evaluated whether their silencing impacted early biofilm formation and cell adhesion after 4 hours. *sarZ* deletion is associated with increased *sarA* expression (a positive biofilm regulator) and capsule gene activation through SigA-dependent Pcap promoter binding [75,77]. Yet, we observed significantly reduced biofilm biomass in the I −P group compared to NI −P. Since cell adhesion was similar between groups, this decrease seems linked to reduced extracellular matrix production. As SarZ activates *mgrA*, which regulates capsule genes (*cap*), disruption of this pathway may have decreased capsule production and thus matrix synthesis in early biofilm. On the other hand, the I +P group showed higher cell viability than NI +P, but similar levels of adherent cells and biofilm biomass, suggesting that phage infection in *sarZ*-silenced

strains impaired not only matrix production but also adhesion. Interestingly, the I +P group produced more biofilm than I −P, despite having fewer planktonic and adherent cells, suggesting phage infection may trigger matrix production via *sarZ*-independent pathways, possibly through eDNA release from lysed cells, as shown in responses to antibiotics and phages [51,85–89].

mgrA silencing led to reductions in both biofilm formation and cell adhesion. Although *mgrA* mutants are associated with increased biofilm formation at later stages [84] this effect appears absent in early stages. Literature shows that *mgrA* regulates *capA* transcription, and its deletion may reduce capsule production [90], potentially impairing initial biofilm formation. Moreover, surface protein overexpression (e.g., Ebh, SraP, SasG) in *mgrA* mutants may hinder cell clustering—a critical early step in biofilm development [49,91,92]. These findings explain the reduction observed in our 4-hour assays, contrasting with studies on mature biofilms (≥16 hours). Notably, in strain MK2139, both I +P and I −P groups had similar levels of adherent cells and biofilm, indicating that phage resistance due to *mgrA* silencing is unrelated to enhanced biofilm formation. Instead, it likely results from WTA glycosylation changes. Conversely, the increased biofilm in the NI +P group, despite reduced bacterial growth, supports the idea that phage-induced lysis promotes biofilm formation via eDNA release.

SAOUHSC_00695 encodes a hypothetical protein with a CobW domain, part of the G3E GTPase superfamily. These proteins share features with COG0523 members and are associated with metal homeostasis and maturation of metalloproteins involved in cobalamin biosynthesis, nickel metabolism, urease activation, and zinc incorporation [93]. Although the function of SAOUHSC_00695 remains unclear, normal bacterial growth in its absence suggests it is non-essential without phage, possibly due to compensatory pathways. However, its role in phage infection may involve cell wall modulation, since metal homeostasis affects WTA, peptidoglycan, and surface protein biosynthesis [74,94,95]. Kuijk *et al*. [74] screened *S. aureus* mutants by immunoblotting with Fab fragments of monoclonal antibodies against α1,4- or β1,4-GlcNAc-modified WTA. The SAUSA300_0673 mutant, corresponding to SAOUHSC_00695 in strain 8325, showed strong binding to α1,4 and weak to β1,4 Fab, suggesting this gene influences WTA glycosylation. SAOUHSC_00695 is also located downstream of *mgrA* and overlaps the 5′ UTR sRNA S266, raising the possibility of co-regulation. The phenotypic similarity between SAOUHSC_00695 and *mgrA* silencing supports this.

Partial restoration of viral replication in the double mutant SAOUHSC_00695/*mgrA* (MK2157) suggests activation of compensatory pathways or baseline expression of infection-enabling genes. *mgrA* regulates metal transporter genes like *mntH*, whose expression increases in its absence, helping maintain manganese and zinc homeostasis [96–98]. Elevated *mntH* in the double mutant may have restored metal balance and thus phage permissiveness. Since *sarZ* and *mgrA* share regulatory targets, their combined silencing (MK2155) may have relieved repression or activated compensatory mechanisms that restored infection. In contrast, no restoration occurred in the *sarZ*/SAOUHSC_00695 mutant (MK2156), suggesting weaker regulatory overlap. This implies that while *sarZ* may indirectly influence *mgrA* expression, it may not suffice to trigger the same compensatory mechanisms observed with direct *mgrA* silencing. Overall, these results suggest a complex regulatory network balancing the expression of genes essential for phage infection—whether involved in WTA modification, as literature suggests, or yet-unidentified pathways.

The *rpiRc* gene, classified as essential, encodes a transcriptional regulator of the pentose phosphate pathway (PPP) and modulates RNAIII levels, acting as a metabolic sensor that controls the *agr* quorum-sensing system [72,73]. Gaupp *et al*. [73] showed that *rpiRc* inactivation in *S. aureus* reduces Protein A production while increasing RNAIII, hemolytic activity, and capsule synthesis, contributing to higher pathogenicity in murine models. Moreover, RNAIII modulates cell wall integrity via peptidoglycan and LTA biosynthesis [99,100], and PPP is involved in cell wall architecture, affecting β-lactam resistance [101]. Thus, increased RNAIII and PPP deregulation caused by *rpiRc* silencing may have disrupted bacterial metabolism, adhesion, and biofilm formation, and altered cell wall structure, increasing phage susceptibility. Furthermore, decreased Protein A expression, which can mask phage receptors [25], may have exposed them. Reduced adhesion in the I −P group, despite similar planktonic counts as NI −P, may reflect lower expression of surface adhesins—known to be downregulated by RNAIII [102]. In both +P groups, adherent cells were undetectable, likely due to low planktonic cell numbers, preventing direct assessment of *rpiRc* silencing on adhesion in the presence of phage. Notably, increased susceptibility to phage infection was observed after 3 hours in the *rpiRc*-silenced strain, even though viral titers did not differ significantly between NI +P and I +P at the 4-hour endpoint. This may reflect the short time between the onset of increased susceptibility and titration, as viral replication requires at least 30 minutes. A viral titer assessment after

4 hours of incubation will be necessary to better evaluate this effect. Further investigations, including gene expression and cell wall characterization, will be essential to elucidate the mechanisms linking *rpiRc* silencing to enhanced phage susceptibility.

Although we did not directly assess the differentially expressed genes after *mgrA* and *sarZ* silencing, literature suggests that these mutants exhibit reduced toxin and virulence factor production, alongside increased adhesin expression [75,77,84,96]. In our study, silencing both reduced phage susceptibility, indicating that resistance may come at the cost of lowered virulence. Conversely, *rpiRc* silencing, which increases RNAIII and enhances toxin production and hemolysis, also increased susceptibility, suggesting a tradeoff where heightened virulence may increase vulnerability to phages. These findings are relevant for phage therapy, highlighting how phage-host interactions modulate bacterial virulence and may uncover therapeutic targets. Moreover, this study identified novel host factors for *S. aureus* phages, including SAOUHSC_00695, a gene of unknown function involved in phage susceptibility.

As next steps, we propose prioritizing phage adsorption kinetics assays to determine whether resistance in mutants results from loss of phage receptors. In parallel, targeted RT-qPCR should evaluate key gene expression levels: WTA glycosylation (*tarM*, *tarS*), capsule production (*capA*), Protein A (*spa*), metal transport (*mntH*), and virulence regulation (RNAIII, *hla*, *sspA*, adhesins). These are essential to confirm our main hypotheses. Subsequently, cell wall analyses (e.g., WTA quantification and characterization) and genetic complementation experiments may strengthen our findings and demonstrate causality. Finally, broader studies—such as RNA-seq or new CRISPRi-seq assays in lysogenic strains—will help uncover additional regulatory mechanisms and clarify how prophages influence the response to lytic phages, contributing to the advancement of phage therapy.

5. CONCLUSIONS

This study presents the first genome-wide CRISPRi-seq screening in *Staphylococcus aureus* to identify host factors that modulate susceptibility or resistance to lytic phage infection. By integrating high-throughput sequencing with targeted gene silencing and phenotypic validation, we uncovered both known and previously uncharacterized bacterial genes involved in the phage-host interaction.

Notably, all genes selected for experimental validation exhibited phenotypes that fully corroborated the CRISPRi-seq predictions, reinforcing the reliability and accuracy of this approach. Our findings demonstrate the practical and high-throughput potential of genome-wide CRISPRi-seq to uncover essential components of bacterial defense and permissiveness to phages—including genes whose study would be impossible with conventional knockouts due to their essentiality. This strategy enables not only the identification of individual host factors but also the detection of dynamic and time-dependent responses to infection.

Among the validated targets, silencing of *mgrA* and SAOUHSC_00695 conferred complete resistance to phage CapO46, likely by disrupting WTA glycosylation required for phage adsorption. Conversely, silencing the essential gene *rpiRc* increased bacterial susceptibility, potentially due to metabolic imbalance and greater exposure of phage receptors. The combined repression of genes such as *sarZ/mgrA* and *SAOUHSC_00695/mgrA* revealed the existence of regulatory compensation mechanisms that influence both phage replication and bacterial survival. Additionally, our results demonstrated that gene silencing influenced early biofilm formation and adhesion, often independently of cell density, highlighting the interconnectedness between virulence regulation, surface architecture, and phage resistance. Interestingly, resistance to phage infection was frequently associated with reduced virulence potential, while increased susceptibility (e.g., in *rpiRc*-silenced strains) coincided with enhanced virulence, revealing a potential trade-off exploitable in therapeutic strategies.

Altogether, this work not only advances our understanding of *S. aureus* phage biology but also highlights the power and practicality of CRISPRi-seq as a discovery platform for host-phage interaction studies. The identification of multiple novel host factors—confirmed by experimental assays—opens new avenues for rational design of phage-based treatments and combinatory approaches in the fight against multidrug-resistant pathogens. Despite its robustness, the CRISPRi-seq technique has limitations, particularly in evaluating genes located within operons or those with strong polar effects, which may hinder the individual assessment of certain targets. Future studies will include adsorption assays, RT-qPCR, and WTA characterization to clarify the molecular basis of these phenotypes and validate the mechanisms proposed.

6. REFERENCES

1. LEE, A.S.; DE LENCASTRE, H.; GARAU, J.; KLUYTMANS, J.; MALHOTRA-KUMAR, S.; PESCHEL, A.; HARBARTH, S. **Methicillin-Resistant Staphylococcus Aureus.** *Nat Rev Dis Primers* **2018**, *4*, 18033, doi:10.1038/nrdp.2018.33.

2. ROWE, S.E.; BEAM, J.E.; CONLON, B.P. **Recalcitrant Staphylococcus Aureus Infections: Obstacles and Solutions.** *Infect Immun* **2021**, *89*, doi:10.1128/IAI.00694-20.

3. BREITBART, M.; ROHWER, F. Here a Virus, **There a Virus, Everywhere the Same Virus?** *Trends Microbiol* **2005**, *13*, 278–284, doi:10.1016/j.tim.2005.04.003.

4. SHKOPOROV, A.N.; HILL, C. **Bacteriophages of the Human Gut: The "Known Unknown" of the Microbiome.** *Cell Host Microbe* **2019**, *25*, 195–209, doi:10.1016/j.chom.2019.01.017.

5. ABEDON, S.T.; GARCÍA, P.; MULLANY, P.; AMINOV, R. **Editorial: Phage Therapy: Past, Present and Future.** *Front Microbiol* **2017**, *8*, doi:10.3389/fmicb.2017.00981.

6. GORDILLO ALTAMIRANO, F.L.; BARR, J.J. **Phage Therapy in the Postantibiotic Era.** *Clin Microbiol Rev* **2019**, *32*, doi:10.1128/CMR.00066-18.

7. NOBREGA, F.L.; COSTA, A.R.; KLUSKENS, L.D.; AZEREDO, J. **Revisiting Phage Therapy: New Applications for Old Resources.** *Trends Microbiol* **2015**, *23*, 185–191, doi:10.1016/j.tim.2015.01.006.

8. MELO, L.D.R.; OLIVEIRA, H.; PIRES, D.P.; DABROWSKA, K.; AZEREDO, J. **Phage Therapy Efficacy: A Review of the Last 10 Years of Preclinical Studies.** *Crit Rev Microbiol* **2020**, *46*, 78–99, doi:10.1080/1040841X.2020.1729695.

9. GENG, H.; ZOU, W.; ZHANG, M.; XU, L.; LIU, F.; LI, X.; WANG, L.; XU, Y. **Evaluation of Phage Therapy in the Treatment of Staphylococcus Aureus-Induced Mastitis in Mice.** *Folia Microbiol (Praha)* **2020**, *65*, 339–351, doi:10.1007/s12223-019-00729-9.

10. MOSIMANN, S.; DESIREE, K.; EBNER, P. **Efficacy of Phage Therapy in Poultry: A Systematic Review and Meta-Analysis.** *Poult Sci* **2021**, *100*, 101472, doi:10.1016/j.psj.2021.101472.

11. ANAND, T.; VIRMANI, N.; KUMAR, S.; MOHANTY, A.K.; PAVULRAJ, S.; BERA, B.CH.; VAID, R.K.; AHLAWAT, U.; TRIPATHI, B.N. **Phage Therapy for Treatment of Virulent Klebsiella Pneumoniae Infection in a Mouse Model**. *J Glob Antimicrob Resist* **2020**, *21*, 34–41, doi:10.1016/j.jgar.2019.09.018.

12. SARKER, S.A.; SULTANA, S.; REUTELER, G.; MOINE, D.; DESCOMBES, P.; CHARTON, F.; BOURDIN, G.; MCCALLIN, S.; NGOM-BRU, C.; NEVILLE, T.; et al. **Oral Phage Therapy of Acute Bacterial Diarrhea With Two Coliphage Preparations: A Randomized Trial in Children From Bangladesh.** *EBioMedicine* **2016**, *4*, 124–137, doi:10.1016/j.ebiom.2015.12.023.

13. JAULT, P.; LECLERC, T.; JENNES, S.; PIRNAY, J.P.; QUE, Y.-A.; RESCH, G.; ROUSSEAU, A.F.; RAVAT, F.; CARSIN, H.; LE FLOCH, R.; et al. **Efficacy and Tolerability of a Cocktail of Bacteriophages to Treat Burn Wounds Infected by**

Pseudomonas Aeruginosa (PhagoBurn): A Randomised, Controlled, Double-Blind Phase 1/2 Trial. *Lancet Infect Dis* **2019**, *19*, 35–45, doi:10.1016/S1473-3099(18)30482-1.

14. EGIDO, J.E.; COSTA, A.R.; APARICIO-MALDONADO, C.; HAAS, P.-J.; BROUNS, S.J.J. **Mechanisms and Clinical Importance of Bacteriophage Resistance.** *FEMS Microbiol Rev* **2022**, *46*, doi:10.1093/femsre/fuab048.

15. MOLLER, A.G.; LINDSAY, J.A.; READ, T.D. **Determinants of Phage Host Range in *Staphylococcus* Species.** *Appl Environ Microbiol* **2019**, *85*, doi:10.1128/AEM.00209-19.

16. JURADO, A.; FERNÁNDEZ, L.; RODRÍGUEZ, A.; GARCÍA, P. **Understanding the Mechanisms That Drive Phage Resistance in Staphylococci to Prevent Phage Therapy Failure**. *Viruses* **2022**, *14*, 1061, doi:10.3390/v14051061.

17. AZAM, A.H.; HOSHIGA, F.; TAKEUCHI, I.; MIYANAGA, K.; TANJI, Y. **Analysis of Phage Resistance in Staphylococcus Aureus SA003 Reveals Different Binding Mechanisms for the Closely Related Twort-like Phages ϕSA012 and ϕSA039**. *Appl Microbiol Biotechnol* **2018**, *102*, 8963–8977, doi:10.1007/s00253-018-9269-x.

18. XIA, G.; CORRIGAN, R.M.; WINSTEL, V.; GOERKE, C.; GRÜNDLING, A.; PESCHEL, A. **Wall Teichoic Acid-Dependent Adsorption of Staphylococcal Siphovirus and Myovirus**. *J Bacteriol* **2011**, *193*, 4006–4009, doi:10.1128/JB.01412-10.

19. LI, X.; GERLACH, D.; DU, X.; LARSEN, J.; STEGGER, M.; KÜHNER, P.; PESCHEL, A.; XIA, G.; WINSTEL, V. **An Accessory Wall Teichoic Acid Glycosyltransferase Protects Staphylococcus Aureus from the Lytic Activity of Podoviridae.** *Sci Rep* **2015**, *5*, 17219, doi:10.1038/srep17219.

20. UCHIYAMA, J.; TANIGUCHI, M.; KUROKAWA, K.; TAKEMURA-UCHIYAMA, I.; UJIHARA, T.; SHIMAKURA, H.; SAKAGUCHI, Y.; MURAKAMI, H.; SAKAGUCHI, M.; MATSUZAKI, S. **Adsorption of Staphylococcus Viruses S13′ and S24-1 on Staphylococcus Aureus Strains with Different Glycosidic Linkage Patterns of Wall Teichoic Acids.** *Journal of General Virology* **2017**, *98*, 2171–2180, doi:10.1099/jgv.0.000865.

21. BROWN, S.; XIA, G.; LUHACHACK, L.G.; CAMPBELL, J.; MEREDITH, T.C.; CHEN, C.; WINSTEL, V.; GEKELER, C.; IRAZOQUI, J.E.; PESCHEL, A.; et al. **Methicillin Resistance in *Staphylococcus Aureus* Requires Glycosylated Wall Teichoic Acids.** *Proceedings of the National Academy of Sciences* **2012**, *109*, 18909–18914, doi:10.1073/pnas.1209126109.

22. BROWN, S.; SANTA MARIA, J.P.; WALKER, S. **Wall Teichoic Acids of Gram-Positive Bacteria.** *Annu Rev Microbiol* **2013**, *67*, 313–336, doi:10.1146/annurev-micro-092412-155620.

23. CHA, Y.; CHUN, J.; SON, B.; RYU, S. **Characterization and Genome Analysis of Staphylococcus Aureus Podovirus CSA13 and Its Anti-Biofilm Capacity**. *Viruses* **2019**, *11*, 54, doi:10.3390/v11010054.

24. UCHIYAMA, J.; TAKEMURA-UCHIYAMA, I.; KATO, S.; SATO, M.; UJIHARA, T.; MATSUI, H.; HANAKI, H.; DAIBATA, M.; MATSUZAKI, S. **In Silico Analysis of**

<scp>AHJD</Scp> -like Viruses, *Staphylococcus Aureus* Phages S24-1 and S13′, and Study of Phage S24-1 Adsorption. *Microbiologyopen* **2014**, *3*, 257–270, doi:10.1002/mbo3.166.

25. NORDSTRÖM, K.; FORSGREN, A. **Effect of Protein A on Adsorption of Bacteriophages to *Staphylococcus Aureus***. *J Virol* **1974**, *14*, 198–202, doi:10.1128/jvi.14.2.198-202.1974.

26. WILKINSON, B.J.; HOLMES, K.M. **Staphylococcus Aureus Cell Surface: Capsule as a Barrier to Bacteriophage Adsorption**. *Infect Immun* **1979**, *23*, 549–552, doi:10.1128/iai.23.2.549-552.1979.

27. DEPARDIEU, F.; DIDIER, J.-P.; BERNHEIM, A.; SHERLOCK, A.; MOLINA, H.; DUCLOS, B.; BIKARD, D. A **Eukaryotic-like Serine/Threonine Kinase Protects Staphylococci against Phages.** *Cell Host Microbe* **2016**, *20*, 471–481, doi:10.1016/j.chom.2016.08.010.

28. CAO, L.; GAO, C.-H.; ZHU, J.; ZHAO, L.; WU, Q.; LI, M.; SUN, B. **Identification and Functional Study of Type III-A CRISPR-Cas Systems in Clinical Isolates of Staphylococcus Aureus.** *International Journal of Medical Microbiology* **2016**, *306*, 686–696, doi:10.1016/j.ijmm.2016.08.005.

29. DAMLE, P.K.; WALL, E.A.; SPILMAN, M.S.; DEARBORN, A.D.; RAM, G.; NOVICK, R.P.; DOKLAND, T.; CHRISTIE, G.E. **The Roles of SaPI1 Proteins Gp7 (CpmA) and Gp6 (CpmB) in Capsid Size Determination and Helper Phage Interference.** *Virology* **2012**, *432*, 277–282, doi:10.1016/j.virol.2012.05.026.

30. RAM, G.; CHEN, J.; KUMAR, K.; ROSS, H.F.; UBEDA, C.; DAMLE, P.K.; LANE, K.D.; PENADÉS, J.R.; CHRISTIE, G.E.; NOVICK, R.P. **Staphylococcal Pathogenicity Island Interference with Helper Phage Reproduction Is a Paradigm of Molecular Parasitism.** *Proceedings of the National Academy of Sciences* **2012**, *109*, 16300–16305, doi:10.1073/pnas.1204615109.

31. XU, S.; CORVAGLIA, A.R.; CHAN, S.-H.; ZHENG, Y.; LINDER, P. **A Type IV Modification-Dependent Restriction Enzyme SauUSI from Staphylococcus Aureus Subsp. Aureus USA300.** *Nucleic Acids Res* **2011**, *39*, 5597–5610, doi:10.1093/nar/gkr098.

32. ADLER, B.A.; KAZAKOV, A.E.; ZHONG, C.; LIU, H.; KUTTER, E.; LUI, L.M.; NIELSEN, T.N.; CARION, H.; DEUTSCHBAUER, A.M.; MUTALIK, V.K.; et al. **The Genetic Basis of Phage Susceptibility, Cross-Resistance and Host-Range in Salmonella.** *Microbiology (N Y)* **2021**, *167*, doi:10.1099/mic.0.001126.

33. ROUSSET, F.; CUI, L.; SIOUVE, E.; BECAVIN, C.; DEPARDIEU, F.; BIKARD, D. **Genome-Wide CRISPR-DCas9 Screens in E. Coli Identify Essential Genes and Phage Host Factors.** *PLoS Genet* **2018**, *14*, e1007749, doi:10.1371/journal.pgen.1007749.

34. LIU, X.; DE BAKKER, V.; HEGGENHOUGEN, M.V.; MÅRLI, M.T.; FRØYNES, A.H.; SALEHIAN, Z.; PORCELLATO, D.; MORALES ANGELES, D.; VEENING, J.-W.; KJOS, M. **Genome-Wide CRISPRi Screens for High-Throughput Fitness Quantification and Identification of Determinants for Dalbavancin Susceptibility in *Staphylococcus Aureus*.** *mSystems* **2024**, *9*, doi:10.1128/msystems.01289-23.

35. WARD, R.D.; TRAN, J.S.; BANTA, A.B.; BACON, E.E.; ROSE, W.E.; PETERS, J.M. **Essential Gene Knockdowns Reveal Genetic Vulnerabilities and Antibiotic Sensitivities in *Acinetobacter Baumannii*.** *mBio* **2024**, *15*, doi:10.1128/mbio.02051-23.

36. JIANG, W.; OIKONOMOU, P.; TAVAZOIE, S. **Comprehensive Genome-Wide Perturbations via CRISPR Adaptation Reveal Complex Genetics of Antibiotic Sensitivity.** *Cell* **2020**, *180*, 1002-1017.e31, doi:10.1016/j.cell.2020.02.007.

37. LIU, X.; KIMMEY, J.M.; MATARAZZO, L.; DE BAKKER, V.; VAN MAELE, L.; SIRARD, J.-C.; NIZET, V.; VEENING, J.-W. **Exploration of Bacterial Bottlenecks and Streptococcus Pneumoniae Pathogenesis by CRISPRi-Seq.** *Cell Host Microbe* **2021**, *29*, 107-120.e6, doi:10.1016/j.chom.2020.10.001.

38. MUTALIK, V.K.; ADLER, B.A.; RISHI, H.S.; PIYA, D.; ZHONG, C.; KOSKELLA, B.; KUTTER, E.M.; CALENDAR, R.; NOVICHKOV, P.S.; PRICE, M.N.; et al. **High-Throughput Mapping of the Phage Resistance Landscape in E. Coli.** *PLoS Biol* **2020**, *18*, e3000877, doi:10.1371/journal.pbio.3000877.

39. BIKARD, D.; JIANG, W.; SAMAI, P.; HOCHSCHILD, A.; ZHANG, F.; MARRAFFINI, L.A. **Programmable Repression and Activation of Bacterial Gene Expression Using an Engineered CRISPR-Cas System.** *Nucleic Acids Res* **2013**, *41*, 7429–7437, doi:10.1093/nar/gkt520.

40. QI, L.S.; LARSON, M.H.; GILBERT, L.A.; DOUDNA, J.A.; WEISSMAN, J.S.; ARKIN, A.P.; LIM, W.A. **Repurposing CRISPR as an RNA-Guided Platform for Sequence-Specific Control of Gene Expression.** *Cell* **2013**, *152*, 1173–1183, doi:10.1016/j.cell.2013.02.022.

41. WANG, T.; GUAN, C.; GUO, J.; LIU, B.; WU, Y.; XIE, Z.; ZHANG, C.; XING, X.-H. **Pooled CRISPR Interference Screening Enables Genome-Scale Functional Genomics Study in Bacteria with Superior Performance.** *Nat Commun* **2018**, *9*, 2475, doi:10.1038/s41467-018-04899-x.

42. HARDING, K.R.; MALONE, L.M.; KYTE, N.A.P.; JACKSON, S.A.; SMITH, L.M.; FINERAN, P.C. **Genome-Wide Identification of Bacterial Genes Contributing to Nucleus-Forming Jumbo Phage Infection**. *Nucleic Acids Res* **2024**, doi:10.1093/nar/gkae1194.

43. CUNHA, P.C.; DE SOUZA, P.S.; ROSSETO, A.J.D.; RODRIGUES, I.R.; DIAS, R.S.; DA SILVA DUARTE, V.; PORCELLATO, D.; DA SILVA, C.C.; DE PAULA, S.O. **Characterization of Newly Isolated Rosenblumvirus Phage Infecting Staphylococcus Aureus from Different Sources.** *Microorganisms* **2025**, *13*, 664, doi:10.3390/microorganisms13030664.

44. KHAN MIRZAEI, M.; NILSSON, A.S. **Isolation of Phages for Phage Therapy: A Comparison of Spot Tests and Efficiency of Plating Analyses for Determination of Host Range and Efficacy.** *PLoS One* **2015**, *10*, e0118557, doi:10.1371/journal.pone.0118557.

45. MARK HANCOCK ADAMS ***Bacteriophages***; Bacteriophages, 1959;

46. TWEST, R.; KROPINSKI, A.M. **Bacteriophage Enrichment from Water and Soil**. In; 2009; pp. 15–21.

47. HYMAN, P.; ABEDON, S.T. **Practical Methods for Determining Phage Growth Parameters**. In; 2009; pp. 175–202.

48. RICE, C.J.; KELLY, S.A.; O'BRIEN, S.C.; MELAUGH, E.M.; GANACIAS, J.C.B.; CHAI, Z.H.; GILMORE, B.F.; SKVORTSOV, T. **Novel Phage-Derived Depolymerase with Activity against Proteus Mirabilis Biofilms**. *Microorganisms* **2021**, *9*, 2172, doi:10.3390/microorganisms9102172.

49. CROSBY, H.A.; SCHLIEVERT, P.M.; MERRIMAN, J.A.; KING, J.M.; SALGADO-PABÓN, W.; HORSWILL, A.R. **The Staphylococcus Aureus Global Regulator MgrA Modulates Clumping and Virulence by Controlling Surface Protein Expression**. *PLoS Pathog* **2016**, *12*, e1005604, doi:10.1371/journal.ppat.1005604.

50. WINSTEL, V.; XIA, G.; PESCHEL, A. **Pathways and Roles of Wall Teichoic Acid Glycosylation in Staphylococcus Aureus.** ***International Journal of Medical*** *Microbiology* **2014**, *304*, 215–221, doi:10.1016/j.ijmm.2013.10.009.

51. MLYNEK, K.D.; CALLAHAN, M.T.; SHIMKEVITCH, A. V.; FARMER, J.T.; ENDRES, J.L.; MARCHAND, M.; BAYLES, K.W.; HORSWILL, A.R.; KAPLAN, J.B. **Effects of Low-Dose Amoxicillin on Staphylococcus Aureus USA300 Biofilms.** ***Antimicrob Agents*** *Chemother* **2016**, *60*, 2639–2651, doi:10.1128/AAC.02070-15.

52. PANLILIO, H.; RICE, C. V. **The Role of Extracellular DNA in the Formation, Architecture, Stability, and Treatment of Bacterial Biofilms.** *Biotechnol Bioeng* **2021**, *118*, 2129–2141, doi:10.1002/bit.27760.

53. BÆK, K.T.; FREES, D.; RENZONI, A.; BARRAS, C.; RODRIGUEZ, N.; MANZANO, C.; KELLEY, W.L. **Genetic Variation in the Staphylococcus Aureus 8325 Strain Lineage Revealed by Whole-Genome Sequencing**. *PLoS One* **2013**, *8*, e77122, doi:10.1371/journal.pone.0077122.

54. PANÉ-FARRÉ, J.; JONAS, B.; HARDWICK, S.W.; GRONAU, K.; LEWIS, R.J.; HECKER, M.; ENGELMANN, S. **Role of RsbU in Controlling SigB Activity in** ***Staphylococcus Aureus*** **Following Alkaline Stress**. *J Bacteriol* **2009**, *191*, 2561–2573, doi:10.1128/JB.01514-08.

55. PALMA, M.; CHEUNG, A.L. **ΣB Activity in Staphylococcus Aureus Is Controlled by RsbU and an Additional Factor(s) during Bacterial Growth.** *Infect Immun* **2001**, *69*, 7858–7865, doi:10.1128/IAI.69.12.7858-7865.2001.

56. KOSSAKOWSKA-ZWIERUCHO, M.; KAŹMIERKIEWICZ, R.; BIELAWSKI, K.P.; NAKONIECZNA, J. **Factors Determining Staphylococcus Aureus Susceptibility to Photoantimicrobial Chemotherapy: RsbU Activity, Staphyloxanthin Level, and Membrane Fluidity**. *Front Microbiol* **2016**, *7*, doi:10.3389/fmicb.2016.01141.

57. FINSTRLOVÁ, A.; MAŠLAŇOVÁ, I.; BLASDEL REUTER, B.G.; DOŠKAŘ, J.; GÖTZ, F.; PANTŮČEK, R. **Global Transcriptomic Analysis of Bacteriophage-Host Interactions between a Kayvirus Therapeutic Phage and Staphylococcus Aureus**. *Microbiol Spectr* **2022**, *10*, doi:10.1128/spectrum.00123-22.

58. PERERA, V.R.; NEWTON, G.L.; POGLIANO, K. **Bacillithiol: A Key Protective Thiol in** ***Staphylococcus Aureus***. *Expert Rev Anti Infect Ther* **2015**, *13*, 1089–1107, doi:10.1586/14787210.2015.1064309.

59. POSADA, A.C.; KOLAR, S.L.; DUSI, R.G.; FRANCOIS, P.; ROBERTS, A.A.; HAMILTON, C.J.; LIU, G.Y.; CHEUNG, A. **Importance of Bacillithiol in the Oxidative Stress Response of Staphylococcus Aureus**. *Infect Immun* **2014**, *82*, 316–332, doi:10.1128/IAI.01074-13.

60. EL YACOUBI, B.; BONNETT, S.; ANDERSON, J.N.; SWAIRJO, M.A.; IWATA-REUYL, D.; DE CRÉCY-LAGARD, V. **Discovery of a New Prokaryotic Type I GTP Cyclohydrolase Family**. *Journal of Biological Chemistry* **2006**, *281*, 37586–37593, doi:10.1074/jbc.M607114200.

61. SANKARAN, B.; BONNETT, S.A.; SHAH, K.; GABRIEL, S.; REDDY, R.; SCHIMMEL, P.; RODIONOV, D.A.; DE CRÉCY-LAGARD, V.; HELMANN, J.D.; IWATA-REUYL, D.; et al. **Zinc-Independent Folate Biosynthesis: Genetic, Biochemical, and Structural Investigations Reveal New Metal Dependence for GTP Cyclohydrolase IB.** *J Bacteriol* **2009**, *191*, 6936–6949, doi:10.1128/JB.00287-09.

62. SCHMALISCH, M.; LANGBEIN, I.; STÜLKE, J. **The General Stress Protein Ctc of Bacillus Subtilis Is a Ribosomal Protein.** *J Mol Microbiol Biotechnol* **2002**, *4*, 495–501.

63. VOLKER, U.; ENGELMANN, S.; MAUL, B.; RIETHDORF, S.; VOLKER, A.; SCHMID, R.; MACH, H.; HECKER, M. **Analysis of the Induction of General Stress Proteins of Bacillus Subtilis.** *Microbiology (N Y)* **1994**, *140*, 741–752, doi:10.1099/00221287-140-4-741.

64. SUZUKI, S.; TANIGAWA, O.; AKANUMA, G.; NANAMIYA, H.; KAWAMURA, F.; TAGAMI, K.; NOMURA, N.; KAWABATA, T.; SEKINE, Y. **Enhanced Expression of Bacillus Subtilis YaaA Can Restore Both the Growth and the Sporulation Defects Caused by Mutation of RplB, Encoding Ribosomal Protein L2**. *Microbiology (N Y)* **2014**, *160*, 1040–1053, doi:10.1099/mic.0.076463-0.

65. JIN, Q.; XIE, X.; ZHAI, Y.; ZHANG, H. **Mechanisms of Folate Metabolism-Related Substances Affecting Staphylococcus Aureus Infection**. *International Journal of Medical Microbiology* **2023**, *313*, 151577, doi:10.1016/j.ijmm.2023.151577.

66. BATOOL, N.; KO, K.S.; CHAURASIA, A.K.; KIM, K.K. **Functional Identification of Serine Hydroxymethyltransferase as a Key Gene Involved in Lysostaphin Resistance and Virulence Potential of Staphylococcus Aureus Strains.** *Int J Mol Sci* **2020**, *21*, 9135, doi:10.3390/ijms21239135.

67. MARTINUSSEN, J.; GLASER, P.; ANDERSEN, P.S.; SAXILD, H.H. **Two Genes Encoding Uracil Phosphoribosyltransferase Are Present in Bacillus Subtilis.** *J Bacteriol* **1995**, *177*, 271–274, doi:10.1128/jb.177.1.271-274.1995.

68. ANDERSON, K.L.; ROUX, C.M.; OLSON, M.W.; LUONG, T.T.; LEE, C.Y.; OLSON, R.; DUNMAN, P.M. **Characterizing the Effects of Inorganic Acid and Alkaline Shock on the *Staphylococcus Aureus* Transcriptome and Messenger RNA Turnover**. *FEMS Immunol Med Microbiol* **2010**, *60*, 208–250, doi:10.1111/j.1574-695X.2010.00736.x.

69. DE AZEVEDO, E.C.; NASCIMENTO, A.S. **Energy Landscape of the Domain Movement in Staphylococcus Aureus UDP-N-Acetylglucosamine 2-Epimerase.** *J Struct Biol* **2019**, *207*, 158–168, doi:10.1016/j.jsb.2019.05.004.

70. DE AZEVEDO, E.C.; NASCIMENTO, A.S. **The β-Lactam Ticarcillin Is a Staphylococcus Aureus UDP-N-Acetylglucosamine 2-Epimerase Binder.** *Biochimie* **2022**, *197*, 1–8, doi:10.1016/j.biochi.2022.01.016.

71. HOTTA, K.; SUNADA, A.; ISHIKAWA, J.; MIZUNO, S.; IKEDA, Y.; KONDO, S. **The Novel Enzymatic 3''-N-Acetylation of Arbekacin by an Aminoglycoside 3-N-Acetyltransferase of Streptomyces Origin and the Resulting Activity**. *J Antibiot (Tokyo)* **1998**, *51*, 735–742, doi:10.7164/antibiotics.51.735.

72. ZHU, Y.; NANDAKUMAR, R.; SADYKOV, M.R.; MADAYIPUTHIYA, N.; LUONG, T.T.; GAUPP, R.; LEE, C.Y.; SOMERVILLE, G.A. **RpiR Homologues May Link Staphylococcus Aureus RNAIII Synthesis and Pentose Phosphate Pathway Regulation.** *J Bacteriol* **2011**, *193*, 6187–6196, doi:10.1128/JB.05930-11.

73. GAUPP, R.; WIRF, J.; WONNENBERG, B.; BIEGEL, T.; EISENBEIS, J.; GRAHAM, J.; HERRMANN, M.; LEE, C.Y.; BEISSWENGER, C.; WOLZ, C.; et al. **RpiRc Is a Pleiotropic Effector of Virulence Determinant Synthesis and Attenuates Pathogenicity in Staphylococcus Aureus**. *Infect Immun* **2016**, *84*, 2031–2041, doi:10.1128/IAI.00285-16.

74. KUIJK, M.M.; TUSVELD, E.; LEHMANN, E.; VAN DALEN, R.; LASA, I.; INGMER, H.; PANNEKOEK, Y.; VAN SORGE, N.M. **The Two-Component System ArlRS Is Essential for Wall Teichoic Acid Glycoswitching in *Staphylococcus Aureus***. *mBio* **2025**, *16*, doi:10.1128/mbio.02668-24.

75. TAMBER, S.; CHEUNG, A.L. **SarZ Promotes the Expression of Virulence Factors and Represses Biofilm Formation by Modulating SarA and *Agr* in *Staphylococcus Aureus*.** *Infect Immun* **2009**, *77*, 419–428, doi:10.1128/IAI.00859-08.

76. BALLAL, A.; RAY, B.; MANNA, A.C. ***SarZ* , a *SarA* Family Gene, Is Transcriptionally Activated by MgrA and Is Involved in the Regulation of Genes Encoding Exoproteins in *Staphylococcus Aureus*.** *J Bacteriol* **2009**, *191*, 1656–1665, doi:10.1128/JB.01555-08.

77. LEI, M.G.; LEE, C.Y. **Regulation of Staphylococcal Capsule by SarZ Is SigA-Dependent**. *J Bacteriol* **2022**, *204*, doi:10.1128/jb.00152-22.

78. INGAVALE, S.; VAN WAMEL, W.; LUONG, T.T.; LEE, C.Y.; CHEUNG, A.L. **Rat/MgrA, a Regulator of Autolysis, Is a Regulator of Virulence Genes in *Staphylococcus Aureus*.** *Infect Immun* **2005**, *73*, 1423–1431, doi:10.1128/IAI.73.3.1423-1431.2005.

79. LUONG, T.T.; DUNMAN, P.M.; MURPHY, E.; PROJAN, S.J.; LEE, C.Y. **Transcription Profiling of the *MgrA* Regulon in *Staphylococcus Aureus*.** *J Bacteriol* **2006**, *188*, 1899–1910, doi:10.1128/JB.188.5.1899-1910.2006.

80. QIAN, Z.; YIN, Y.; ZHANG, Y.; LU, L.; LI, Y.; JIANG, Y. **Genomic Characterization of Ribitol Teichoic Acid Synthesis in Staphylococcus Aureus: Genes, Genomic Organization and Gene Duplication.** *BMC Genomics* **2006**, *7*, 74, doi:10.1186/1471-2164-7-74.

81. PEREIRA, M.P.; D'ELIA, M.A.; TROCZYNSKA, J.; BROWN, E.D. **Duplication of Teichoic Acid Biosynthetic Genes in *Staphylococcus Aureus* Leads to**

Functionally Redundant Poly(Ribitol Phosphate) Polymerases. *J Bacteriol* **2008**, *190*, 5642–5649, doi:10.1128/JB.00526-08.

82. D'ELIA, M.A.; PEREIRA, M.P.; CHUNG, Y.S.; ZHAO, W.; CHAU, A.; KENNEY, T.J.; SULAVIK, M.C.; BLACK, T.A.; BROWN, E.D. **Lesions in Teichoic Acid Biosynthesis in *Staphylococcus Aureus* Lead to a Lethal Gain of Function in the Otherwise Dispensable Pathway**. *J Bacteriol* **2006**, *188*, 4183–4189, doi:10.1128/JB.00197-06.

83. MEREDITH, T.C.; SWOBODA, J.G.; WALKER, S. **Late-Stage Polyribitol Phosphate Wall Teichoic Acid Biosynthesis in *Staphylococcus Aureus***. *J Bacteriol* **2008**, *190*, 3046–3056, doi:10.1128/JB.01880-07.

84. TROTONDA, M.P.; TAMBER, S.; MEMMI, G.; CHEUNG, A.L. MgrA **Represses Biofilm Formation in *Staphylococcus Aureus*.** *Infect Immun* **2008**, *76*, 5645–5654, doi:10.1128/IAI.00735-08.

85. BOWDEN, L.C.; FINLINSON, J.; JONES, B.; BERGES, B.K. **Beyond the Double Helix: The Multifaceted Landscape of Extracellular DNA in Staphylococcus Aureus Biofilms.** *Front Cell Infect Microbiol* **2024**, *14*, doi:10.3389/fcimb.2024.1400648.

86. SUGIMOTO, S.; SATO, F.; MIYAKAWA, R.; CHIBA, A.; ONODERA, S.; HORI, S.; MIZUNOE, Y. **Broad Impact of Extracellular DNA on Biofilm Formation by Clinically Isolated Methicillin-Resistant and -Sensitive Strains of Staphylococcus Aureus**. *Sci Rep* **2018**, *8*, 2254, doi:10.1038/s41598-018-20485-z.

87. KAPLAN, J.B.; IZANO, E.A.; GOPAL, P.; KARWACKI, M.T.; KIM, S.; BOSE, J.L.; BAYLES, K.W.; HORSWILL, A.R. **Low Levels of β-Lactam Antibiotics Induce Extracellular DNA Release and Biofilm Formation in Staphylococcus Aureus.** *mBio* **2012**, *3*, doi:10.1128/mBio.00198-12.

88. GÖDEKE, J.; PAUL, K.; LASSAK, J.; THORMANN, K.M**. Phage-Induced Lysis Enhances Biofilm Formation in *Shewanella Oneidensis* MR-1**. *ISME J* **2011**, *5*, 613–626, doi:10.1038/ismej.2010.153.

89. CARROLO, M.; FRIAS, M.J.; PINTO, F.R.; MELO-CRISTINO, J.; RAMIREZ, M. **Prophage Spontaneous Activation Promotes DNA Release Enhancing Biofilm Formation in Streptococcus Pneumoniae**. *PLoS One* **2010**, *5*, e15678, doi:10.1371/journal.pone.0015678.

90. LEI, M.G.; LEE, C.Y. **MgrA Activates Staphylococcal Capsule via SigA-Dependent Promoter.** *J Bacteriol* **2020**, *203*, doi:10.1128/JB.00495-20.

91. KRAGH, K.N.; HUTCHISON, J.B.; MELAUGH, G.; RODESNEY, C.; ROBERTS, A.E.L.; IRIE, Y.; JENSEN, P.Ø.; DIGGLE, S.P.; ALLEN, R.J.; GORDON, V.; et al. **Role of Multicellular Aggregates in Biofilm Formation**. *mBio* **2016**, *7*, doi:10.1128/mBio.00237-16.

92. SORROCHE, F.G.; SPESIA, M.B.; ZORREGUIETA, Á.; GIORDANO, W. **A Positive Correlation between Bacterial Autoaggregation and Biofilm Formation in Native Sinorhizobium Meliloti Isolates from Argentina.** *Appl Environ Microbiol* **2012**, *78*, 4092–4101, doi:10.1128/AEM.07826-11.

93. EDMONDS, K.A.; JORDAN, M.R.; GIEDROC, D.P. **COG0523 Proteins: A Functionally Diverse Family of Transition Metal-Regulated G3E P-Loop GTP Hydrolases from Bacteria to Man.** *Metallomics* **2021**, *13*, doi:10.1093/mtomcs/mfab046.

94. FORMOSA-DAGUE, C.; SPEZIALE, P.; FOSTER, T.J.; GEOGHEGAN, J.A.; DUFRÊNE, Y.F. **Zinc-Dependent Mechanical Properties of *Staphylococcus Aureus* Biofilm-Forming Surface Protein SasG.** *Proceedings of the National Academy of Sciences* **2016**, *113*, 410–415, doi:10.1073/pnas.1519265113.

95. CASSAT, J.E.; SKAAR, E.P. **Metal Ion Acquisition in Staphylococcus Aureus: Overcoming Nutritional Immunity**. *Semin Immunopathol* **2012**, *34*, 215–235, doi:10.1007/s00281-011-0294-4.

96. CROSBY, H.A.; TIWARI, N.; KWIECINSKI, J.M.; XU, Z.; DYKSTRA, A.; JENUL, C.; FUENTES, E.J.; HORSWILL, A.R. **The *Staphylococcus Aureus* ArlRS Two-component System Regulates Virulence Factor Expression through MgrA.** *Mol Microbiol* **2020**, *113*, 103–122, doi:10.1111/mmi.14404.

97. KEHL-FIE, T.E.; ZHANG, Y.; MOORE, J.L.; FARRAND, A.J.; HOOD, M.I.; RATHI, S.; CHAZIN, W.J.; CAPRIOLI, R.M.; SKAAR, E.P. **MntABC and MntH Contribute to Systemic Staphylococcus Aureus Infection by Competing with Calprotectin for Nutrient Manganese.** *Infect Immun* **2013**, *81*, 3395–3405, doi:10.1128/IAI.00420-13.

98. PRICE, E.E.; BOYD, J.M. **Genetic Regulation of Metal Ion Homeostasis in Staphylococcus Aureus.** *Trends Microbiol* **2020**, *28*, 821–831, doi:10.1016/j.tim.2020.04.004.

99. CHUNHUA, M.; YU, L.; YAPING, G.; JIE, D.; QIANG, L.; XIAORONG, T.; GUANG, Y. **The Expression of LytM Is Down-regulated by RNAIII in *Staphylococcus Aureus*.** *J Basic Microbiol* **2012**, *52*, 636–641, doi:10.1002/jobm.201100426.

100. YAN, J.; LIU, Y.; GAO, Y.; DONG, J.; MU, C.; LI, D.; YANG, G. **RNAIII Suppresses the Expression of LtaS via Acting as an Antisense RNA in *Staphylococcus Aureus*.** *J Basic Microbiol* **2015**, *55*, 255–261, doi:10.1002/jobm.201400313.

101. ZEDEN, M.S.; GALLAGHER, L.A.; BUENO, E.; NOLAN, A.C.; AHN, J.; SHINDE, D.; RAZVI, F.; SLADEK, M.; BURKE, Ó.; O'NEILL, E.; et al. **Metabolic Reprogramming and Altered Cell Envelope Characteristics in a Pentose Phosphate Pathway Mutant Increases MRSA Resistance to β-Lactam Antibiotics**. *PLoS Pathog* **2023**, *19*, e1011536, doi:10.1371/journal.ppat.1011536.

102. TAN, X.; RAMOND, E.; JAMET, A.; BARNIER, J.-P.; DECAUX-TRAMONI, B.; DUPUIS, M.; EUPHRASIE, D.; TROS, F.; NEMAZANYY, I.; ZIVERI, J.; et al. **Transketolase of Staphylococcus Aureus in the Control of Master Regulators of Stress Response During Infection**. *J Infect Dis* **2019**, *220*, 1967–1976, doi:10.1093/infdis/jiz404.

GENERAL CONCLUSIONS

This thesis reinforces the potential of bacteriophages as promising tools for bacterial control in both food safety and microbiological research. The first chapter described the isolation and comprehensive characterization of UFVCit2, a polyvalent lytic phage targeting members of the Enterobacteriaceae family, including *Salmonella Enteritidis*. The phage demonstrated high genetic safety, environmental stability, and efficacy in reducing bacterial loads in food matrices such as lettuce and chicken meat, highlighting its potential application in food biocontrol strategies.

The second chapter expanded the investigation into bacteriophage applications by characterizing phage CapO46, a member of the *Rosenblumvirus* genus, with lytic activity against *Staphylococcus aureus*, an important pathogen in both foodborne diseases and healthcare-associated infections. Beyond its robust lytic profile and favorable biological characteristics, CapO46 also demonstrated the ability to reduce S. aureus counts in UHT milk, suggesting its potential use as a biocontrol agent in dairy products.

In the third chapter, a genome-wide CRISPRi screen was employed to identify host factors in *S. aureus* that influence phage susceptibility. This approach revealed key genes involved in cell wall biosynthesis, regulatory networks, metal homeostasis, and metabolism that impact phage infection dynamics. These findings contribute to a deeper understanding of phage-host interactions and provide essential knowledge for improving phage therapy design, mitigating resistance, and informing the rational development of phage-based antimicrobials.

Collectively, the data presented in this work highlight the versatility of bacteriophages not only as biocontrol agents in food systems but also as tools for dissecting bacterial physiology and vulnerability. Furthermore, this thesis emphasizes the importance of integrating genomic, functional, and application-driven approaches to advance the development of phage-based interventions in both industrial and clinical settings.